



**Development of
Recommendations for
Compaction Temperatures
in the Field to Achieve
Density and Limit As-Built
Permeability of HMA in
Wisconsin**

SPR # 0092-07-17

Robert Schmitt
Department of Civil Engineering
University of Wisconsin - Platteville
Hussain Bahia, Carl Johnson, and Andrew Hanz
Department of Civil and Environmental Engineering
University of Wisconsin Madison

March 2009

WHRP 08-08

(this page intentionally left blank)

1. Report Number 08-08	2. Govt. Accession No.	3 Recipient's Catalog No.	
4. Title and Subtitle Development of Recommendations for Compaction Temperatures in the Field to achieve Density and Limit as-built Permeability of HMA in Wisconsin		5. Report Date March 2009	
		6. Performing Organization Code WisDOT 0092-07-17	
7. Authors Schmitt, Robert; Bahia, Hussain; Johson, Carl; Hanz, Andrew		8. Performing Organization Report No. WHRP 08-08	
9. Performing Organization Name and Address University of Wisconsin-Platteville Civil and Environmental Engineering Dept. 1 University Plaza Platteville, WI 53818		10 Work Unit No.	
		11. Contract or Grant No. WHRP SPR #0092-07-17	
12. Sponsoring Agency Name and Address Wisconsin Department of Transportation Division of Business Services Research Coordination Section 4802 Sheboygan Avenue, Room 104 Madison, WI 53707		13. Type of Report and Period Covered Final Report, 2007 – 2009	
		14. Sponsoring Agency Code	
15. Supplementary Notes			
16. Abstract <p>The objectives of this study were to (1) evaluate the effect of compaction effort and temperature on densification of HMA in the field and in the lab, (2) quantify the effects of Warm Mix additives on the compaction, and (3) create a dataset capable of determining the effect of as-built density and permeability on asphalt pavement performance. Field testing and loose-mix sampling occurred on 30 unique layers of HMA during the 2007 paving season, and a single Warm Mix project during the 2008 paving season. Loose-mix samples from the construction projects were compacted in the Superpave Gyrotory compactor at two pressure settings, 300 kPa and 600 kPa; and at three temperatures of 248, 194, and 140°F.</p> <p>Factors affecting field density gain in rank order were mat temperature, number of roller passes, roller type, vibratory setting, and PG binder grade. Density of 92% Gmm can be achieved, however at lower temperatures, more roller passes are necessary. A 300 kPa pressure yields a density (@ Ndes) about 1.8 % less than 600 kPa at 248°F. The density was reduced by about 0.4% when compacting at 194°F, and 2.4% at 140°F. Aggregate source and fine aggregate angularity had a marginal effect on compactive effort. A moderate correlation was found between lab temperature and field temperature to achieve a mutual density. Higher Ndes mix will require more field passes.</p> <p>A lab and field evaluation of single Warm Mix Asphalt (WMA) E-1 mixture determined that the average final density for WMA and tradition Hot Mix Asphalt were nearly identical. For a similar number of roller passes, 30% RAP content averaged 2.6% greater density values than 40% RAP content. The results of the laboratory evaluation demonstrate that the use of the WMA additive allowed for an increased amount of RAP in the mix without a significant detriment to mixture workability as shown using the CDI. Both the HMA and WMA 30% mixes approached the Superpave criteria of 4% air voids at Ndes over all compaction temperatures, the air void levels in the WMA 40% were considerably lower than the 4% target.</p> <p>A single database was created to model pavement performance and establish specific density and permeability criteria. A stand-alone spreadsheet file is included with this report to be used in performance modeling after several years from the 2007 construction season.</p>			
17. Key Words Asphalt, Pavement, Permeability, Density, Performance		18. Distribution Statement. No Restriction. This document is available through the National Technical Information Service 5285 Port Royal Road Sterling, Virginia 22161	
19. Security Classif.(of this report) None	20. Security Classif. (of this page) None	21. No. of Pages 146	22. Price -0-

DISCLAIMER

This research was funded through the Wisconsin Highway Research Program by the Wisconsin Department of Transportation (WisDOT) under Project # 0092-07-17. The contents of this report reflect the views of the authors who are responsible for the facts and the accuracy of the data presented herein. The contents do not necessarily reflect the official views of the WisDOT at the time of publication.

EXECUTIVE SUMMARY

The objectives of this study are to (1) evaluate the effect of compaction effort and temperature on densification of HMA in the field and in the lab, (2) quantify the effects of Warm Mix additives on the minimum temperature and the temperature-stress profiles, and (3) create a dataset capable of determining the effect of as-built density and permeability on asphalt pavement performance in Wisconsin. The field study investigated the minimum limiting temperatures at which 92% Gmm field density can be achieved with commonly used compaction effort. The lab study was conducted to determine if a relationship similar to the field can be found for lab compaction using varying temperatures and compaction pressures. To accomplish these objectives, field testing and loose-mix sampling occurred on 23 unique construction projects, totaling 30 unique layers of HMA during the 2007 paving season, and a single Warm Mix project during the 2008 paving season. Field data included nuclear density, core density, temperature, roller passes, roller type, and vibratory setting. Loose-mix samples from the construction projects were compacted in the Superpave Gyrotory compactor at two pressure settings, 300 kPa and 600 kPa; and at three temperatures, 120, 90, and 60°C (248, 194, and 140°F).

Analysis of field data found that factors affecting density gain in importance rank order were temperature of mat surface, number of roller passes, roller type, vibratory setting, and PG binder grade. The results from field data indicate that a density of 92% Gmm can always be achieved, however at lower temperatures, more roller passes are necessary. For lab compaction, pressure and temperature showed significant main effects and significant interactive effects. Using 300 kPa pressure yields a density (@ Ndes) about 1.8 % less than 600 kPa at a baseline temperature of 248°F. The density was reduced by about 0.4% when compacting at 194°F, and 2.4% at 140°F. Aggregate source and fine aggregate angularity were identified as having a marginal effect on compactive effort. Lab and field data sets were merged by density; a moderate correlation was found between lab temperature and field temperature to achieve a mutual density, and a higher Ndes mix will require more field passes. The results, in general, point out the possibility of optimizing the compaction process by understanding the role of temperature and pressure, which are mixture-type specific.

A lab and field evaluation of single Warm Mix Asphalt (WMA) E-1 mixture determined that the average final density for WMA and tradition Hot Mix Asphalt were nearly identical. Variability in WMA final density was larger by a factor of 2.5 for the standard deviation, which was the result of different RAP levels in the mix. For a similar number of roller passes, 30% RAP content averaged 2.6% greater density values than 40% RAP content. Variability (standard deviation) in 30% RAP was much higher by a factor of 3. The results of the laboratory evaluation demonstrate that the use of the WMA additive allowed for an increased amount of RAP in the mix without a significant detriment to mixture workability as shown using the CDI. Both the HMA and WMA 30% mixes approached the Superpave criteria of 4% air voids at Ndes over all compaction temperatures, the air void levels in the WMA 40% were considerably lower than the 4% target.

A single database was created to model pavement performance and establish specific density and permeability criteria. As-built construction data were collected from 29 construction projects paved in 2007. Air and water permeability were measured on the surface layer of 15 of the construction projects, where initial air and water permeability will begin. A stand-alone

spreadsheet file is included with this report to be used in performance modeling after several years from the 2007 construction season.

ACKNOWLEDGMENTS

The authors thank Wisconsin DOT and contractors for their valuable cooperation during this research study. Project personnel allowed the research to be conducted in an efficient manner with minimal impact to construction operations.

TABLE OF CONTENTS

EXECUTIVE SUMMARY	4
ACKNOWLEDGMENTS	6
LIST OF FIGURES	9
LIST OF TABLES.....	11
CHAPTER 1 INTRODUCTION.....	12
1.1 Background and Problem Statement.....	12
1.2 Objective.....	12
1.3 Background and Significance of Work.....	12
1.4 Benefits.....	13
CHAPTER 2 LITERATURE REVIEW	14
2.1 Introduction	14
2.2 Wisconsin DOT Compaction Studies	16
2.3 TRB Workshop 2006.....	17
2.4 Density Models.....	19
2.5 Washington DOT Studies (Variability in Mat Density)	20
2.6 Density and Permeability.....	21
2.7 Warm Mix Asphalt	22
CHAPTER 3 DATA COLLECTION	23
3.1 Introduction	23
3.2 Projects	23
3.3 Density Testing.....	25
3.4 Water and Air Permeability Testing	27
3.5 Field Compaction Experimental Design.....	28
3.6 Lab Compaction Experimental Design.....	33
3.7 Density and Permeability Criteria.....	35
Chapter 4 Field Compaction Data Analysis.....	36
4.1 Statistical Modeling Approach	36
4.2 Project-by-Project Regression	36
4.3 GLM Full Model	38
4.4 Breakdown Roller	48
4.5 Pneumatic Roller	52
4.6 Finish Roller	54
4.7 Limiting Field Temperature.....	58
Chapter 5 Data Analysis for Lab Compaction.....	61
5.1 Statistical Modeling Approach	61
5.2 ANOVA for Ndes	61
5.3 Ndes=60 Gyration.....	65
5.4 Ndes=75 Gyration.....	66
5.5 Ndes=100 Gyration.....	69
5.6 Summary of Lab Compaction Models.....	71
5.7 Compaction Densification Index	71
5.8 Field and Lab Correlation.....	74
5.8.1 Merging Process	74
5.8.2 Data Analysis - Correlations.....	77
CHAPTER 6 WARM MIX ASPHALT.....	82
6.1 Introduction	82
6.2 Lab Investigation	82
6.2.1 Data Collection and Comparison to QC Data.....	82
6.2.3 Experimental Design	84
6.2.4 Results and Analysis.....	85
6.3 Field Investigation	90

6.3.1 Data Collection	90
6.3.2 Data Analysis – WMA versus HMA during Compaction	92
6.3.3 Data Analysis – WMA versus HMA Final Density	94
6.3.4 Data Analysis – WMA at Varying RAP	95
CHAPTER 7 Development of Permeability and Density Criteria	97
7.1 Introduction	97
7.2 Location Referencing Based on Reference Point System	97
7.3 Conversion of Construction Stationing to Reference Point	98
7.4 Assignment of Construction Data to Sequence Numbers	99
7.4.1 Job Mix Formulas	99
7.4.2 Density	100
7.4.3 Mix Properties	101
7.5 Assignment of Permeability Data to Sequence Numbers	102
7.6 Performance-Construction Data Set	104
CHAPTER 8 CONCLUSIONS AND RECOMMENDATIONS	106
8.1 Conclusions from Field Compaction	106
8.2 Conclusions from Lab Compaction	109
8.3 Recommendations for Achieving Field Density	110
8.4 Recommendations for Continued Research – Evaluation of Warm Mix Asphalt	111
8.4.1 Warm Mix Asphalt Field Experiment	111
8.4.2 Warm Mix Asphalt Lab Experiment	112
8.4.3 Density and Permeability Criteria	113
REFERENCES	115
Appendix A Breakdown Roller Plots	118
Appendix B Intermediate Pneumatic Roller Plots	125
Appendix C Finish Roller Plots	132
Appendix D Lab Compaction Models	140
Appendix E	144
Aggregate Source Analysis	144

LIST OF FIGURES

FIGURE 3.1 TESTING FOR PERMEABILITY AND DENSITY (USH 41 FOND DU LAC COUNTY)	25
FIGURE 3.2 PERMEABILITY TESTING (STH 60 WASHINGTON COUNTY).....	27
FIGURE 4.1 GLM OUTPUT FOR FULL MODEL.....	38
FIGURE 4.2 GLM OUTPUT FOR FULL MODEL INCLUDING 2-WAY INTERACTIONS.....	39
FIGURE 4.3 DELTA DENSITY AND TEMPERATURE BY ROLLER TYPE	41
FIGURE 4.4 DELTA DENSITY AND ROLLER TYPE.....	42
FIGURE 4.5 DELTA DENSITY AND TEMPERATURE BY PG GRADE.....	43
FIGURE 4.6 DELTA DENSITY AND RANGE TO 96% GMM.....	44
FIGURE 4.7 DELTA DENSITY AND VIBRATORY SETTING (0=OFF, 1=ON)	45
FIGURE 4.8 DELTA DENSITY AND RANGE TO 96% GMM BY ROLLER TYPE.....	46
FIGURE 4.9 COMPARISON OF MEANS BY PG GRADE	47
FIGURE 4.10 COMPARISON OF MEANS BY ROLLER TYPE.....	47
FIGURE 4.11 COMPARISON OF LEAST SQUARES MEANS BY VIBRATORY SETTING.....	48
FIGURE 4.12 BREAKDOWN ROLLER GLM RESULTS	49
FIGURE 4.13 BREAKDOWN ROLLER GLM RESULTS WITH MAIN EFFECTS AND INTERACTIONS.....	50
FIGURE 4.14 BREAKDOWN ROLLER COMPARISON OF MEANS BY PG GRADE	51
FIGURE 4.15 BREAKDOWN ROLLER COMPARISON OF MEANS BY VIBRATORY SETTING	51
FIGURE 4.16 PNEUMATIC ROLLER GLM RESULTS	52
FIGURE 4.17 PNEUMATIC ROLLER GLM RESULTS FOR MAIN EFFECTS AND INTERACTIONS.....	53
FIGURE 4.18 FINISH ROLLER GLM RESULTS	54
FIGURE 4.19 FINISH ROLLER GLM RESULTS FOR MAIN EFFECTS AND INTERACTIONS	55
FIGURE 4.20 FINISH ROLLER MEANS COMPARISON BY PG GRADE	56
FIGURE 4.21 FINISH ROLLER MEANS COMPARISON BY VIBRATORY SETTING	56
FIGURE 4.22 FINISH ROLLER MODEL	57
FIGURE 4.23 ROLLER PASSES TO ACHIEVE 92% GMM (E-1).....	58
FIGURE 4.24 ROLLER PASSES TO ACHIEVE 92% GMM (E-3).....	59
FIGURE 4.25 ROLLER PASSES TO ACHIEVE 92% GMM (E-10).....	59
FIGURE 5.1 BASIC STATISTICS FOR LAB COMPACTION VARIABLES BY CLASSIFICATION	62
FIGURE 5.2 ANOVA RESULTS FOR LAB COMPACTION VARIABLES	63
FIGURE 5.3 ANOVA RESULTS FOR LAB COMPACTION VARIABLES	64
FIGURE 5.4 NDES=60 GYRATIONS ANOVA RESULTS FOR MAIN EFFECTS	65
FIGURE 5.5 NDES=60 GYRATIONS MAIN EFFECTS AND INTERACTIONS.....	66
FIGURE 5.6 NDES=75 GYRATIONS ANOVA RESULTS.....	67
FIGURE 5.7 NDES=75 GYRATIONS ANOVA RESULTS WITH MAIN EFFECTS AND INTERACTIONS.....	68
FIGURE 5.8 INTERACTION OF NMAS AND TEMPERATURE (NDES=75 GYRATIONS).....	68
FIGURE 5.9 NDES=100 GYRATIONS ANOVA RESULTS.....	69
FIGURE 5.10 NDES=100 GYRATIONS ANOVA WITH MAIN EFFECTS AND INTERACTIONS	70
FIGURE 5.11 CDI FOR E-1 MIXTURES	72
FIGURE 5.12 CDI FOR E-3 MIXTURES	72
FIGURE 5.13 CDI FOR E-10 MIXTURES	73
FIGURE 5.14 LAB COMPACTION DATA SORTED BY PROJECT, TEMPERATURE, AND DENSITY	74
FIGURE 5.15 LAB COMPACTION AVERAGING BY DENSITY AND GYRATION	75
FIGURE 5.16 FIELD COMPACTION DATA SORTED BY PROJECT AND DENSITY	75
FIGURE 5.17 LAB COMPACTION AVERAGING BY DENSITY AND GYRATION	76
FIGURE 5.18 MERGED LAB AND FIELD COMPACTION DATA	76
FIGURE 5.20 CORRELATION MATRIX OF MERGED DATA	77
FIGURE 5.21 CORRELATION OF LAB GYRATIONS WITH ROLLER PASSES	78
FIGURE 5.22 CORRELATION OF LAB GYRATIONS WITH ROLLER PASSES	79
FIGURE 5.23 EFFECT OF PRESSURE ON LAB GYRATIONS WITH ROLLER PASSES	79
FIGURE 5.24 600 KPA PRESSURE FOR LAB GYRATIONS AND ROLLER PASSES.....	80
FIGURE 5.25 TEMPERATURE AT 600 KPA PRESSURE FOR LAB GYRATIONS AND ROLLER PASSES ..	80
FIGURE 5.26 CORRELATION OF LAB GYRATIONS WITH FIELD MAT TEMPERATURE.....	81
FIGURE 6.1 AIR VOIDS VS. TEMPERATURE – NDES = 60 GYRATIONS AT 300KPA	85

FIGURE 6.2 AIR VOIDS VS. TEMPERATURE – NDES = 60 GYRATIONS AT 600KPA	86
FIGURE 6.3 CDI VS. TEMPERATURE AT 300KPA.....	88
FIGURE 6.4 CDI VS. TEMPERATURE AT 600KPA.....	88
FIGURE 6.5 WARM MIX TEMPERATURE READING AT DRUM DISCHARGE.....	91
FIGURE 6.6 WARM MIX TEMPERATURE READING BEHIND PAVER	92
FIGURE 6.7 GLM FOR DENSITY READINGS BETWEEN WMA AND HMA	93
FIGURE 6.8 GLM FOR DELTA DENSITY BETWEEN WMA AND HMA	93
FIGURE 6.9 GLM FOR DELTA DENSITY MAIN EFFECTS AND INTERACTIONS.....	94
FIGURE 6.10 GLM FOR FINAL DENSITY BETWEEN WMA AND HMA.....	94
FIGURE 6.11 FINAL DENSITY COMPARISON FOR WMA AND HMA	95
FIGURE 6.12 GLM FOR VARYING RAP LEVELS IN WMA	96
FIGURE 6.13 FINAL DENSITY COMPARISON FOR RAP CONTENTS.....	96
FIGURE 7.1 OVERLAY OF DATABASES USING REFERENCE POINT SYSTEM.....	98
FIGURE 7.2 RIDE QUALITY MEASUREMENT METHODOLOGY.....	98
FIGURE 7.3 COMPARISON OF PERMEABILITY METHODS	102
FIGURE 7.4 COMPARISON OF AIR PERMEABILITY AND CORE DENSITY.....	103
FIGURE 7.5 COMPARISON OF WATER PERMEABILITY AND CORE DENSITY	103

LIST OF TABLES

TABLE 2.1 LITERATURE SUMMARY OF FACTORS RELATED TO FIELD DENSIFICATION.....	14
TABLE 3.1 PROJECTS FOR FIELD COMPACTION TESTING.....	24
TABLE 3.2 CORE AND NUCLEAR READING COMPARISON	26
TABLE 3.3 SAMPLE OF VARIABLE CHANGES DURING FIELD COMPACTION.....	29
TABLE 3.4 VARIABLES MEASURED DURING FIELD COMPACTION OF 30 LAYERS.....	31
TABLE 3.5 VARIABLES ANALYZED FOR FIELD COMPACTION	32
TABLE 3.6 LAB COMPACTION LAYERS.....	34
TABLE 3.7 LAB COMPACTION VARIABLES AND LEVELS	34
TABLE 4.1 PROJECT-BY-PROJECT MULTIPLE REGRESSION MODELS	37
TABLE 5.1 SUMMARY OF LAB COMPACTION ANALYSIS	71
TABLE 6.1 SUMMARY OF MIX PROPORTIONS.....	82
TABLE 6.2 SUMMARY OF JOB MIX PROPERTIES.....	83
TABLE 6.3 SUMMARY OF FIELD QC DATA	83
TABLE 6.4 EXPERIMENTAL DESIGN – EVALUATION OF WMA	84
TABLE 6.5 ANOVA ANALYSIS – AIR VOIDS AT NDES.....	87
TABLE 6.6 RESULTS OF TUKEY PAIRWISE COMPARISON TEST	87
TABLE 6.7 ANOVA ANALYSIS – CDI	89
TABLE 6.8 RESULTS OF TUKEY PAIRWISE COMPARISON TEST – CDI.....	89
TABLE 6.9 TEST SITE SUMMARY	90
TABLE 7.1 SEQUENCE NUMBER/PROJECT STATIONING OVERLAY (USH 18, PROJECT I.D. 1660-04-73)	99
TABLE 7.2 SEQUENCE NUMBER/JMF DATA OVERLAY (USH 45, PROJECT I.D. 9847-03-60)	100
TABLE 7.3 SEQUENCE NUMBER AND DENSITY DATA OVERLAY (USH 45, PROJECT I.D. 9847-03-60)	101
TABLE 7.4 SEQUENCE NUMBER AND MIX PROPERTIES OVERLAY (USH 45, I.D. 9847-03-60).....	101
TABLE 7.5 SEQUENCE NUMBER AND MIX PROPERTIES OVERLAY	105

CHAPTER 1 INTRODUCTION

1.1 Background and Problem Statement

The placement of adequately densified and impermeable HMA pavements has been recognized as an effective means to protect against rapid oxidation of the binder materials and excessive moisture damage in HMA pavement layers. National studies have shown that the desired air void content of in-place HMA pavements is below 8% and that the desired permeability is below 150×10^{-5} cm/sec. These critical values for in-place air voids and permeability were based solely on their relationship and are only empirically derived. Intuitively, an excessive amount of permeability significantly increases the potential for poor performing pavements; however the relationships of both air voids and permeability with actual performance have not been clearly defined. The degree of compaction, and varying mat temperatures during laydown operations, need to be understood to better achieve the desired target density values and corresponding permeability.

1.2 Objective

The objectives of this research study are to:

- (1) Investigate the minimum limiting temperatures at which required density of HMA can be achieved with commonly used compaction effort;
- (2) Investigate the effect of density achieved “as-built” on water and air permeability and measure how density and permeability (as-built) affect asphalt pavement performance in Wisconsin;
- (3) Understand the inter-relations between HMA mixture properties (aggregate gradations and volumetrics), temperature and in-place density and permeability;
- (4) Establish target minimum temperatures needed to achieve permeability and density values suitable for use within contract specifications;
- (5) Develop temperature-stress profiles to provide guidelines for field compaction; and
- (6) Quantify the effects of Warm Mix additives on the minimum temperature and the temperature-stress profiles.

1.3 Background and Significance of Work

In 2006, WHRP sponsored a study to evaluate density and permeability of in-service asphaltic pavements throughout the state (Schmitt et al. 2007). During this Phase I study, in-service density and permeability were related to performance, and it was not possible to establish definitive criteria for density and permeability. Pavements having a lower as-built density, generally below 92%, had a lower pavement performance as measured by higher PDI values and more cracking. There was no definitive relationship between permeability and performance.

In a related UW-Madison study entitled, “Effect of Temperature and Pressure on HMA Compaction,” a field and laboratory study was conducted in the 2006 paving season to study the effect of stress and temperature on the compaction process (Delgadillo and Bahia 2008). Field data indicated that compaction predominantly occurred where temperatures ranged from 125°C to 60°C; however, below a certain temperature limit, no more density was achieved. Results of the study indicated that the determination of the lower temperature limit for compaction is an important task that is missing in the current specifications and construction manuals. Current specification methods may have compaction temperatures that are too high and do not have too much meaning in the field.

Since both studies have related objectives, namely achieving a desired level of density and permeability to yield a higher performing pavement, a new set of objectives was created. Emerging Warm Mix Asphalt (WMA) technology was also included in the study since it has similar objectives.

1.4 Benefits

The potential benefits of this study include:

- Enhance the understanding of field and lab compaction of HMA pavements to achieve target density of 92%.
- Define target minimum temperatures needed to achieve permeability and density values suitable for use within contract specifications and material manuals.
- Investigate compaction characteristics of Warm Mix Asphalt both in the lab and field.
- Create a database to yield models between in-place permeability, density, mixture characteristics, and performance for a full range of in-place HMA pavements in Wisconsin.

CHAPTER 2 LITERATURE REVIEW

2.1 Introduction

In the previous WHRP Phase I study, a literature review synthesized previous studies that attempted to relate in-place permeability and pavement performance (Schmitt et al. 2007). During this study, the literature review documented recent and relevant studies relating as-built density of HMA pavements to traditional construction and materials factors. Table 2.1 cross-lists the reference with factors affecting field densification. Following this table is a detailed review of each reference document.

Table 2.1 Literature Summary of Factors related to Field Densification

Reference (1)	Factors related to Field Densification (3)
Diefenderfer et al., 2007	<ul style="list-style-type: none"> • WMA can be successfully placed using conventional HMA paving practices
Faheem et al., 2007 (lab study)	<ul style="list-style-type: none"> • Interaction between compaction pressure and temperature. • Density increase with temperature did not apply for all mixtures. • There are clearly optimum temperature and pressure ranges. • Under -asphalted mixes depend mainly on the type of binder used. • Over asphalted mixtures had identical behavior regardless of compaction temperature, pressure or binder type.
Scherocman, 2006	<ul style="list-style-type: none"> • Keep the rollers directly behind the paver while the mix is hot. • Most efficient roller pattern typically uses a pneumatic tire roller for initial compaction followed by a double drum vibratory roller for intermediate and finish, rolling. • Two double-drum vibratory rollers in echelon directly behind the paver with tender mixtures.
Nose, 2006	<ul style="list-style-type: none"> • Significantly higher level of density can be achieved from a combination of a high-frequency double-drum vibratory roller and a vibrator pneumatic roller (VPT). • VPT making 6 roller passes at medium amplitude achieved the same level of density as a conventional static pneumatic tire (having 3 times the weight) and making 12 roller passes. • VPT roller is more versatile and efficient than a much heavier SPT roller. • Density distribution measured by cores show that the density in middle or bottom portion is higher than that in the top portion.

Table 2.1 (cont.)

Kearney, 2006	<ul style="list-style-type: none"> • Oscillatory compaction can achieve higher densities with fewer passes when compared to a vibratory roller. • Compaction is possible at lower temperatures around 150°F.
Decker, 2006	<ul style="list-style-type: none"> • Pavements can be successfully placed at low temperatures
Starry, 2006	<ul style="list-style-type: none"> • Three factors that influence the ability to achieve target density are mix design, mix placement, and the temperature.
El Halim et al., 2006	<ul style="list-style-type: none"> • Layers compacted by steel drum rollers were 20 times more permeable than those compacted by the asphalt multi-integrated roller immediately after construction, and as much as 10 times more permeable after 1 year.
Christensen and Bonaquist, 2005	<ul style="list-style-type: none"> • The most important factor affecting rut resistance is binder grade, followed by aggregate fineness relative to VMA. • Both VMA and aggregate fineness should be tightly controlled.
Russell et al., 2005	<ul style="list-style-type: none"> • Base type, source, gradation, and Ndes level all influenced field density and permeability. • For fine-graded mixes, the t/NMAS ratio showed an influence on achieving density, particularly below a ratio of 2 for gravel-source mixes and a ratio of 3 for limestone-source mixes. For limestone-source mixes outside the current WisDOT t/NMAS range of 3 to 5, it was more difficult to achieve density below a ratio of 3, and possible to achieve a 92% density above a ratio of 5. • Factors that affected density growth during compaction included mat temperature, number of passes, and their interaction (a declining mat temperature occurs with more passes).
Willoughby, 2003	<ul style="list-style-type: none"> • Temperature differentials of 25°F or greater cannot be compacted to the same level as the surrounding mat. • A uniform temperature mat greatly increases the ability to achieve a uniform density.
Klaus, 2003	<ul style="list-style-type: none"> • Use of wax in Warm Mix Technology can produce flow improvement that enable mixing temperatures to be reduced by 40 to 80°F.
Hanna et al., 2002	<ul style="list-style-type: none"> • Nuclear density testing the morning following paving will not result in a significant difference in density than if it is tested the same day of paving.
Willoughby et al., 2002	<ul style="list-style-type: none"> • When the mat temperature differential exceeded 25° F, 89% of the density profiles failed to meet the density criteria, but only 19% failed to meet the density criteria when the temperature differential was less than 25°F. • Pavements that experienced large temperature differentials during placement produced substantial density differentials.

Table 2.1 (cont.)

Willoughby et al., 2001	<ul style="list-style-type: none"> • No one single piece of equipment or operation will guarantee that temperature differentials will not occur. • Techniques can be utilized to offset the effects of the temperature differentials.
Cooley et al., 2001	<ul style="list-style-type: none"> • There is a significant relationship between density and permeability of fine-graded mixes. • 9.5- and 12.5-mm NMAS mixtures become excessively permeable at approximately 7.7% in-place air voids,
Huh and Nam, 2000	<ul style="list-style-type: none"> • Developed a mathematical model to quantify density versus number of roller passes (coverage). Variables considered were compaction density, mix viscosity, temperature, frequency, and amplitude, in addition to the number of roller passes. • Minimum number of passes required to finish a certain compaction job and the maximum compaction density achievable by a certain compaction operation are suggested.
Mahoney et al., 2000	<ul style="list-style-type: none"> • Gradation and asphalt content analysis showed no significant aggregate segregation within the cooler areas of the compacted mat.

2.2 Wisconsin DOT Compaction Studies

A Wisconsin study from Faheem et al. (2007) evaluated the influence of binder viscosity, compaction temperature, compaction pressure, and binder content upon the densification of asphalt test mixtures produced using Process Modified Asphalt and Polymer Modified Asphalt. The effects upon densification were evaluated through a two stage laboratory study. The first stage was concerned with comparing the effort needed to compact each mix using two compaction levels and three compaction temperatures. One type of aggregate and one type of mix gradation were used in this evaluation. The second stage was concerned with the effect of the binder content on the mixture resistance to compaction and densification while varying the compaction temperatures, and pressure for mixtures made with the two types of binders tested. The results of the first stage showed that mixes vary in their sensitivity to the compaction level and the compaction temperature. A high level of interaction between compaction pressure and temperature was observed. Surprisingly, the conventional thinking of density always increasing with temperature did not apply for all mixtures. The second stage showed that the behavior of under asphalted mixtures depend mainly on the type of binder used. While for the over asphalted mixtures, their behavior was identical regardless of compaction temperature, pressure or binder type. While some studies have reported on what are known as Tender Zones, very few could quantify this in the laboratory and report on what makes a mixture tender and how to give guidelines to contractors to avoid Tender Zones. The authors suggested that these zones could be asphalt binder specific and should be defined in a 3-domain chart showing pressure, temperature sensitivity, and asphalt binder type and content in the mixture.

Russell et al. (2005) investigated the density and permeability characteristics of Superpave mixes on 10 paving projects. Base type, source, gradation, and Ndes level all

influenced field density and permeability. No discernible trend was observed between density and permeability for coarse-graded mixes. A clear relationship between layer thickness and permeability was not established. Layer thickness was a factor on a project-specific basis, with some projects indicating it was significant, while others found it not significant. Fine-graded limestone-source mixes compacted on PCC, and those designed at a higher Ndes level, were more permeable than other mixes produced from different sources or constructed on different subsurface layers. For fine-graded mixes, the t/NMAS ratio showed an influence on achieving density, particularly below a ratio of 2 for gravel-source mixes and a ratio of 3 for limestone-source mixes. For limestone-source mixes outside the current WisDOT t/NMAS range of 3 to 5, it was more difficult to achieve density below a ratio of 3, and possible to achieve a 92% density above a ratio of 5. The factors that affected density growth during compaction included mat temperature, number of passes, and their interaction (a declining mat temperature occurs with more passes).

Hanna et al. (2002) evaluated discrepancies between contractors' and Wisconsin Department of Transportation readings, in particular, the relationship between the temperature and density of newly placed hot mix asphalt. The theory states that as asphalt cools, it becomes denser. Hence, if a nuclear gauge is used to measure density after the asphalt has been allowed to cool, it should record a higher reading than when the asphalt was measured just after cold rolling the previous day. This research investigation has found a model that has not reinforced this theory. The research has shown that testing a road for density the morning following paving will not result in a significant difference in density than if it is tested the same day of paving.

2.3 TRB Workshop 2006

An all-day workshop at the 84th TRB Annual Meeting addressed asphalt practitioners' concerns related to specifying and achieving density during HMA pavement construction (TRB 2006). The workshop was divided into four mini-sessions with the following themes: Optimizing HMA Construction Temperatures; Recent Advances in Compaction Equipment, including "Intelligent Compaction"; Longitudinal Joint Density; and Incentives-Disincentives for Construction Quality. Several relevant papers were reviewed in detail from this workshop.

A paper by Scherocman (2006) reported some of the possible causes for both stiff and tender asphalt concrete mixtures and to discuss how to properly compact each type of mix. To properly densify Superpave mixtures, it is necessary to keep the rollers directly behind the paver in order to apply the compactive effort while the mix is hot. Several different roller patterns can be employed, but the most efficient roller pattern typically uses a pneumatic tire roller for initial compaction followed by a double drum vibratory roller for intermediate, and often finish, rolling. Some Superpave designed mixtures, however, are very tender and move under the compactive effort of the rollers. These tender mixes shove in both the longitudinal and transverse direction and often check or crack while being compacted. For tender mixtures, three temperature zones typically exist--both an upper and a lower temperature zone where density can be obtained and an intermediate temperature zone where de-compaction of the mix occurs during the rolling process. For tender mixes, it is necessary to alter the roller patterns in order to achieve the required level of density in the upper temperature zone--before the mix starts to move and shove. The use of two double-drum vibratory (DDV) rollers operated in echelon directly behind the

paver is the most efficient and effective method to achieve the desired level of density in such mixtures.

Nose (2006) reported that to improve the efficiency of the compaction process for both stiff and tender Superpave mixtures, use a vibratory pneumatic tire (VPT) roller developed by Sakai Heavy Industries, Limited, in 2002. The roller has been used on various types of paving projects in the United States since the first production unit was introduced in March 2003. For the evaluations conducted on normal paving operations, the VPT roller was used in the intermediate rolling position after breakdown rolling by a high-frequency double-drum vibratory (DDV) roller. Based on the evaluation of results obtained at San Francisco International Airport, King City, California, and Traverse City, Michigan, the following conclusions were reached. First, the minimum required density of the pavement was significantly exceeded with a combination of a high-frequency DDV roller and a VPT roller. Second, a vibratory pneumatic roller weighing only 20,580 lb and making six roller passes at medium amplitude achieved the same level of density as a conventional static pneumatic tire (SPT) roller weighing 60,000 lb, or nearly 3 times the weight, and making 12 roller passes. It is obvious that the VPT roller is more versatile and efficient than a much heavier SPT roller. Third, the density distribution measured by cores cut from the pavement show that the density in middle or bottom portion is higher than that in the top portion. It is believed that the density in the top portion was lower due to excessive compactive effort applied during breakdown rolling when the pavement surface temperature was relatively low.

Kearney (2006) evaluated oscillation technology that uses dual, opposed, eccentric weights rotating in the same direction around the roller drum axis to produce a rocking motion. This rocking motion produces horizontal and downward shear forces that achieve greater compaction by "massaging" the HMA--even at lower mix temperatures. Since the drum does not leave the pavement surface or bounce like a conventional vibratory roller drum, the compacted mat surface is smooth and flat and there is no damage to utilities, buildings, or bridges. Numerous tests have shown that oscillatory compaction can achieve higher densities with fewer passes when compared to a vibratory roller. Plus compaction is possible at lower temperatures (down to 150°F).

Decker (2006) reported many agencies have specification requirements which force the contractor to discontinue paving operations at some arbitrary temperature or calendar date. Yet pavements can be successfully placed at low temperatures. Public safety concerns often force the owner-agency and contractor to complete paving operations at adverse climatic conditions.

Starry (2006) discussed three factors that influence the ability of a paving train to achieve target density air void content on paving projects. These factors are mix design, mix placement, and the temperature of the hot mix asphalt during the compaction process. The temperature factor is the one contractors are most likely to miss on paving jobs. The case of a contractor's night paving job is highlighted to illustrate the importance of temperature, mix delivery and proper location of the compactors behind the paver.

El Halim et al. (2006) investigated the asphalt multi-integrated roller (AMIR), an innovative compaction technology, offers a more effective alternative for overcoming problems of steel drum rollers by reducing permeability and, in turn, improving long-term performance of flexible pavements. A multi-staged laboratory and field-testing program that measures permeability in terms of hydraulic conductivity was performed on pavement sections constructed using an AMIR side by side with a conventional steel roller. Asphalt concrete layers compacted by steel drum rollers were found, on average, to be up to 20 times more permeable than those

compacted by the AMIR immediately after construction and as much as 10 times more permeable after 1 year. The major steps leading to the understanding of how rolling affects the permeability of asphalt layers and, consequently, the long-term performance of newly compacted pavements are discussed and presented.

2.4 Density Models

Christensen and Bonaquist (2005) described a model for estimating mixture rut resistance using the concept of mixture resistivity, which is the inverse of the permeability of the mixture aggregate to the specific binder used in the mixture at the temperature of interest. Laboratory testing using the repeated shear at constant height test showed very good correlations between resistivity, compaction effort, and maximum permanent shear strain as determined using the repeated shear at constant height test. To verify the usefulness of the proposed model field rutting data from Mn/Road, WesTrack and the National Center for Asphalt Technology (NCAT) Test Track were modeled, using resistivity, N sub design, and relative field density as predictor variables. The resulting model predicted rutting rates for all three projects simultaneously with an R-squared value of 89%. This model was used to analyze the effects of changes in mixture composition, binder grade, and compaction on rut resistance, and also in a preliminary analysis of the current Superpave mix design system. The most important factor affecting rut resistance in HMA mixtures is binder grade, followed by aggregate fineness relative to voids in mineral aggregates (VMA). This suggests that both VMA and aggregate fineness should be tightly controlled to ensure that a given mixture exhibits the desired level of rut resistance.

Huh and Nam (2000) developed a closed formula to quantify density versus number of roller passes (coverage). Variables considered were compaction density, mix viscosity, temperature, frequency, and amplitude, in addition to the number of roller passes. Their effects are included in the proposed formula. The experimental data found in the literature are used to verify the equation. Excellent prediction of the data confirms the success of the formulation. As a result of this mathematical modeling, the minimum number of passes required to finish a certain compaction job and the maximum compaction density achievable by a certain compaction operation are suggested. The equation and its features will be an effective tool for using rolling compaction in an effort to construct better roadway pavements.

Mahoney et al. (2000) researched a cyclic occurrence of premature failure of open-textured asphalt concrete (AC) pavement sections by fatigue cracking, raveling, or both, generally called "cyclic segregation" or "end-of-load segregation." This resulted in an initial study in which mat temperature differentials were observed during laydown. In turn, this led to the current study and the reported results. Pavement temperature differentials result from placement of a cooler portion of the hot-mix mass into the mat. This cooler mass generally constitutes the crust, which can develop during hot-mix transport from the mixing plant to the job site. Placement of this cooler hot mix can create pavement areas near cessation temperature that tend to resist proper compaction (they may also exhibit tearing or roughness or appear to be open textured). These areas were observed to have decreased densities and a higher percentage of air voids (higher air voids). Four 1998 WSDOT paving projects were examined to determine the existence and extent of mat temperature differentials and associated material characteristics. An infrared camera was used to identify cooler portions of the mat, which were then sampled along with normal-temperature pavement sections. Gradation and asphalt content analysis

showed no significant aggregate segregation within the cooler areas. However, these cooler portions of the mat consistently showed higher air voids than the surrounding pavement. On the basis of numerous studies that have related AC deterioration and high air voids in a mix, it is known that the areas of a mat with higher air voids may experience premature failure compared with the time to failure of the mat as a whole.

2.5 Washington DOT Studies (Variability in Mat Density)

Willoughby (2003) reported on research in Washington State to examine the systematic occurrence and variability in pavement mat density. Temperature differentials of 25°F or greater generally cannot be compacted to the same level of density as the surrounding mat and therefore lead to significant density differentials (increase in air voids of 2% or more). A cyclic pattern typically occurs, matching each delivered truckload of mix, although temperature differentials can occur randomly or not at all, depending on the remixing device. The largest extent of pavement is affected when no remixing occurs and temperature differentials develop for every truckload of hot mix. These temperature differentials can cover the entire width and affect up to 50% of the mat. If the delivered hot mix is thoroughly remixed before placement, temperature differentials are minimal. Although density will vary in any paving operation, it was found that a uniform temperature mat greatly increases the ability to achieve a uniform density. Because of this cyclic pattern of variable density, random sampling for in-place density does not properly identify or quantify this problem. It is recommended that temperature differential areas be determined during construction and excluded from the random sampling used for acceptance testing. The issue of variable densities due to temperature differences or aggregate segregation should be identified and eliminated at the start of the project.

Willoughby et al. (2002) examined temperature differentials in hot-mix asphalt paving over four construction seasons. From those studies it was found that low-density areas can be caused by temperature differentials in the mat. The study summarized is based on an examination of 17 projects during the 2000 Washington State DOT paving season to determine density differentials in the mat with a "density profile." A density profile is a series of density readings taken in a longitudinal direction over a 15-m (50-ft) section through a low-temperature area. From this collection of density readings, the density range (the difference between the maximum and the minimum readings) and the density drop (the difference between the average and the minimum readings) are determined. The density range and drop are used to determine if low-temperature areas result in inadequate compaction. The criteria set forth by the Washington State DOT included temperature differentials greater than or equal to 14°C (25°F), a maximum density range of 96 kg/cu m (6.0 lb/cu ft), and a maximum density drop of 48 kg/cu m (3.0 lb/cu ft). Evaluation of the density profiles showed that when the temperature differential exceeded 14°C (25°F), 89% of the density profiles failed to meet the density criteria, but only 19% failed to meet the density criteria when the temperature differential was less than 14°C (25°F). It was found that pavements that experienced large temperature differentials during placement produced substantial density differentials.

Willoughby et al. (2001) investigated what kind of problem the Washington State Department of Transportation (WSDOT) experiences with hot-mix paving, whether temperature differentials or aggregate segregation or both, the possible causes of those problems, and how WSDOT can remedy the problem. The study found that WSDOT experiences temperature

differentials on many projects and to some extent aggregate segregation (typically in longitudinal streaks). The study also found that because many factors are involved with paving operations, no one single piece of equipment or operation will guarantee that temperature differentials will not occur, but that techniques can be utilized to offset the effects of the temperature differentials. The study utilized a density profile procedure that provides a method of determining the effect of the temperature differentials in the HMA mat on performance. It can locate potential areas of low density, test those areas, and provide results (via a nuclear asphalt content gauge) to determine the extent of the problem. Density differentials are a primary concern in hot-mix paving. If temperature differentials exist, but the finished pavement has a uniform density of 93% or greater for dense-graded mixes, then the pavement should attain acceptable performance over its service life. The density profile procedure does not guarantee a uniform mat density, but it can be used as a quality control tool to help attain a uniform density. This could be a major step in achieving a higher quality hot-mix product.

2.6 Density and Permeability

Cooley et al. (2001) evaluated the density-permeability relationship. Within the hot mix asphalt (HMA) community, it is generally accepted that the proper compaction of al for a stable and durable pavement. Low in-place air voids have been shown to lead to rutting and shoving while high in-place air voids have been shown to reduce a pavement's durability through moisture damage and excessive oxidation of the asphalt binder. Recent research has suggested that coarse-graded Superpave designed mixes are more permeable than conventionally designed pavements at a given air void content. This higher permeability can lead to durability problems. The pavement density at which coarse-graded Superpave mixes become permeable was evaluated by using a field permeability device. On the basis of the data collected, 9.5- and 12.5-mm nominal maximum size (NMA) mixtures become excessively permeable at approximately 7.7% in-place air voids, which corresponded to a field permeability value of $100 \times (10^{-5})$ cm/sec. Mixtures having a 19.0-mm NMA became permeable at an in-place air void content of 5.5% air voids which provided a field permeability value of $120 \times (10^{-5})$ cm/sec. Coarse-graded mixes having an NMA of 25.0-mm became permeable at 4.4% air voids, which corresponded to a field permeability value of $150 \times (10^{-5})$ cm/sec.

Cooley (2006) is conducting an on-going study for the Mississippi DOT (MDOT). MDOT's current lift thickness requirements for a single lift of HMA is based on nominal maximum aggregate size (NMA), with maximum lift thickness limited to generally 4 times the NMA. Most current gravel sources in Mississippi are producing particle sizes that are in the range of 37.5 to 50 mm. Once crushed to provide the needed particle angularity for HMA, most of the aggregate particles are less than 12.5-mm in diameter. This means that the most rut resistant mixes (mixtures containing the most angular aggregates) have a relatively small NMA. Under the current Mississippi aggregate requirements, the highest quality HMA mix used in Mississippi, a 9.5-mm NMA, cannot be used in 50-mm mill and fill overlay projects, and a high quality 12.5-mm NMA mix cannot be utilized in a 67.5 or 75 mm upper binder layer. The proposed research evaluates the use of 9.5-mm NMA aggregate HMA in a 50-mm maximum lift thickness and a 12.5-mm NMA aggregate HMA in a 3-inch maximum lift thickness in a total of 12 field projects. For each of these projects the compaction process will be monitored for roller types and pavement temperature and pavement density between roller passes. The

collected data will be used to estimate the relative ability to compact the lift and provide information on whether the thicker lifts result in better density using a typical compactive effort. Uniformity of compaction throughout the depth of the compacted layer and the permeability of the layer will also be addressed. Based upon the research findings, MDOT would be provided with the requisite information to modify the currently specified lift thickness for for 9.5-mm and 12.5-mm NMAS HMA mixes.

2.7 Warm Mix Asphalt

A Virginia DOT study by Diefenderfer et al. (2007) evaluated the installation of warm mix asphalt (WMA) to compile experiences and offer recommendations for future use. Three trial sections were installed using warm mix technologies between August and November of 2006. Two used the Sasobit technology, and the third employed the Evotherm technology. This report discusses the material makeup of these technologies and documents the production and placement of the three trial sections. Trial sections were initiated through cooperative efforts by the Virginia Transportation Research Council; VDOT districts, residencies, and area headquarters; and participating contractors. Construction used typical mixture designs and practices so that performance under typical construction conditions could be evaluated. The study showed that WMA can be successfully placed using conventional HMA paving practices and procedures with only minor modifications to account for the reduction in temperature. The technologies evaluated affected mixture properties in slightly different ways such as changes in tensile strength ratios and variability in air voids. Additional monitoring of constructed sections was recommended to evaluate long-term performance. It is hypothesized that lower production temperatures may increase mixture durability by reducing production aging of the mix. Benefits to contractors may include the allowance for increased hauling distances, reduced plant emissions, and cost savings due to reduced energy costs. Because of the experimental nature of this study, no cost savings data are yet available to justify or refute the use of WMA technologies.

Klaus (2003) described how asphalt flow improvers in the form of Fischer-Tropsch wax and Romontan wax have emerged successfully from an extensive program of laboratory testing and road trials to assess their suitability as modifiers for rolled asphalts and Guss asphalt. They produce flow improvement effects in hot asphalt mixes that enable mixing temperatures to be reduced by 20-40°C. Below the temperatures used in laying and compaction, these materials produce a stepwise increase in asphalt viscosity and stiffness. This results in a significant improvement in the stability (resistance to deformation) of the asphalt under operational conditions of high ambient temperatures and heavy traffic. The data presented by Klaus indicates low temperature properties are not adversely affected. It is hypothesized that the higher density achieved during compaction will greatly improve the performance of the asphalt over the intended service life. The use of flow improvers also showed promise as a co-modifier with polymer modified binders for German PMB 45 and PMB 25 grades due to significant improvements in mixture workability and compatibility between the polymer and asphalt. Based on current practice, the recommended concentration of these waxes is 3% by weight of the binder. Until the end of 2002, about 3 million square meters of asphalt pavements would be laid successfully in Germany.

CHAPTER 3 DATA COLLECTION

3.1 Introduction

Six separate data sets were generated to meet the objectives of the study, with four data sets related to achieving field and lab compaction, and two data sets for establishing long-term density and permeability criteria.

Compaction Data

1. Field cores to adjust nuclear density readings for data analysis.
2. Field density growth as roller passes are added while the temperature decreases and the mat densifies.
3. Field permeability immediately after field compaction is completed and the mat has cooled.
4. Lab loose mix compaction by controlling traditional field variables of pressure and temperature.

Density and Permeability Criteria Data

1. As-built construction data that include Job Mix Formulas, Running Average Calculation Sheets, Density Reports, and permeability test results.
2. Project referencing data that overlay construction project stationing across Reference Point / Sequence Number system.

3.2 Projects

During the summer 2007, field testing and loose-mix sampling occurred on 22 unique construction projects totaling 30 unique layers, as summarized in Table 3.1. On some projects, only a single layer was tested, while on others two or three layers were tested. Projects were selected based on ESAL series, paving schedule, and cooperation with field staff. Effort was made to collect data from E-3 and E-10 mixtures since compaction is more difficult than E-1 mixtures. One E-30 mixture was tested, USH 41 in Fond du Lac County.

Table 3.1 Projects for Field Compaction Testing

Layer (1)	Functional Class (2)	Highway Number (3)	County (4)	NMAS, mm (5)	Design ESALs (6)	Coarse Aggregate (7)	Binder PG Grade (8)	Base (9)
1	USH	8	Oneida	12.5	E-3	Gravel	58-28	Milled AC
2	USH	18	Iowa	12.5	E-3	Limestone	64-22	Pulverized AC
3	USH	18	Iowa	19	E-3	Limestone	64-22	Pulverized AC
4	USH	18	Milwaukee	12.5	E-3	Limestone	64-22	Milled AC
5	USH	18	Milwaukee	19	E-3	Limestone	64-22	Milled AC
6	STH	32	Racine	19	E-3	Limestone	64-22	CABC
7	STH	33	LaCrosse	19	E-1	Limestone	58-28	CABC
8	IH	39	Marquette	12.5	E-10	Gravel	58-28	Dowel PCC
9	IH	39	Portage	12.5	E-10	Gravel	58-28	Dowel PCC
10	USH	41	Fond du Lac	12.5	E-30	Limestone	64-22	Dowel PCC
11	STH	44	Fond du Lac	12.5	E-1	Limestone	58-28	Milled AC
12	USH	45	Langlade	12.5	E-3	Gravel	58-28	Milled AC
13	USH	53	Chippewa	12.5	E-10	Gravel	58-28	Rubb. PCC
14	USH	53	Chippewa	19	E-10	Gravel	58-28	Rubb. PCC
15	USH	53	Chippewa	25	E-10	Gravel	58-28	Rubb. PCC
16	USH	53	Trempealeau	12.5	E-3	Limestone	64-22	Pulverized AC
17	STH	32/57	Brown	12.5	E-3	Limestone	58-28	Milled AC
18	STH	59	Waukesha	19	E-3	Limestone	64-22	CABC
19	STH	60	Richland	12.5	E-1	Limestone	64-22	Pulverized AC
20	STH	60	Richland	19	E-1	Limestone	64-22	Pulverized AC
21	STH	60	Washington	12.5	E-10	Gravel	64-28	Milled AC
22	STH	60	Washington	19	E-10	Gravel	64-28	Milled AC
23	STH	67	Waukesha	19	E-1	Limestone	58-28	CABC
24	STH	70	Vilas	12.5	E-1	Gravel	58-28	Milled AC
25	STH	77	Ashland	12.5	E-1	Gravel	58-28	Milled AC
26	STH	96	Waupaca	12.5	E-3	Limestone	58-28	Pulverized AC
27	STH	153	Marathon	12.5	E-3	Gravel	58-28	Milled AC
28	STH	153	Marathon	19	E-3	Gravel	58-28	Milled AC
29	STH	181	Milwaukee	12.5	E-10	Limestone	64-22	CABC
30	STH	181	Milwaukee	19	E-10	Limestone	64-22	CABC

3.3 Density Testing

Twenty (20) test sites were randomly selected on each layer for field compaction testing. The reason for sampling 20 sites was to provide a balance with statistical requirements and available budget, while minimizing interference with construction operations. Then, five (5) of the 20 test sites were randomly selected for water and air permeability testing, and core sampling. Figure 3.1 illustrates permeability testing and nuclear density testing on the USH 41 project in Fond du Lac County.



Figure 3.1 Testing for Permeability and Density (USH 41 Fond du Lac County)

Nuclear readings of 15 seconds in duration were taken between roller passes since there was insufficient time to conduct a WisDOT standard 4-minute test. Effort was made to conduct a minimum of 2 readings after each roller pass, and in most cases this was possible. In a few cases, only a single 15-second reading was possible due to the roller reversing direction back across the test site. Multiple readings taken after each roller pass were averaged. During the final nuclear tests immediately prior to coring, a minimum of three 15-second readings were recorded and averaged. The 15-second readings produce more test error, however, with approximately 2,100 unique tests after the roller passes across 30 layers, the test error can be overcome by trends in the data.

Cores were tested at the UW-Madison lab using the Corelok device. Contractor G_{mm} values were collected to determine core density as percentage of theoretical maximum density. Initially, 5 cores were planned per project, however, the constraints of field testing under traffic and other factors reduced the sample number to as few as one. Cores were not sampled on STH

60 in Richland County due to equipment failure, and on STH 60 in Washington County from a decision by the WisDOT project staff to not allow coring in the surface layer.

Table 3.2 provides a comparison of core densities with the research nuclear density gauge readings (CPN Model MC-3, Serial #M391105379) across the 30 layers. The difference in average core densities and nuclear readings were used to adjust all nuclear readings for the data analysis. Relative to cores, the nuclear gauge ranged from 4.4% higher density on the STH 70 project, and 3.0% lower on the STH 33 project. On STH 70 for example, all original nuclear readings were reduced by 4.4% density. Comparison was made with the project QC or QV gauge; however, adjustments were only made to the cores.

Table 3.2 Core and Nuclear Reading Comparison

Functional Class (1)	Hwy Number (2)	County (3)	NMAS, mm (4)	Comparison Sites, n (5)	Core Density, % (6)	Nuclear Density, % (7)	Mean Diff., % (8)	Std. Dev., of Diff., % (9)
USH	8	Oneida	12.5	1	91.7	90.6	1.1	0.00
USH	18	Iowa	12.5	6	92.0	92.0	0.0	0.60
USH	18	Iowa	19	5	92.7	93.3	-0.6	0.63
USH	18	Milwaukee	12.5	5	90.6	91.2	-0.6	0.81
USH	18	Milwaukee	19	1	90.3	87.7	2.6	0.00
STH	32	Racine	19	5	91.5	91.8	-0.2	0.42
STH	33	LaCrosse	19	4	91.5	88.6	3.0	1.12
IH	39	Marquette	12.5	5	87.9	91.0	-3.1	0.54
IH	39	Portage	12.5	5	90.1	89.8	0.3	0.65
USH	41	Fond du Lac	12.5	5	91.5	91.7	-0.2	0.34
STH	44	Fond du Lac	12.5	4	90.8	91.3	-0.5	0.52
USH	45	Langlade	12.5	2	91.8	92.4	-0.6	0.47
USH	53	Chippewa	12.5	5	92.9	93.3	-0.3	1.21
USH	53	Chippewa	19	4	92.8	93.3	-0.4	1.68
USH	53	Chippewa	25	3	91.4	92.7	-1.3	1.70
USH	53	Trempealeau	12.5	5	91.9	91.8	0.1	0.81
STH	32/57	Brown	12.5	4	90.9	91.1	-0.2	0.27
STH	59	Waukesha	19	5	91.2	92.3	-1.1	0.66
STH	60	Richland	12.5	0	---	---	---	---
STH	60	Richland	19	4	92.8	92.6	0.2	0.68
STH	60	Washington	12.5	0	---	---	---	---
STH	60	Washington	19	5	91.9	94.1	-2.2	0.75
STH	67	Waukesha	19	5	94.0	95.7	-1.6	1.13
STH	70	Vilas	12.5	3	88.1	92.5	-4.4	0.88
STH	77	Ashland	12.5	2	89.7	92.4	-2.6	2.42
STH	96	Waupaca	12.5	5	91.3	91.2	0.1	0.49
STH	153	Marathon	12.5	3	93.1	91.8	1.3	0.09
STH	153	Marathon	19	2	93.4	91.9	1.5	0.43
STH	181	Milwaukee	12.5	5	90.1	92.0	-1.8	2.11
STH	181	Milwaukee	19	5	93.3	94.9	-1.7	0.65

3.4 Water and Air Permeability Testing

After the pavement cooled, water and air permeability testing occurred on five (5) of the 20 test site per layer. The reason for sampling only 5 sites was the limited time to perform testing under traffic and the available budget to test one layer per day.

The NCAT water permeameter was centered within the rectangular base used for nuclear density testing, sealant was applied to a rubber gasket between the pavement and permeameter base, and weights were added to prevent uplift force from the water head. The NCAT permeameter was filled and the drop in water height was recorded per unit time. Several trials were conducted at each test site for repeatability information and to average the test results. There were no leaks with the seal between the water permeameter and pavement, and all mixtures were fine graded. Figure 3.2 illustrates water and air permeability testing on STH 60 in Washington County.



Figure 3.2 Permeability Testing (STH 60 Washington County)

The ROMUS air permeameter was used to collect data for a comparative analysis with the water permeameter on each of the 30 layers. Air permeability testing was conducted after water permeability testing, with test locations offset 6 to 12 inches longitudinally to avoid the wet pavement surface. The ROMUS device is based on the falling-head air permeameter principle with one noted exception: a vacuum chamber is used to draw air through the pavement as opposed to a pressurized chamber forcing air into the pavement (Schmitt et al. 2007). While fundamentally consistent with air flow measures of earlier devices, the vacuum chamber also serves to enhance the seal between the device and the pavement surface. This is in contrast to a

pressurized water permeameter chamber which must be ballasted to remain in contact with the pavement surface.

The main components of the ROMUS air permeameter include a hand-operated grease gun, base seal reservoir, vacuum chamber, automatic vacuum pump and valve, digital pressure gauge, and digital display. To initiate testing, the bottom of the ROMUS device is first sealed to the pavement surface by way of a grease seal. The sealant grease is manually pumped through the device or blotted into a recessed base ring which was sized to replicate the opening of the NCAT water permeameter.

Once the device has been sealed to the pavement surface, pressing of the start button initiates a fully automated system that first creates a vacuum within the internal pressure chamber. When the vacuum pressure reaches a value of approximately 25 inches of water (47mm Hg), effectively simulating the maximum head of water used with the NCAT device, a valve automatically opens to allow air to be drawn through the pavement layer into the vacuum chamber. For this research project, the ROMUS device was programmed to record a single timing increment, to the nearest millisecond, representing a change in vacuum pressure equivalent to 8 inches of water. This set-up simulates a falling head water permeability test with a head drop from 20 to 12 inches of water. Once the test is complete, the timing increment is displayed on a digital display for manual recordation.

3.5 Field Compaction Experimental Design

There are an abundance of variables that affect the ability to achieve density on a given project. Many contractors and owners rely on past experience to manage those variables affecting field compaction, such as layer thickness with difficulty orienting larger coarse aggregate, lab air voids where lower values usually yield higher density, asphalt content where higher concentration usually yields higher density, amount of fine aggregate, angularity of fine aggregate, gyration design values, etc. Because of so many variables, a roller test pattern is established on a project-by-project basis by trial and error. However, the pattern becomes quickly outdated when the variables change, many simultaneously. The conditions on the given day when establishing a roller pattern can partially change later in the day, and/or on the following days. The most straight-forward corrective action is to re-establish a new rolling pattern. Table 3.3 highlights some of the changes that can occur within a few project stations, or among paving days.

Table 3.3 Sample of Variable Changes during Field Compaction

Variable (1)	Sample of Potential Changes (2)
Material Properties	<ul style="list-style-type: none"> • Asphalt content% and viscosity • Air voids • Gradation, relative ratio of coarse to fine. • FAA
Layer Thickness	<ul style="list-style-type: none"> • Can change randomly throughout the paving day • Uneven base profile when paving first layer. • Wedging for slope correction • Wedging for superelevation correction • Horizontal curve runout • Pavement structures – manholes, valve shutoffs, etc. • Any miscellaneous screed setting corrections, yield changes, etc. • Matching centerline joint – possibility of straddling fresh mat • Joint type – Michigan or vertical
NMAS	<ul style="list-style-type: none"> • 19mm lower layer and 12.5mm surface layer • Thickness-to-NMAS ratio
Base Type	<ul style="list-style-type: none"> • PCC and associated k-value • Rubblized PCC • Milled or Pulverized HMA • CABC • Any combination of the above within a few stations • Soil Support Value
Mat Temperature	<ul style="list-style-type: none"> • 275, 223, 211, 188, 151 °F, etc. • Varying by 20 °F just a few feet between test sites • Ambient air temperature • Wind speed
Roller Type	<ul style="list-style-type: none"> • Breakdown - vibratory on or off, width, contact pressure • Pneumatic – tire width, inflation pressure, contact pressure • Finish – vibratory on or off, width, contact pressure • Weight of steel rollers changing with water reduction • Vibratory setting, amplitude, frequency, oscillation vs vertical • Mat overlap with tandem breakdown rollers
Roller Operator	<ul style="list-style-type: none"> • Speed variability • Pass overlap • Preferred number of passes • Adjoining traffic and ability to compact centerline joint • V-pattern to change direction

The list in this table is not comprehensive as there are many other variables that can be added, along with changes in their individual characteristics. It is hoped that research in intelligent compaction will capture many of these variables and measure their relative effect on achieving density. Since the ability to accurately measure all variables can be a daunting task, focus was placed upon those variables that can be measured and managed during a typical paving operation in alignment with the study objectives.

A new approach was investigated by creating and testing a key variable that measures the relative increase in density during roller compaction. Previous studies have used the traditional density value in their investigations, such as 92.7%, 92.1%, etc., however, this new approach

assesses the relative densification growth under repeated roller passes as the pavement cools. This variable, named “Density Delta”, measures the relative increase in density between successive roller passes, as shown by Equation 3.1.

$$\text{Density Delta} = \text{Density Roller Pass}_j - \text{Density Roller Pass}_i \quad (3.1)$$

Where,

Density Roller Pass_j = Density after Roller Pass j, %;

Density Roller Pass_i = Density after Roller Pass i, %;

i < j; and

i and j are integer values.

Density Delta is a random variable that responds to independent variables presented in Table 3.3, as well as others that have not been defined or measured. It is treated as a dependent variable, and simply reacts to forces and characteristics of the HMA and paving operation, along with their interactive effects. The goal is to receive as much “Density Delta” as possible from the field effort, so that specified density thresholds are met, such as 91.0%, 91.5% or 92.0%. The goal of the contractor is to maximize Density Delta so that the requisite density is met, while minimizing the input effort and resources. There is considerable effort and money resources spent compacting the pavement, such as \$80 to \$90/hr for a typical roller plus operator. This unit cost multiplied by the number of hours spent compacting (and associated job overhead, traffic control, supervision, etc.) can lead to a real cost around \$5/ton for the paving train (minus trucks). It is equally the goal of the owner to have the contractor achieve density, so that a durable, long-lasting pavement is constructed. In addition, rapid construction reduces risk levels of accidents and impediments to the traveling public.

Table 3.4 presents the variables measured during the field portion of the study and supporting notes. Based on an evaluation of the data enumerated in this table, only certain data were retained for the analysis. Those data are described in Table 3.5, along with rationale for retaining or removing the variable from the analysis.

Table 3.4 Variables Measured during Field Compaction of 30 Layers

Variable (1)	Sample Data (2)	Notes (3)
PG	58, 64	Three PG grades were identified: 58-28, 64-22, and 64-28
Gyration	60, 75, 100	E-1, E-3, and E-10 mixes were tested, along with a single E-30 mix on USH-41, so gyrations ranged from 60 to 100.
Thickness	73mm, 66mm, etc.	Layer thickness was recorded from cores and averaged.
NMAS	12.5mm, 19mm	Only two stone sizes were encountered.
ThkNMAS	3.1, 4.3, 4.8	Computed from the ratio of layer thickness and NMAS.
Mix Properties	Air Voids, VMA, VFA, gradation, etc.	It was not possible to assign the specific mix test properties to the tested layer segment, due to the uncertainty of the truck/mix sample location with respect to the field test site locations. This data is currently being collected from WisDOT Regional Offices and incomplete for analysis.
Source	Granite, Limestone	Two coarse aggregate sources were encountered; No granite sources tested.
Base	Rigid, Flexible	Rigid included undisturbed PCC panels and rubblized PCC; Flexible included milled, pulverized, CABC, and previously paved HMA layers.
Sites	10, 20	There were 20 randomly selected test sites per layer, with 15-second nuclear readings taken after each or every other roller pass. Multiple readings were averaged. Time constraints limited testing on STH 153 Stratford to 10 sites per layer.
Temperature	278, 222, 174, 135 F	Readings were recorded from behind the screed until completion of finish rolling with a heat gun. The contractor's heat gun readings and research heat gun readings were always within 5F.
Passes	2, 4, 3, 1	A grouping of passes between nuclear density tests. In most cases, readings were collected after 2 passes across a test site.
TotalPasses	2, 5, 8, 11, 14, 16	Total number of cumulative passes applied a specific test site. This measure provides an indication of relative energy applied to a given location on the pavement.
Roller	Breakdown, Pneumatic, Finish	All projects had both a breakdown and finish roller. About half of the projects had a pneumatic roller (generally higher ESAL pavements, such as E-3 and E-10).
Vibratory	On or Off	Only measured with steel drum rollers – breakdown and finish.
Density	89.1%, 92%	Random dependent variable in response to several input variables, such as roller type, temp, material properties, etc.
DensDelta	2.3% (92.4% minus 90.1%)	Density Delta. Can also be referred to as density growth. Random variable that responds to independent variables.
Dens96	4.2% (96.0% minus 91.6%)	Difference between actual density after successive roller passes and 96% Gmm. This measure provides a relative degree of compaction to an upper threshold of 96% Gmm. The goal when designing an asphalt mixture is to achieve 96% Gmm during the service life, where the addition of as-built density and traffic loading are estimated to achieve the target 96% Gmm. A value of 4% air voids during the service life is thought to produce a long-lasting, durable pavement.

Table 3.5 Variables Analyzed for Field Compaction

Variable (1)	Retained for Analysis (2)	Rationale or Research Question (3)
PG	Yes	Understand the effect of asphalt grade on densification, leading to experimental design for Warm Mix research.
Temp	Yes	How does mat temperature affect densification?
Passes	Yes	What is effect of a group of passes on density growth?
TotalPasses	Yes	What is effect of total passes applied to a given test site?
Roller	Yes	What is relative effect of Breakdown, Pneumatic, and Finish rollers?
Vib	Yes	What is effect of vibratory setting (on or off) on densification?
DensDelta	Yes	Key dependent variable in this research.
Dens96	Yes	What is ability to densify the pavement as it approaches 96% of the Gmm value? Anecdotally speaking, it should be more difficult to increase density as this value is approached.
<i>Gyration</i>	<i>No</i>	Cannot be controlled on a typical project.
<i>Thick</i>	<i>No</i>	This would have reduced the allowable data for analysis by about 75% since only 5 cores were sampled from 20 test sites. The average core thickness could be averaged for a layer, but applying one value to the layer during analysis would have confounded whether the thickness had an effect, or whether the project as a whole had an effect. Thus, it was removed.
<i>NMAS</i>	<i>No</i>	This variable cannot be controlled for a given layer on a given day.
<i>ThkNMAS</i>	<i>No</i>	This variable can be controlled for a given layer on a given day; however, is generally constant based on structural layer design, job mix formulas, specifications, yield limits, etc.
<i>Mix Properties</i>	<i>No</i>	It was not possible to assign the specific mix test properties (3 to 4 per day) to the tested layer segment, since properties change within a day's production.
<i>Source</i>	<i>No</i>	This variable is seldom changed on a project.
<i>Base</i>	<i>No</i>	On several projects the base changed within a project.
<i>Sites</i>	<i>No</i>	Sites were randomly located, so no assignment of this variable.
<i>Density</i>	<i>No</i>	Important measure, but Delta Density chosen as dependent variable in this study. Also, the difference between actual density and 96% Gmm is measured as an alternative measure, and having both actual Density and difference with 96% of Gmm would have created a 100% collinear relationship and invalidated the statistical models.

A sample of the data used during analysis are illustrated Figure 3.3. This figure helps understand how the data were managed, namely the Delta Density (designated ‘densdelta’ for programming code) and density difference from 96% Gmm (‘dens96’). ‘Pass’ is a group of passes between nuclear density tests, ‘Roller’ is an indicator for roller type (0=paver; 1=breakdown steel drum; 2=pneumatic; 3=finish steel drum), ‘Vib’ is vibratory setting (0=off; 1=on).

Project	PG	Gyrations	Site	Temp	Pass	TotalPass	Roller	Vib	Density	DensDelta	Dens96
8	58	75	1	275	0	0	0	0	81.1	.	.
8	58	75	1	256	2	2	2	1	90.5	9.4	5.5
8	58	75	1	134	2	4	4	3	91.3	0.8	4.7
8	58	75	2	275	0	0	0	0	81.1	.	.
8	58	75	2	247	2	2	2	1	90.8	9.7	5.3
8	58	75	2	137	2	4	4	3	91.4	0.6	4.6
8	58	75	3	275	0	0	0	0	81.1	.	.
8	58	75	3	255	2	2	2	1	90.6	9.5	5.4
8	58	75	3	137	2	4	4	3	90.2	-0.4	5.8
8	58	75	4	275	0	0	0	0	81.1	.	.
8	58	75	4	253	2	2	2	1	92.2	11.1	3.8
8	58	75	4	137	2	4	4	3	92.5	0.3	3.5
8	58	75	5	275	0	0	0	0	81.1	.	.
8	58	75	5	260	2	2	2	1	89.7	8.6	6.3
8	58	75	5	131	1	3	3	3	90.7	1.0	5.3
8	58	75	5	130	1	4	4	3	90.9	0.2	5.1

Figure 3.3 Sample Data for Field Compaction Analysis

3.6 Lab Compaction Experimental Design

A total of 20 layers of loose mix were compacted at the UW-Madison Lab. Because of time and budget constraints, it was not possible to test all 30 layers in the lab. By ESAL series, 4 layers tested were E-1, and 8 layers each were tested for E-3 and E-10. Table 3.6 provides the layers and associated attributes.

A factorial design was used to understand attributes in lab compaction. Initially, only E-3 and E-10 samples were considered for the analysis; however, E-1 samples were added for future Warm Mix Asphalt research. This created 3 levels, as opposed to 2 levels, for total number of design gyrations. Each of the loose mix samples were tested at three temperatures: 120°C, 90°C, and 60°C (248°F, 194°F, and 140°F); two pressures, 600 kPa and 300 kPa. During the analysis, temperatures were analyzed in °F to normalize with field compaction data. Binder viscosity data were not readily available, so high-temperature PG ratings were used as a surrogate measure for viscosity. Table 3.7 provides the levels of each variable for analysis of lab compaction data.

Table 3.6 Lab Compaction Layers

Layer Number (1)	Project Name (2)	Project I.D. (3)	County (4)	Design ESALs (5)	Coarse Aggregate (6)	NMAS, mm (7)	Binder Grade (8)
1	USH 8	1590-12-60	Oneida	E-3	Gravel	12.5	58-28
5	USH 18	2200-10-70	Milwaukee	E-3	Limestone	19	64-22
6	STH 32	3240-05-71	Racine	E-3	Limestone	19	64-22
7	STH 33	5121-09-71	LaCrosse	E-1	Limestone	19	58-28
8	IH 39	1166-04-80	Marquette	E-10	Gravel	12.5	58-28
9	IH 39	1166-04-76	Portage	E-10	Gravel	12.5	58-28
10	USH 41	2120-06-71	Fond du Lac	E-30	Limestone	12.5	64-22
11	STH 44	6090-00-70	Fond du Lac	E-1	Limestone	12.5	58-28
12	USH 45	9847-03-60	Langlade	E-3	Gravel	12.5	58-28
13	USH 53	1191-09-74	Chippewa	E-10	Gravel	12.5	58-28
14	USH 53	1191-09-74	Chippewa	E-10	Gravel	19	58-28
15	USH 53	1191-09-74	Chippewa	E-10	Gravel	25	58-28
18	STH 59	2230-01-70	Waukesha	E-3	Limestone	19	64-22
19	STH 60	5190-06-71	Richland	E-1	Limestone	12.5	58-28
21	STH 60	2310-02-60	Washington	E-10	Gravel	12.5	64-22
25	STH 77	9260-03-71	Ashland	E-1	Gravel	12.5	58-28
26	STH 96	1510-01-73	Waupaca	E-3	Limestone	12.5	58-28
27	STH 153	6370-01-60	Marathon	E-3	Gravel	12.5	58-28
28	STH 153	6370-01-60	Marathon	E-3	Gravel	19	58-28
30	STH 181	2140-08-71	Milwaukee	E-10	Limestone	19	64-22

Table 3.7 Lab Compaction Variables and Levels

Variable Name (1)	Variable Levels (2)
Binder Performance Grade, High Temperature °C	58, 64
NMAS, mm	12.5, 19, 25
Coarse Aggregate Source	1=Gravel, 2=Limestone
Gyrations to Ndes	60, 75, 100
Gyratory Pressure, kPa	300, 600
Compaction Temperature, °F (°F used for field)	140, 194, 248

3.7 Density and Permeability Criteria

During Phase I of this research (Schmitt et al. 2007), it was shown that pavements with higher as-built densities tend to exhibit better performance as measured by the change in PDI per year. Higher as-built densities result in less permeable pavements, and water permeability increases in a non-linear fashion with increasing pavement deterioration. However, based on limited data, it was not possible to establish definitive criteria for permeability and density.

A work plan was proposed for Phase II research, included as a component of this project, to produce performance models that will establish specific criteria. The Phase I report recommended that a long-term study be conducted for a period of at least 5 years. As-built construction data were to be collected on projects throughout the state having varying density requirements, then performance data are collected and monitored every other year until the pavement reaches 4-5 years of age.

This project created the data set, as described in Chapter 7, where a single database system modeled after the Meta-Manager system will model pavement performance. It consists of individual data sets for 29 construction projects paved in 2007. Air and water permeability were measured on the surface layer of 15 of the construction projects, where initial air and water permeability will begin. A stand-alone spreadsheet file is included with this report to be used in performance modeling after several years from the 2007 construction season.

Chapter 4 Field Compaction Data Analysis

4.1 Statistical Modeling Approach

Several statistical methods were used during this analysis, with Density Delta the dependent variable. Traditional statistical tests were used as well, and the reader is encouraged to consult statistical textbooks for descriptions.

Two primary modeling methods were used to explore the key relationship between achieving gains in density with numerous project variables. The first method was traditional multiple regression (REG) models, using both forward selection and backward elimination techniques to test variables in the trial models. A p-value cutoff of 0.10 was specified since the “noise” in construction data and nuclear density testing error may inadvertently drop a marginally significant variable when the p-value is just beyond a traditional 0.05 cutoff value.

The second modeling method was generalized linear models (GLM). The key distinction between these approaches is that the GLM procedure first finds the mean of the data, then the function; while the REG procedure first finds the function, then the mean. During the analysis, the advantages of using GLM were realized. The key objective was to understand what variables provide an increase in the mean Delta Density, and the GLM output naturally provides this mean in the function. In addition, the GLM procedure has the ability to test the significance of a variable when entered last into the model using Type III Sum of Squares, while regression computes the Sum of Squares in the specified model order using Type II SS. Both methods were used at the start of the analysis, then only GLM during the latter portion of the analysis.

4.2 Project-by-Project Regression

Multiple regression models were computed for each of the 30 layers, with model coefficients provided in Table 4.1. All model coefficients retained were significant at the 0.10 level. The R-squared value and Cp statistic are also reported. A high R-squared value indicates the ability to assign variability to the model parameters, while the Cp is an indicator of model misspecification. When the Cp is much larger than the number of model parameters, it is usually a good indicator of model underspecification. It is recommended that a model be selected having Cp less than the number of model parameters, even though the parameters meet a significance level of 0.10, 0.05, or less.

Table 4.1 Project-by-Project Multiple Regression Models

Layer #	Project Name	County	Model Selection	NMAS, mm	n	Intercept	Temp	Total Passes	Roller	Vib	Dens96	Rsquare	Cp
(1)	(2)	(3)	(4)	(5)	(6)	(7)	(8)	(9)	(10)	(11)	(12)	(14)	(15)
1	USH 8	Oneida	Both	12.5	47	-10.474	0.047		1.580	6.700		92.5	3.27
2	USH 18	Iowa	Both	12.5	77	-23.642	0.147			3.020		75.9	4.88
3	USH 18	Iowa	Both	19	80	-32.363	0.166	-0.344	4.301	2.026	-0.602	86.5	6.00
4	USH 18	Milwaukee	BW	12.5	69	2.053	0.051	-0.863			-0.666	60.8	2.17
	USH 18	Milwaukee	FW	12.5	69	-8.439	0.065					53.7	9.68
5	USH 18	Milwaukee	SAME	19	103	-13.262	0.069		1.086	1.449		47.4	5.55
6	STH 32	Racine	SAME	19	78	-8.359	0.061					50.9	1.06
7	STH 33	LaCrosse	back	19	65	-9.981	0.078	-0.697	1.553			50.0	4.43
	STH 33	LaCrosse	forward	19	65	-6.456	0.062					44.6	7.14
8	IH 39	Marquette	Both	12.5	91	-13.978	0.095		0.687			65.0	0.65
9	IH 39	Portage	Both	12.5	78	-7.680	0.059					73.7	0.93
10	USH 41	Fond du Lac	Both	12.5	72	5.907		-0.715		3.017	-0.425	73.8	2.49
11	STH 44	Fond du Lac	Both	12.5	46	12.813	0.038	-1.481	-1.610	-2.098	-0.759	91.4	6.00
12	USH 45	Langlade	Both	12.5	41	-7.464	0.093				-0.628	93.8	3.04
13	USH 53	Chippewa	Both	12.5	69	14.406		-0.832	-3.441	4.111	-0.592	92.5	4.08
14	USH 53	Chippewa	Both	19	86	-3.343	0.041		-1.732	2.868		68.1	4.49
15	USH 53	Chippewa	Both	25	75	-0.833	0.039	-0.663		1.669	-0.278	61.6	6.09
16	USH 53	Trempealeau	Both	12.5	83	-23.318	0.106	-0.767	4.420	2.734	-0.261	56.7	6.00
17	STH	Brown	Both	12.5	101	-10.185	0.063	-0.241	1.197	1.069		69.9	4.49
18	STH 59	Waukesha	Both	19	62	1.894	0.051	-1.907	1.382		-0.520	61.6	4.13
19	STH 60	Richland	Both	12.5	65	-32.626	0.141		3.709	5.266		68.0	6.31
20	STH 60	Richland	Both	19	57	-44.698	0.237	-1.824	6.587		-1.159	77.3	5.00
21	STH 60	Washington	Both	12.5	89	-17.711	0.116	-0.193	1.592	1.128	-0.671	81.6	6.00
22	STH 60	Washington	Both	19	89	-7.968	0.059					54.9	0.20
23	STH 67	Waukesha	Both	19	101	-4.623	0.046		-0.758			39.7	4.75
24	STH 70	Vilas	Both	12.5	69	0.796	0.066		-2.945			82.0	2.03
25	STH 77	Ashland	Both	12.5	55	-7.027	0.059	-1.075	3.469	6.108	-0.967	81.4	6.00
26	STH 96	Waupaca	Both	12.5	56	-23.044	0.142	-1.759	5.571		-1.055	90.5	5.00
27	STH 153	Marathon	Both	12.5	28	4.954	0.049	0.709	-4.023		-0.695	96.6	4.05
28	STH 153	Marathon	Both	19	26	30.707	-0.051	-1.004	-5.494		-0.978	97.2	4.00
29	STH 181	Milwaukee	Both	12.5	69	-3.212	0.061	-0.574			-0.478	63.1	5.59
30	STH 181	Milwaukee	Both	19	103	-12.343	0.113				-0.839	75.9	4.70

Bold indicates PG64 asphalt binder

Both indicates both Forward Selection and Backward Elimination selected the same model

BW = Backward Elimination model

FW = Forward Selection model

Models from each project provide valuable insight for those factors thought to influence increases in density. First, the positive temperature coefficients in Column 8 indicate that higher temperatures yield greater increases in density. Secondly, total passes has a negative coefficient, indicating that the ability to achieve more density diminishes as the number of passes is added. Another interesting finding is that a third of the projects did not successfully model total passes. Roller type (1=Breakdown, 2=Pneumatic, 3=Finish) have a computed blend of positive and

negative coefficients, suggesting inconsistency in density gains by roller type on a given project. Vibratory setting (0=OFF, 1=ON) have positive coefficients, indicating that an ON setting yields greater Density Delta. As the density approaches 96% Gmm, the density gain decreases, depicted by the negative coefficient. Finally, the R-Squared values are fairly high, with several layers having 90% values. However, Cp statistics suggest that the models may be misspecified since many are at or above the number of model parameters. No diagnostic checks were performed on the models to validate their accuracy; they simply provide a representation of potential factors and their relative effects.

Based on the models above, the following preliminary conclusions can be reached:

- Higher temperatures yield greater increases in density.
- Roller type has an inconsistent effect across a range of projects.
- Vibratory ON setting yields greater density increases.
- As the density approaches 96% Gmm, the density gain decreases.
- No discernible trend could be found for PG grade

4.3 GLM Full Model

The next phase of analysis involves GLM, where the mean density gain is calculated, then Sum of Squares assigned to the variables to explain variation in the mean. As discussed earlier, Type III SS were used to determine significance. All layers were placed in the model to strengthen the analysis. Indicator variables were created for PG grade (58 or 64), Roller (1,2, or 3), and vibratory (ON or OFF). Figure 4.1 provides the GLM output for 2,125 tests.

Source	DF	Sum of Squares	Mean Square	F Value	Pr > F
Model	8	18953.92528	2369.24066	407.80	<.0001
Error	2116	12293.70482	5.80988		
Corrected Total	2124	31247.63010			
R-Square	Coeff Var	Root MSE	densdelta Mean		
0.606572	75.71150	2.410369	3.183624		
Source	DF	Type III SS	Mean Square	F Value	Pr > F
pg	1	81.148462	81.148462	13.97	0.0002
roller	2	822.546597	411.273298	70.79	<.0001
vib	1	152.231060	152.231060	26.20	<.0001
temp	1	2347.334350	2347.334350	404.02	<.0001
passes	1	1138.305670	1138.305670	195.93	<.0001
totalpasses	1	917.943837	917.943837	158.00	<.0001
dens96	1	232.966723	232.966723	40.10	<.0001

Figure 4.1 GLM Output for Full Model

The interesting finding is that all variables were significant in explaining a portion of the density change. Temperature and number of passes accumulated the greatest sum of squares. The model R-square = 60.6%, leaving 40% of the variability unexplained (from testing error, lab air voids, AC%, base rigidity, etc.).

The average density gain was 3.2% density, however, this is not representative of successive roller passes. The growth from screed to the first pass of the breakdown roller was about 8% (for

example, 80% after the screed then to 88% after 2 passes). When all tests are taken into account, including latter breakdown rolling, intermediate rubber-tired rolling, and finish rollers, the average was computed at 3.2%.

The greatest factors affecting density gain in order, as measured by the Type III SS, were mat temperature, number of passes, roller type (breakdown, rubber-tired, and finish), density approaching 96% Gmm, vibratory setting, and PG grade.

Interactions were then investigated. Three-way and larger interactions are difficult to interpret, so only the 2-way interactions were included in the model. Figure 4.2 provides the output. Insignificant interactions are italicized to offset from those that are significant. Dens96 main effect is insignificant, but is retained since the interactions are significant.

Source	DF	Sum of Squares	Mean Square	F Value	Pr > F
Model	35	26104.63025	745.84658	302.95	<.0001
Error	2089	5142.99985	2.46194		
Corrected Total	2124	31247.63010			
R-Square	0.835412	Coeff Var 49.28529	Root MSE 1.569058	densdelta Mean 3.183624	
Source	DF	Type III SS	Mean Square	F Value	Pr > F
pg	1	13.4112126	13.4112126	5.45	0.0197
roller	2	120.0494735	60.0247367	24.38	<.0001
pg*roller	2	27.1895488	13.5947744	5.52	0.0041
vib	1	7.2652358	7.2652358	2.95	0.0860
<i>pg*vib</i>	1	<i>5.2392802</i>	<i>5.2392802</i>	<i>2.13</i>	<i>0.1448</i>
<i>roller*vib</i>	2	<i>10.2213789</i>	<i>5.1106895</i>	<i>2.08</i>	<i>0.1257</i>
temp	1	127.8608258	127.8608258	51.93	<.0001
temp*pg	1	39.4057922	39.4057922	16.01	<.0001
temp*roller	2	17.9055302	8.9527651	3.64	0.0265
<i>temp*vib</i>	1	<i>4.9748363</i>	<i>4.9748363</i>	<i>2.02</i>	<i>0.1553</i>
passes	1	32.3647214	32.3647214	13.15	0.0003
passes*pg	1	7.2601587	7.2601587	2.95	0.0861
passes*roller	2	380.6719757	190.3359879	77.31	<.0001
<i>passes*vib</i>	1	<i>3.3099040</i>	<i>3.3099040</i>	<i>1.34</i>	<i>0.2464</i>
temp*passes	1	185.3055978	185.3055978	75.27	<.0001
totalpasses	1	444.6241385	444.6241385	180.60	<.0001
totalpasses*pg	1	15.9233319	15.9233319	6.47	0.0111
totalpasses*roller	2	771.6062200	385.8031100	156.71	<.0001
<i>totalpasses*vib</i>	1	<i>1.6079617</i>	<i>1.6079617</i>	<i>0.65</i>	<i>0.4191</i>
temp*totalpasses	1	735.0260667	735.0260667	298.56	<.0001
passes*totalpasses	1	11.8518588	11.8518588	4.81	0.0283
dens96	1	2.7640680	2.7640680	1.12	0.2895
dens96*pg	1	8.9914674	8.9914674	3.65	0.0561
dens96*roller	2	151.9147797	75.9573899	30.85	<.0001
<i>dens96*vib</i>	1	<i>0.2759935</i>	<i>0.2759935</i>	<i>0.11</i>	<i>0.7378</i>
temp*dens96	1	8.0521375	8.0521375	3.27	0.0707
passes*dens96	1	6.8580093	6.8580093	2.79	0.0953
totalpasses*dens96	1	121.5884229	121.5884229	49.39	<.0001

Figure 4.2 GLM Output for Full Model including 2-way Interactions

Aside from the main effects identified earlier, several interactions collected a relatively high sum of squares. Passes*Roller and Totalpasses*Roller were most likely significant since the finish roller records a higher number of cumulative passes. Totalpasses*Temperature indicates that as total passes increases, temperature decreases. From the top of the model list, there is a relationship between PG and roller type (this will be investigated later on a roller-by-

roller basis). Temp*PG is difficult to interpret, as measured binder viscosity from the projects was not available. Dens96*Roller would be the breakdown roller compacting at levels further from 96% Gmm, and the finish roller compacting at levels closer to 96% Gmm. Totalpasses*Dens96 is simply a total cumulative number of passes are recorded as the density approaches 96% Gmm.

To help further understand the main effects and interactions, plots were prepared in Figures 4.3 through 4.8, and mean differences were tested in Figure 4.9 through 4.11.

The test of mean differences in Figures 4.9 through 4.11 used least squares means, or what are called adjusted means. They are different than the pure arithmetic mean found at the top of the output. The least squares mean test compares the means of the subsets, and in this application, the means of the independent variables.

Based on the GLM output, plots, and tests for mean differences, the following were observed:

- Breakdown roller had the greatest density increases (Figures 4.3 and 4.4), however, the test of least squares means (Figure 4.9) found no statistical difference at the 5% level with the pneumatic roller. This is because, on average, the breakdown had an increase of approximately 6% per measurable pass, but the standard deviation was equally high at 4%. This was caused from high initial compaction on the first passes, and less on the subsequent passes. The pneumatic roller had a much smaller mean increase of 1%, but the standard deviation was also much smaller at 1%, indicating more consistent growth. Thus, when considering the covariate of the mean for the breakdown and pneumatic rollers, no mean difference was detected.
- Negative values for Delta Density in the figures was the result of testing error with the nuclear gauge, or the reduction in density from displacement during final rolling (or a combination of both).
- Temperature has an effect on density with the greatest density gains made above 170°F with the breakdown roller. Density gains are possible with temperatures as low as 120°F, but there was negative scatter as well (from testing error and/or shoving).

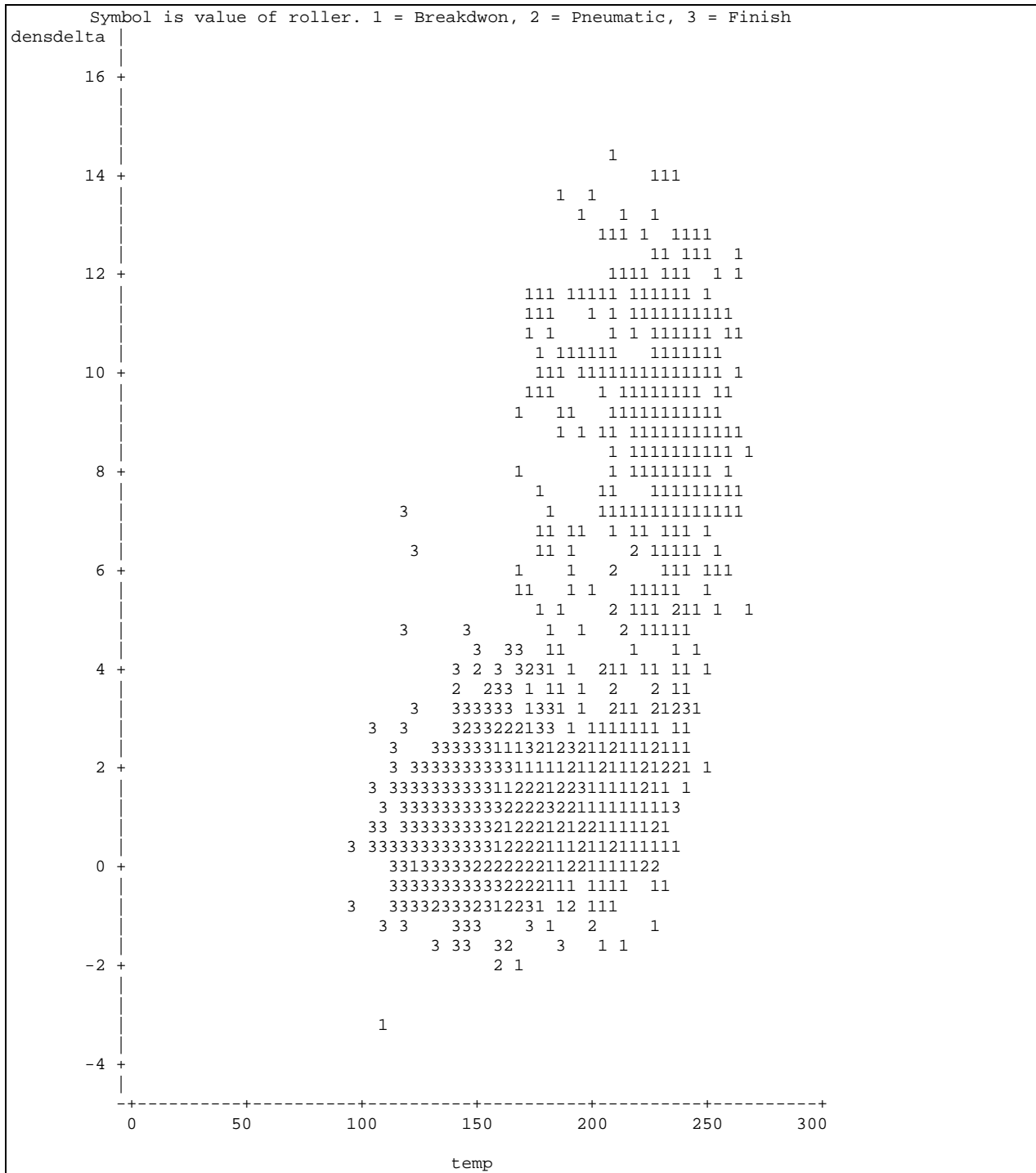


Figure 4.3 Delta Density and Temperature by Roller Type

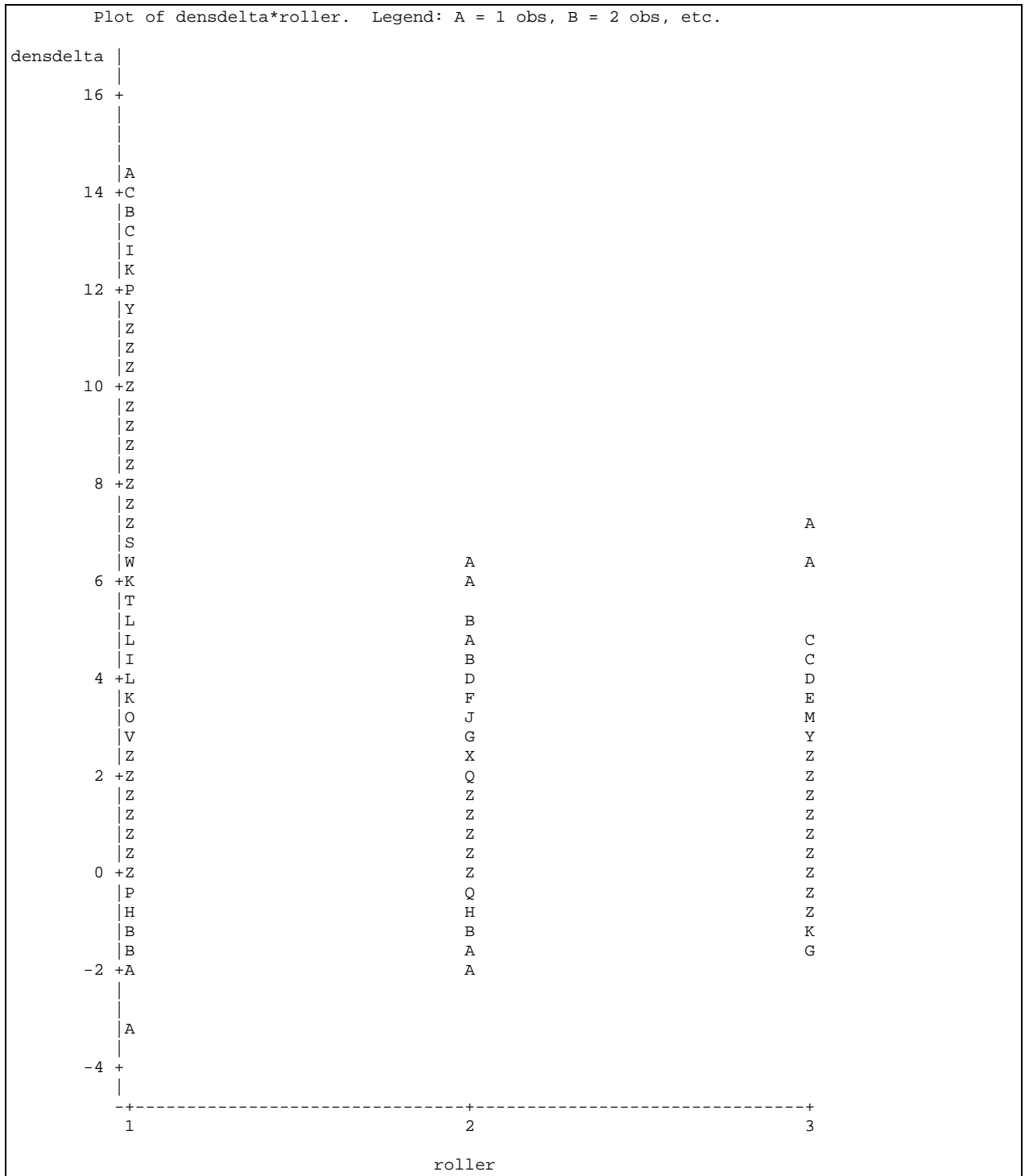


Figure 4.4 Delta Density and Roller Type

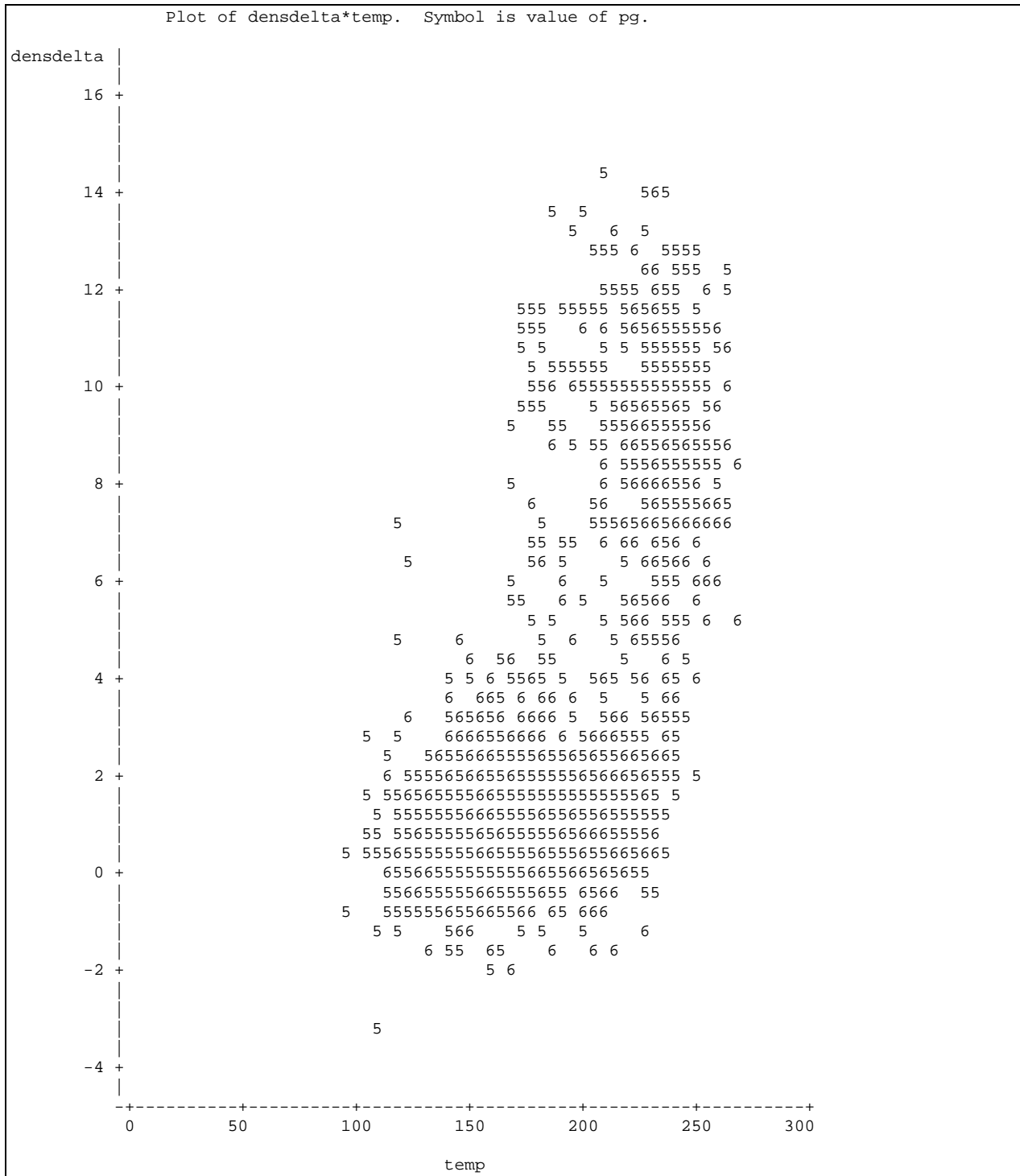


Figure 4.5 Delta Density and Temperature by PG Grade

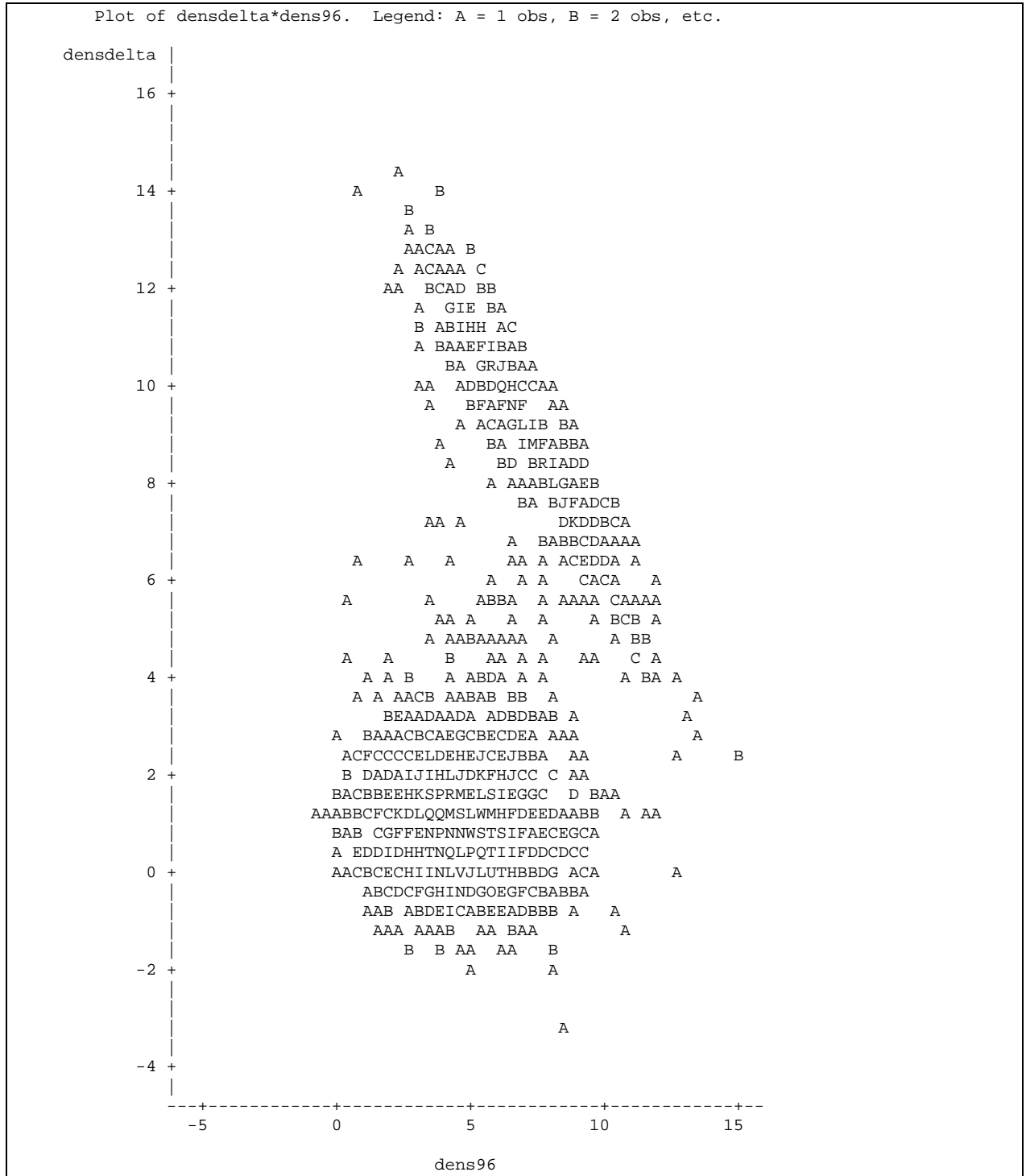


Figure 4.6 Delta Density and range to 96% Gmm

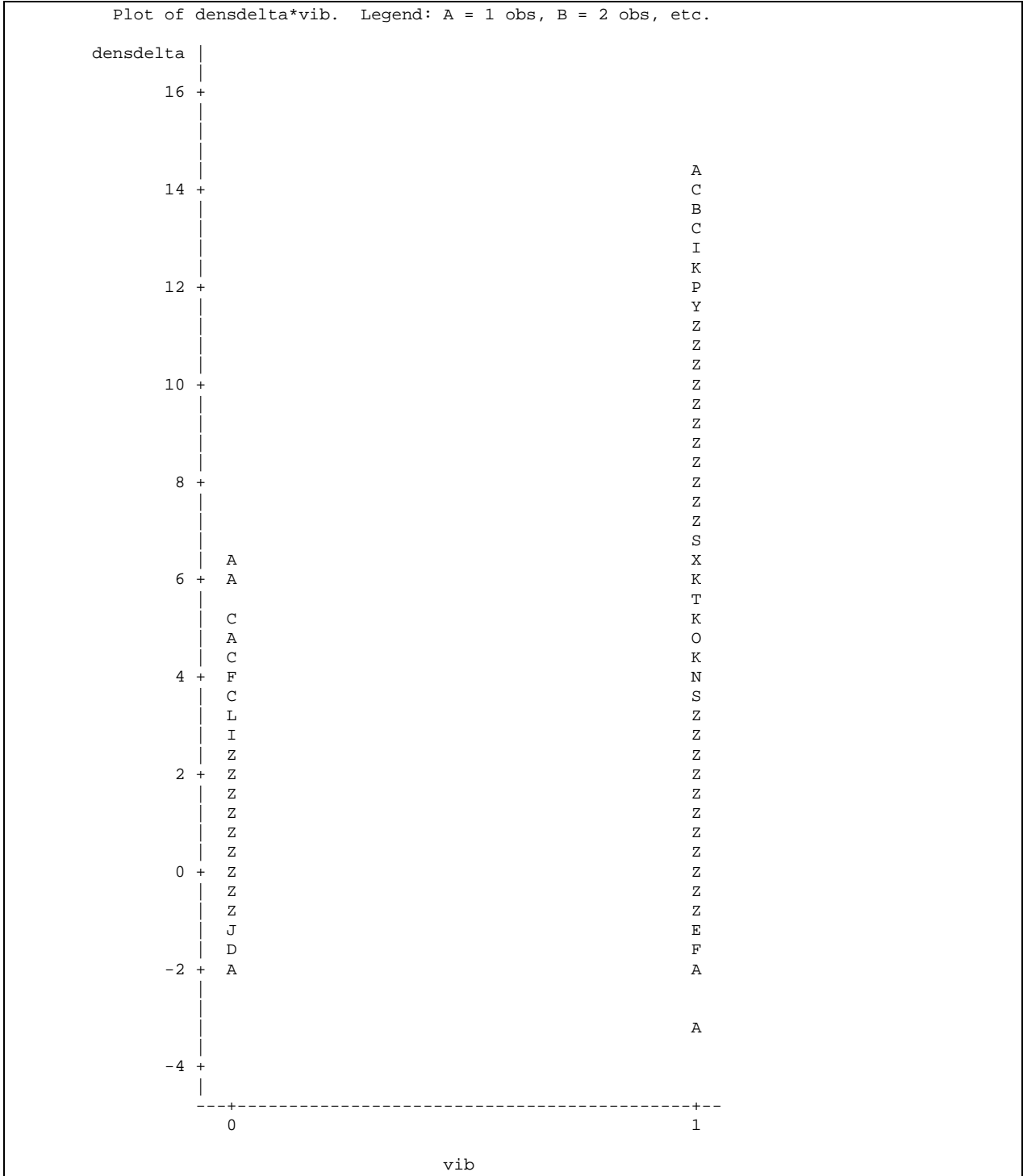


Figure 4.7 Delta Density and Vibratory Setting (0=Off, 1=On)

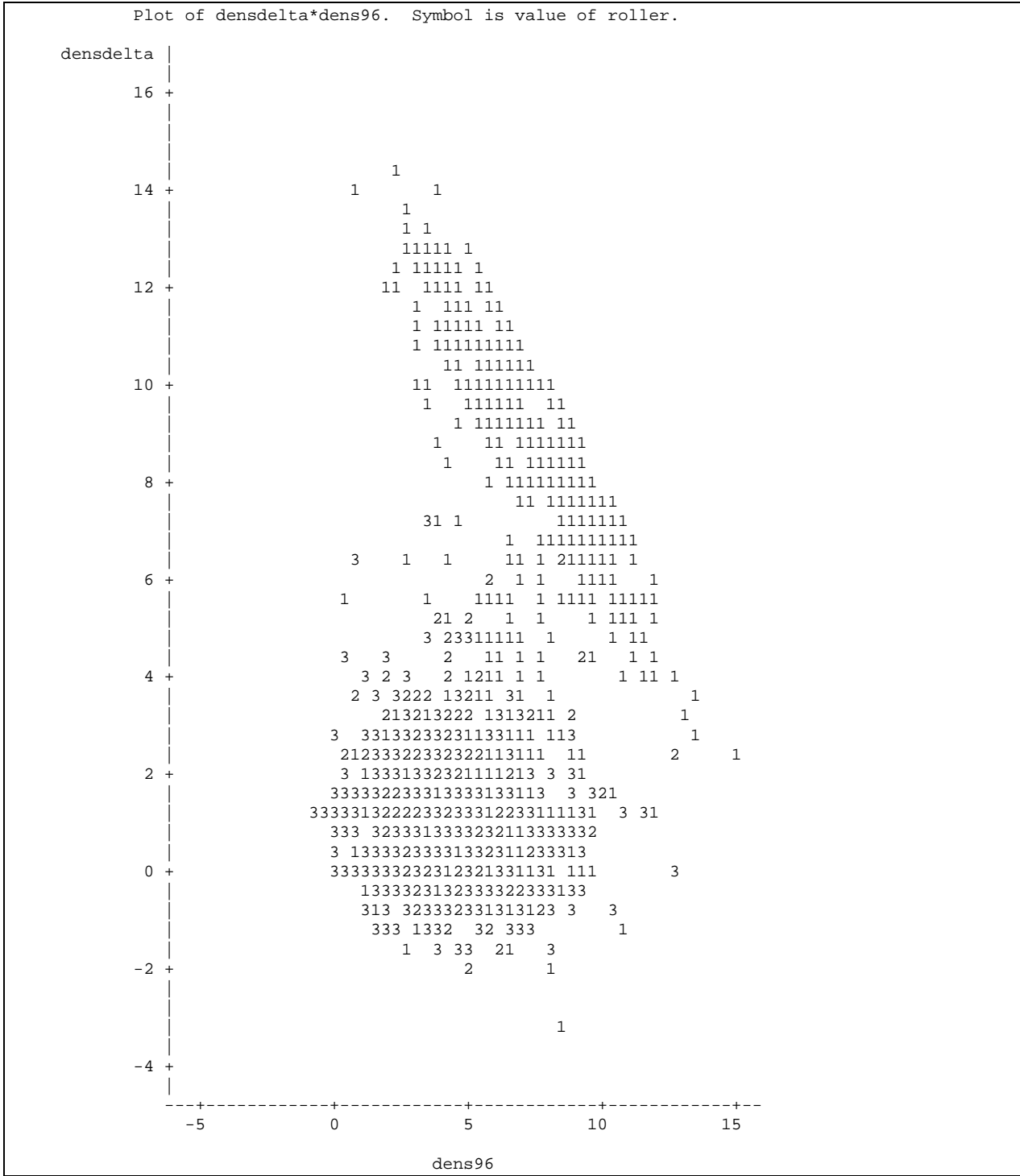


Figure 4.8 Delta Density and range to 96% Gmm by Roller Type

Level of		-----densdelta-----			-----temp-----	
pg	N	Mean	Std Dev	Mean	Std Dev	
58	1393	3.36389088	3.99282885	182.692904	42.4691585	
64	732	2.84057377	3.49398642	181.815574	39.4673167	

Level of		-----passes-----		-----totalpasses-----	
pg	N	Mean	Std Dev	Mean	Std Dev
58	1393	1.74084709	1.05640010	4.09978464	2.74975573
64	732	1.67486339	0.89122296	4.63251366	2.81245670

Level of		-----dens96-----	
pg	N	Mean	Std Dev
58	1393	5.34989232	2.24349675
64	732	5.46762295	2.30267871

Least Squares Means
Adjustment for Multiple Comparisons: Tukey-Kramer

		H0:LSMean1=	
		LSMean2	
pg	densdelta	LSMEAN	Pr > t
58	2.38068276		0.0287
64	2.16401237		

Figure 4.9 Comparison of Means by PG Grade

Level of		-----densdelta-----			-----temp-----	
roller	N	Mean	Std Dev	Mean	Std Dev	
1	955	5.95193717	4.14267608	216.845251	28.2577986	
2	317	1.07539432	1.25351162	179.214511	27.2331363	
3	853	0.86776084	1.12395148	144.996483	19.4971705	

Level of		-----passes-----		-----totalpasses-----	
roller	N	Mean	Std Dev	Mean	Std Dev
1	955	1.47015707	0.56625908	2.26910995	1.29902348
2	317	2.68138801	1.67711720	5.54258675	2.25626770
3	853	1.63774912	0.82725327	6.07033998	2.68095780

Level of		-----dens96-----	
roller	N	Mean	Std Dev
1	955	6.48816754	2.17066305
2	317	4.92807571	1.74012596
3	853	4.33329426	1.95766654

Least Squares Means for effect roller
Pr > |t| for H0: LSMean(i)=LSMean(j)

Dependent Variable: densdelta

i/j	1	2	3
1		0.2375	0.6746
2	0.2375		0.0207
3	0.6746	0.0207	

Figure 4.10 Comparison of Means by Roller Type

Level of		-----densdelta-----		-----temp-----	
vib	N	Mean	Std Dev	Mean	Std Dev
0	650	0.78384615	1.13698191	160.450769	30.1277436
1	1475	4.24115254	4.11962837	192.059129	42.0782006
Level of		-----passes-----		-----totalpasses-----	
vib	N	Mean	Std Dev	Mean	Std Dev
0	650	2.10000000	1.40793481	5.67384615	2.48597154
1	1475	1.54983051	0.69554087	3.67050847	2.68442757
Level of		-----dens96-----			
vib	N	Mean	Std Dev		
0	650	4.53830769	1.85639948		
1	1475	5.76596610	2.32565648		
Least Squares Means					
Adjustment for Multiple Comparisons: Tukey-Kramer					
		H0:LSMean1=			
	densdelta	LSMean2			
vib	LSMEAN	Pr > t			
0	1.94753907	0.0005			
1	2.59715606				

Figure 4.11 Comparison of Least Squares Means by Vibratory Setting

4.4 Breakdown Roller

The ability of the breakdown roller to achieve an increase in density was investigated separately from the pneumatic roller and finish rollers. This data reduction allowed an isolation on those variables within the breakdown rolling operation where the contractor can make rolling pattern adjustments. Specifically, how many passes should be applied to the mat, what should be known about the temperature effect, and should the vibratory setting be ON or OFF.

The GLM procedure was used once again to understand changes in mean density gain after a measurable series of breakdown roller passes, rather than the REG procedure that first determines the function, then overall mean. Figure 4.12 provides summary output from the GLM procedure.

There are very interesting features to glean from the output. First, from a sample size of 955 tests, the average density gain after a measurable series of roller passes (1 pass or 2 passes) was about 6% density. This relatively large gain is to be expected since initial density behind the screed is about 80%. Subsequent passes have a much smaller Delta Density, of say 2% or 4%, after an additional 2 passes, reducing the overall mean.

Source	DF	Sum of Squares	Mean Square	F Value	Pr > F
Model	6	11286.74908	1881.12485	350.66	<.0001
Error	948	5085.57484	5.36453		
Corrected Total	954	16372.32392			
R-Square	Coeff Var	Root MSE	densdelta Mean		
0.689380	38.91415	2.316146	5.951937		
Source	DF	Type III SS	Mean Square	F Value	Pr > F
pg	1	2.004780	2.004780	0.37	0.5411
vib	1	30.447872	30.447872	5.68	0.0174
temp	1	356.639373	356.639373	66.48	<.0001
passes	1	3139.275669	3139.275669	585.19	<.0001
totalpasses	1	3973.431438	3973.431438	740.69	<.0001
dens96	1	995.759395	995.759395	185.62	<.0001

Figure 4.12 Breakdown Roller GLM Results

Important additional observations from the output include:

- 68.9% of the variation in breakdown density growth is explained by vibratory setting, temperature, successive passes, cumulative passes, and approaching 96% density.
- PG grade does not have an effect on density gain with the breakdown roller. The very small sum of squared of 2.00478 densdelta%² yielded an insignificant p-value of 0.54. This finding suggests that a similar density gain can be expected from PG58-series and PG64-series asphalt binders with the breakdown roller.
- Vibratory setting is important, with the ON setting providing added density gain.
- Temperature is equally important, and in fact, more sum of squares are assigned to this variable than vibratory setting.
- Passes are very important. The sum of squares assigned to the successive passes after the roller and the total cumulative passes have a greater magnitude of impact than the other variables combined. About two-thirds of the variability is allocated to combined successive passes and cumulative passes.
- The greater the mat density (relative to 96% of Gmm), the more difficult it is to achieve density gains. This finding is intuitive, since after 2 initial passes the resultant density may be around 88%, while after 2 more passes, the resultant density may be 90%, which is closer to 96% of Gmm.

The findings in the initial GLM warranted further investigation, so 2-way interactions were added to the model, and output is provided in Figure 4.13.

Source	DF	Sum of Squares	Mean Square	F Value	Pr > F
Model	21	13585.28372	646.91827	216.56	<.0001
Error	933	2787.04020	2.98718		
Corrected Total	954	16372.32392			
R-Square	Coeff Var	Root MSE	densdelta Mean		
0.829771	29.03838	1.728346	5.951937		
Source	DF	Type III SS	Mean Square	F Value	Pr > F
pg	1	46.8342093	46.8342093	15.68	<.0001
vib	1	10.4516190	10.4516190	3.50	0.0617
pg*vib	1	3.4680024	3.4680024	1.16	0.2815
temp	1	123.5343380	123.5343380	41.35	<.0001
temp*pg	1	2.4949835	2.4949835	0.84	0.3610
temp*vib	1	0.7588120	0.7588120	0.25	0.6144
passes	1	7.0842324	7.0842324	2.37	0.1239
passes*pg	1	6.0456713	6.0456713	2.02	0.1552
passes*vib	1	33.6046253	33.6046253	11.25	0.0008
temp*passes	1	20.9392957	20.9392957	7.01	0.0082
totalpasses	1	552.7922582	552.7922582	185.05	<.0001
totalpasses*pg	1	223.7787042	223.7787042	74.91	<.0001
totalpasses*vib	1	57.7978079	57.7978079	19.35	<.0001
temp*totalpasses	1	602.1136373	602.1136373	201.57	<.0001
passes*totalpasses	1	114.0685824	114.0685824	38.19	<.0001
dens96	1	74.3670497	74.3670497	24.90	<.0001
dens96*pg	1	97.0019224	97.0019224	32.47	<.0001
dens96*vib	1	20.7255288	20.7255288	6.94	0.0086
temp*dens96	1	59.7282561	59.7282561	19.99	<.0001
passes*dens96	1	6.2630514	6.2630514	2.10	0.1480
totalpasses*dens96	1	157.2362366	157.2362366	52.64	<.0001

Figure 4.13 Breakdown Roller GLM Results with Main Effects and Interactions

With both main effects and interactions in the model, some new insight was provided into breakdown compaction. The same n=955 sample had a natural increase in the R-squared from 69% to 83% with additional parameters, but the vibratory setting became marginally significant, and *individual passes became insignificant*. This is an alarming finding, given that passes are needed to densify the pavement. But, this finding is better understood when evaluating all interactions with Total Passes. A majority of the sum of squares were assigned to Total Passes and its interactive effects with PG grade, vibratory setting, temperature, number of successive passes, and density approaching 96% Gmm. Thus, the very important finding here is that more cumulative passes are the most significant factor affecting the mean density gain with a breakdown roller. For example, 4 passes are more important than 2 passes during breakdown compaction. However, vibratory ON, high temperatures, and approaching 96% Gmm are important as well. Means and standard deviations for PG and vibratory setting are provided in Figures 4.14 and 4.15, respectively.

Level of		-----densdelta-----		-----temp-----	
pg	N	Mean	Std Dev	Mean	Std Dev
58	611	6.46497545	4.17858131	217.823592	28.0231012
64	344	5.04069767	3.92158199	215.107558	28.6284645

Level of		-----passes-----		-----totalpasses-----	
pg	N	Mean	Std Dev	Mean	Std Dev
58	611	1.44189853	0.54123023	2.03109656	1.10617430
64	344	1.52034884	0.60574884	2.69186047	1.49570543

Level of		-----dens96-----	
pg	N	Mean	Std Dev
58	611	6.45319149	2.12639203
64	344	6.55029070	2.24895179

Figure 4.14 Breakdown Roller Comparison of Means by PG Grade

Level of		-----densdelta-----		-----temp-----	
vib	N	Mean	Std Dev	Mean	Std Dev
0	20	0.53500000	1.25416149	197.200000	29.0110687
1	935	6.06780749	4.10554295	217.265471	28.1076436

Level of		-----passes-----		-----totalpasses-----	
vib	N	Mean	Std Dev	Mean	Std Dev
0	20	1.20000000	0.41039134	3.85000000	1.69441808
1	935	1.47593583	0.56788476	2.23529412	1.26906670

Level of		-----dens96-----	
vib	N	Mean	Std Dev
0	20	4.93500000	2.45384231
1	935	6.52139037	2.15346745

Figure 4.15 Breakdown Roller Comparison of Means by Vibratory Setting

Densdelta means for 58-series and 64-series binders were similar, with a slight difference of 1.4%, however, the standard deviations were relatively high (as discussed earlier). The sample size for testing the difference between vibratory ON and OFF was very unbalanced, with only 20 of 955 tests with vibratory OFF. Plots were prepared to visualize the findings from GLM and means output, and are shown in Appendix A.

4.5 Pneumatic Roller

Next, the pneumatic roller was evaluated. About half of the projects in the field study used a pneumatic rubber-tired roller, and on all of those projects, it was sequenced behind the breakdown steel-drum roller. Total sample size was n=320 tests. On a few projects, it was positioned within the same roller zone as the breakdown roller, while on other projects, it would follow about 10 to 15 minutes behind the breakdown roller. Thus, the analysis was limited to the job conditions presented. Figure 4.16 provides summary output from the GLM procedure.

Source	DF	Sum of Squares	Mean Square	F Value	Pr > F
Model	5	92.8413353	18.5682671	13.32	<.0001
Error	314	437.6573834	1.3938133		
Corrected Total	319	530.4987188			

R-Square	Coeff Var	Root MSE	densdelta Mean
0.175008	107.9096	1.180599	1.094063

Source	DF	Type III SS	Mean Square	F Value	Pr > F
pg	1	1.34282541	1.34282541	0.96	0.3271
temp	1	40.13057386	40.13057386	28.79	<.0001
passes	1	25.47985604	25.47985604	18.28	<.0001
totalpasses	1	9.06149865	9.06149865	6.50	0.0113
dens96	1	6.76323131	6.76323131	4.85	0.0283

Parameter	Estimate	Standard Error	t Value	Pr > t
Intercept	-1.346452175 B	0.68231086	-1.97	0.0493
pg 58	0.156181970 B	0.15911951	0.98	0.3271
pg 64	0.000000000 B	.	.	.
temp	0.015545170	0.00289708	5.37	<.0001
passes	0.208713324	0.04881508	4.28	<.0001
totalpasses	-0.106227575	0.04166195	-2.55	0.0113
dens96	-0.087405189	0.03967915	-2.20	0.0283

Figure 4.16 Pneumatic Roller GLM Results

An immediate observation is the weakness of the model, as measured by the R-squared = 17.5 %. Unexplained variability in the mean Delta Density outweighs explained variability by a factor of greater than 4-to-1. For what variability remains, PG is insignificant, temperature and passes are highly significant, and both total passes and differences with 96% Gmm are moderately significant. The greatest allocation of sum of squares is to temperature and passes. Average density gain per successive roller passes is about 1%.

To further support the findings, at the bottom of the output is a statistical model created with parameter estimates and statistical t tests. The key parameter estimates for temperature and passes have stronger estimates than the other parameters, as indicated by the t statistics. The coefficients estimate a 0.15% increase in density for each additional 10°F, and 0.21% density for each initial roller pass. Total passes were moderately significant. From a practical perspective, the greatest density gain is achieved from the initial 4 passes, and not repeated passes. Two-way interactions are also computed, with resulting output in Figure 4.17.

Source	DF	Sum of Squares	Mean Square	F Value	Pr > F
Model	15	149.0215557	9.9347704	7.92	<.0001
Error	304	381.4771631	1.2548591		
Corrected Total	319	530.4987188			
R-Square	Coeff Var	Root MSE	densdelta Mean		
0.280908	102.3895	1.120205	1.094063		
Source	DF	Type III SS	Mean Square	F Value	Pr > F
pg	1	10.06626364	10.06626364	8.02	0.0049
temp	1	6.60937813	6.60937813	5.27	0.0224
temp*pg	1	14.22074810	14.22074810	11.33	0.0009
passes	1	0.39504795	0.39504795	0.31	0.5752
passes*pg	1	1.64578241	1.64578241	1.31	0.2530
temp*passes	1	2.90946674	2.90946674	2.32	0.1289
totalpasses	1	21.12141833	21.12141833	16.83	<.0001
totalpasses*pg	1	2.91791269	2.91791269	2.33	0.1283
temp*totalpasses	1	30.11022216	30.11022216	23.99	<.0001
passes*totalpasses	1	0.38769666	0.38769666	0.31	0.5787
dens96	1	0.00586179	0.00586179	0.00	0.9456
dens96*pg	1	0.00065206	0.00065206	0.00	0.9818
temp*dens96	1	0.02478034	0.02478034	0.02	0.8883
passes*dens96	1	0.33391921	0.33391921	0.27	0.6063
totalpasses*dens96	1	2.86538579	2.86538579	2.28	0.1318

Figure 4.17 Pneumatic Roller GLM Results for Main Effects and Interactions

The R-squared value naturally increases with the addition of interactions to the main effects, from 17.5% to 28.1%. With a larger model, total passes and the interaction of totalpasses*temperature accumulate the greatest sum of squares. The adjusted model indicates total passes are a function of temperature, which is to be expected (more passes, more cooling). So, it is more beneficial for a contactor to use the rubber-tired roller at a higher temperature, and with a greater number of initial passes. PG grade and PG*Temperature interaction also accumulate a greater sum of squares, indicating that binder dynamic viscosity and its relationship to temperature are influential in density gains.

Plots in Appendix B were prepared to illustrate the relationships. A majority of Density Delta readings ranged from -1% (15-second testing error) to +4% below 200°F, with greater gains on PG 58-series binders or temperatures greater than 200F. A trend was observed where higher temperatures yield greater density gains. Passes up to n=4 provide the greatest initial densification, and a greater number of passes provide diminishing return on effort investment. Based on the data collected in the presence of a relatively large amount of error (gauge seating, etc.) or unexplained variability, it is recommended that a rubber-tired roller be applied to the mat at higher temperatures and with a minimum of 4 initial passes. Again, multiple coverage is key, as is temperature.

4.6 Finish Roller

Lastly, the finish (or cold) steel-drum roller is analyzed. A typical observation on all projects was the finish roller operating in either a vibratory or static setting at lower mat temperatures, generally in the range of 170°F down to 120°F. Total sample size was n=853 tests. Figure 4.18 provides summary output from the GLM procedure.

Source	DF	Sum of Squares	Mean Square	F Value	Pr > F
Model	6	250.898428	41.816405	42.86	<.0001
Error	846	825.404995	0.975656		
Corrected Total	852	1076.303423			

R-Square	Coeff Var	Root MSE	densdelta Mean
0.233111	113.8278	0.987753	0.867761

Source	DF	Type III SS	Mean Square	F Value	Pr > F
pg	1	8.32753230	8.32753230	8.54	0.0036
vib	1	62.17838724	62.17838724	63.73	<.0001
temp	1	7.14707089	7.14707089	7.33	0.0069
passes	1	51.92626891	51.92626891	53.22	<.0001
totalpasses	1	95.01983316	95.01983316	97.39	<.0001
dens96	1	60.86265455	60.86265455	62.38	<.0001

Figure 4.18 Finish Roller GLM Results

The average density gain from successive finish roller passes (typically 1 or 2) is about 0.9%. Similar to the intermediate pneumatic roller, the R-squared = 23.3% is relatively small. Unexplained variability in the mean Delta Density outweighs explained variability by a factor of about 3-to-1. All main effects were significant in density gain, including PG grade, vibratory setting, temperature, passes, cumulative passes, and density approaching 96% Gmm. The greatest sum of squares was found with total cumulative passes, followed by vibratory setting and difference with 96% Gmm.

Note that temperature had the lowest sum of squares, suggesting that passes a greater factor, and temperature has little effect at achieving density gains with the cold roller. Passes are key. Two-way interactions were also investigated, with resulting output in Figure 4.19.

Source	DF	Sum of Squares	Mean Square	F Value	Pr > F		
Model	21	292.631457	13.934831	14.78	<.0001		
Error	831	783.671966	0.943047				
Corrected Total	852	1076.303423					
R-Square	0.271886	Coeff Var	111.9094	Root MSE	0.971106	densdelta Mean	0.867761
Source	DF	Type III SS	Mean Square	F Value	Pr > F		
pg	1	0.33996734	0.33996734	0.36	0.5484		
vib	1	1.50858191	1.50858191	1.60	0.2063		
pg*vib	1	5.53061964	5.53061964	5.86	0.0157		
temp	1	9.22431129	9.22431129	9.78	0.0018		
temp*pg	1	0.96521189	0.96521189	1.02	0.3120		
temp*vib	1	0.00806937	0.00806937	0.01	0.9263		
passes	1	2.38325426	2.38325426	2.53	0.1123		
passes*pg	1	2.30795854	2.30795854	2.45	0.1181		
passes*vib	1	0.12446396	0.12446396	0.13	0.7165		
temp*passes	1	0.44114470	0.44114470	0.47	0.4942		
totalpasses	1	9.50331535	9.50331535	10.08	0.0016		
totalpasses*pg	1	0.81896096	0.81896096	0.87	0.3517		
totalpasses*vib	1	1.53338272	1.53338272	1.63	0.2026		
temp*totalpasses	1	13.13904264	13.13904264	13.93	0.0002		
passes*totalpasses	1	10.62847319	10.62847319	11.27	0.0008		
dens96	1	0.49102424	0.49102424	0.52	0.4708		
dens96*pg	1	0.46188741	0.46188741	0.49	0.4842		
dens96*vib	1	1.60404489	1.60404489	1.70	0.1925		
temp*dens96	1	1.45682148	1.45682148	1.54	0.2143		
passes*dens96	1	5.77146499	5.77146499	6.12	0.0136		
totalpasses*dens96	1	0.00887966	0.00887966	0.01	0.9227		

Figure 4.19 Finish Roller GLM Results for Main Effects and Interactions

There was an expected increase in the R-squared, with the resulting value of 27.2%. Again, there is still a great deal of unexplained variability from such sources as testing error, base type, layer thickness, thickness-to-NMAS ratio, air voids, etc. With more parameters in the model, it became difficult for the previous main effects to maintain significance, including PG grade, passes, and difference with 96% Gmm.

The greatest assignment in mean variability is with interactions of temperature*totalpasses (decrease in temp with more passes) and passes*totalpasses, along with the main effect of temperature. Moderate significance is found with the interactions of PG*vib and passes*dens96. This suggests that in order to achieve gains in density, it is necessary to increase the cumulative number of passes at a higher temperature, setting the vibratory amplitude and frequency with respect to binder grade (with the help of IC research), and number of successive passes as 96% Gmm is approached.

To further investigate these effects, arithmetic means and least squares means (that incorporate the covariate) are assessed in Figures 4.20 and 4.21. Commentary follows the figures.

Level of		-----densdelta-----		-----temp-----	
pg	N	Mean	Std Dev	Mean	Std Dev
58	545	0.84605505	1.09137159	143.673394	21.5225542
64	308	0.90616883	1.18023666	147.337662	15.0184342

Level of		-----passes-----		-----totalpasses-----	
pg	N	Mean	Std Dev	Mean	Std Dev
58	545	1.65871560	0.79811485	5.74678899	2.65167015
64	308	1.60064935	0.87654911	6.64285714	2.64064589

Level of		-----dens96-----	
pg	N	Mean	Std Dev
58	545	4.22990826	1.93056039
64	308	4.51623377	1.99478051

Least Squares Means
Adjustment for Multiple Comparisons: Tukey-Kramer

	H0:LSMean1=	
	densdelta	LSMean2
pg	LSMEAN	Pr > t
58	0.75802700	0.0148
64	0.94961143	

Figure 4.20 Finish Roller Means Comparison by PG Grade

Level of		-----densdelta-----		-----temp-----	
vib	N	Mean	Std Dev	Mean	Std Dev
0	342	0.56315789	0.96309586	141.450292	16.6058901
1	511	1.07162427	1.17743369	147.369863	20.8950269

Level of		-----passes-----		-----totalpasses-----	
vib	N	Mean	Std Dev	Mean	Std Dev
0	342	1.61988304	0.83294481	5.84210526	2.62822135
1	511	1.64970646	0.82402343	6.22309198	2.70749414

Level of		-----dens96-----	
vib	N	Mean	Std Dev
0	342	4.14385965	1.81822164
1	511	4.46007828	2.03760990

Least Squares Means
Adjustment for Multiple Comparisons: Tukey-Kramer

	H0:LSMean1=	
	densdelta	LSMean2
vib	LSMEAN	Pr > t
0	0.57157722	<.0001
1	1.13606121	

Figure 4.21 Finish Roller Means Comparison by Vibratory Setting

From Figure 4.20, the PG 64-series binders have a slightly larger density gain than PG 58-28, with a near equal number of successive passes (1.6) and density from 96% Gmm (~ 4%). The least squares test for PG means found that there was a moderate difference. Note that the 64-series binders were compacted with 4°F greater temperature (147°F minus 143°F). This finding is interesting, given the fact that a 64-22 or 64-28 binder has a greater shear resistance during compaction.

From Figure 4.21, vibratory setting is an important factor in achieving density gain with the finish roller. A comparison of both arithmetic means and least-squares means finds that a

vibratory setting ON yields 0.5% more density gain (1.1% minus 0.6%) after successive roller passes. A key finding is how much total density can be gained with the finish roller. If the average density gain is about 0.86% after an average 1.6 successive roller passes, and the total passes is about 6 for the layer, the total calculated average density gain for a full 6-pass coverage is a multiplier of 3.75 ($6 / 1.6 = 3.75$), yielding a total of about 3.2%. This a pure averaging estimate, however, it provides a relative sense of how much density can be gained with a finish roller. Many contractors can expect a finish roller to achieve at least 1.5% to 2% added density, and a total number of passes = 6 will provide approximately 3%. This relationship is the average across 30 layers of pavement. Figures in Appendix C help illustrate the relationships in finish rolling.

Figure 4.22 provides the GLM parameter model. The coefficients generally support the earlier findings, however, with multiple parameters competing to explain the increase in density gain, some parameter estimates may seem counterintuitive. Even though these model parameters help predict future finish roller compaction, the model is only 23.3% accurate, primarily because of testing error and other key variables that affect cold rolling, such as layer thickness, thickness-to-NMAS ratio, base rigidity, roller size, weight change with water loss, and different contact pressures.

Parameter		Estimate	Standard Error	t Value	Pr > t
Intercept		1.510702424 B	0.35313262	4.28	<.0001
pg	58	-0.212996547 B	0.07290591	-2.92	0.0036
pg	64	0.000000000 B	.	.	.
vib	0	-0.565368744 B	0.07082074	-7.98	<.0001
vib	1	0.000000000 B	.	.	.
temp		0.005007094	0.00184999	2.71	0.0069
passes		0.306894180	0.04206719	7.30	<.0001
totalpasses		-0.140381591	0.01422497	-9.87	<.0001
dens96		-0.151533341	0.01918585	-7.90	<.0001

NOTE: The X'X matrix has been found to be singular, and a generalized inverse

Figure 4.22 Finish Roller Model

An assessment of model parameters is as follows:

- **PG grade.** An indicator variable for 58-series and 64-series binders where a 58-series reduces the mean gain by 0.21% density, and a zero for 64-series.
- **Vibratory setting.** Indicator variable where OFF has -0.56% density gain, and ON has 0% density gain.
- **Temperature.** A multiplier of 0.005 is applied for every 1°F. So, a mat temp that is 10F warmer, will yield a 0.05% density increase, a negligible change. This is an important finding, when comparing with the breakdown roller and pneumatic roller, that are more temperature dependent.
- **Passes.** This is where the greatest gains are made with a finish roller. More successive passes, more density gain. A multiplier of 0.3 is applied to each successive pass. An application of 2 successive passes would achieve a 0.6% density gain.
- **Total Passes.** More cumulative passes provides diminishing return on density gain. This is counter to what would be expected, but with the negative coefficient in the model, a large number of cumulative passes will not provide enhanced density gain (Figure 6.10 supports this). The figures generally indicate a total of 6 to 8 passes should be sufficient. But, this brings in the

question of trying to achieve density gains with the cold roller at lower temperatures, when the breakdown (and pneumatic) have the greatest impact.

- Density approaching 96% Gmm. With the negative coefficient, it is increasingly difficult to densify the mat when approaching 96% of Gmm.

4.7 Limiting Field Temperature

A primary objective in this study is to investigate the minimum limiting temperatures at which required density of HMA can be achieved with commonly used compaction effort. To achieve this objective, field data were stratified by ESAL series, then the data were compared to a target density of 92% Gmm, a common density requirement. From the 20 test sites per layer, the average number of roller passes and average beginning and ending temperature to achieve 92% density were computed. Then, a visual assessment was made to aid in determining the limiting temperature. There are variations of this density requirement, namely lower ESAL pavements, or those layers paved directly on crushed aggregate base course; however, the threshold of 92% Gmm was established for this investigation since it is the baseline standard requisite field density.

Figures 4.23 through 4.25 for E-1, E-3, and E-10 mixes, respectively, plot the number of roller passes against the beginning and ending pass temperatures when 92% density was achieved. Only one of the 30 layers tested in this study did not achieve 92% density – STH 33 in LaCrosse County. On the day of paving, a rapidly moving cold front cooled the surface temperature to around 110°F, and the average final density was approximately 91.3% density.

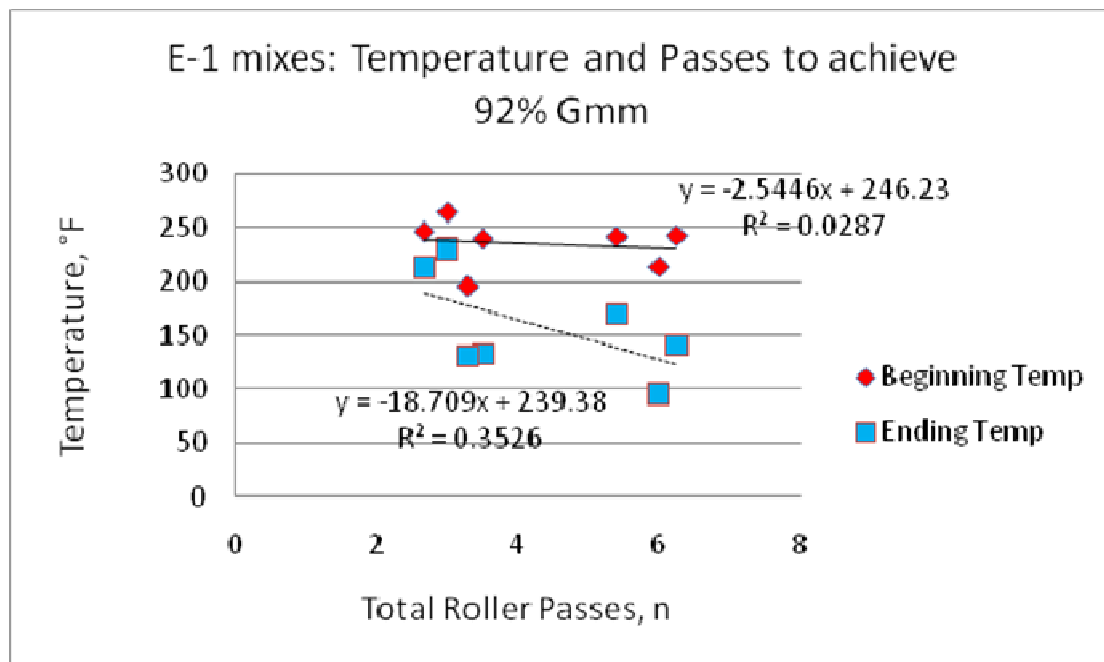


Figure 4.23 Roller Passes to Achieve 92% Gmm (E-1)

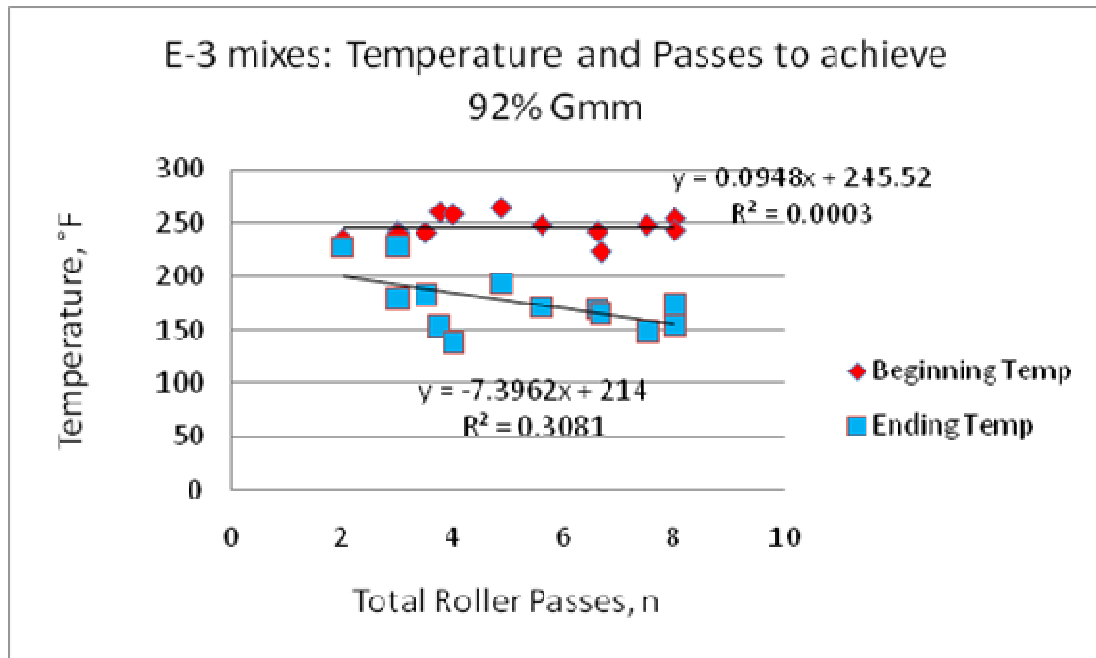


Figure 4.24 Roller Passes to Achieve 92% Gmm (E-3)

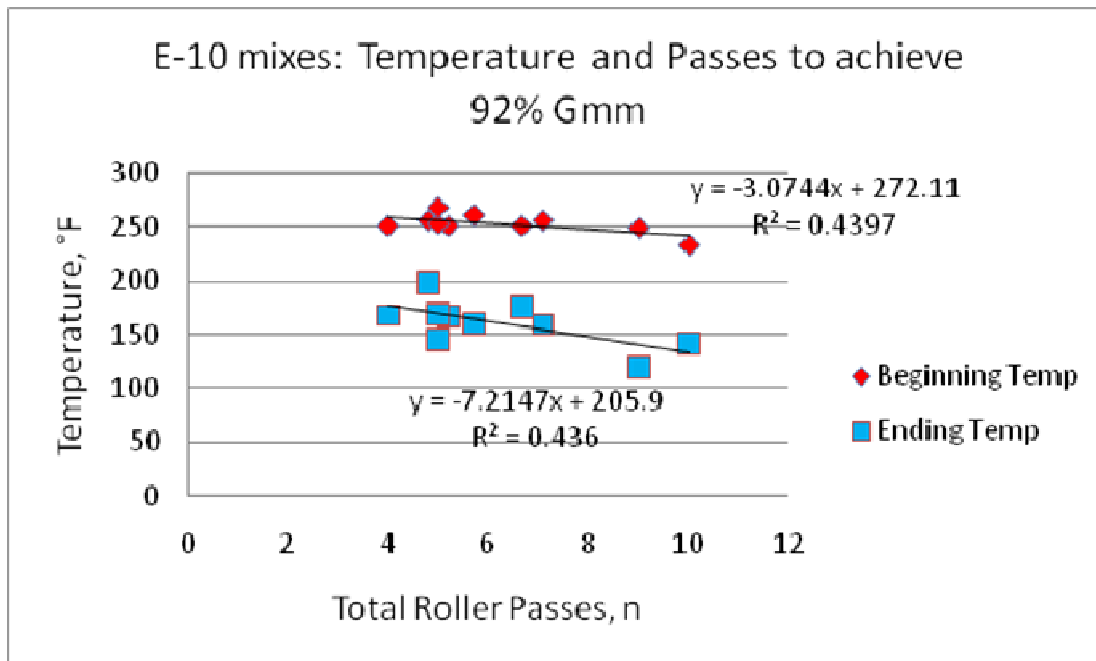


Figure 4.25 Roller Passes to Achieve 92% Gmm (E-10)

An important finding was 29 of 30 layers met the 92% density requirement, requiring a range of 4 to 10 cumulative roller passes. A consistent result across all ESAL mixtures was higher ending compaction temperature yielding 92% density with a lesser number of roller passes. In general, beginning mat temperatures hovered around 250°F, and no strong trend was observed with number of roller passes. A slight trend was also observed on E-10 mixes where higher beginning compaction temperatures reduced the number of total roller passes to achieve 92% density.

In conclusion, there is no limiting temperature at which 92% density can be achieved, based on the random data collected in this study. If a sufficient number of roller passes are applied to the pavement, the 92% density requirement will be met. It is recommended that compaction occur at higher temperatures to minimize the total number of roller passes; however, this must be balanced with the ability to achieve surface smoothness.

Chapter 5 Data Analysis for Lab Compaction

5.1 Statistical Modeling Approach

The analysis of field compaction data used a key response variable, known as “Density Delta”, to measure the relative increase in density between successive roller passes. Lab compaction data were analyzed in a different manner, using the traditional density measure, % of Gmm, as the response variable to understand the relative degree of compaction. The incremental approach using Density Delta was not used since the final resultant density after gyratory compaction is of key interest. Initial compaction (Nini) and final compaction (Nmax) were considered, but Ndes was chosen to better align with densification at traditional field compaction levels.

Several statistical methods were used during this analysis, Traditional statistical tests were used as well, and the reader should refer to statistical textbooks for further background on their methods and assumptions.

Because the analysis was largely the evaluation of factors at stated levels (factorial), ANOVA methods were used. ANOVA is a statistical technique used to compare the means of two or more groups of observations or treatments. General Linear Models (GLM) was used to perform the ANOVA analysis, where the mean of the data are first computed, then the contribution of each independent variable in explaining deviations of the mean. The key objective was to understand what variables have an effect on changes in density. Type III Sum of Squares were used to determine relative significance in the independent variables by measuring the reduction in unexplained variability when the variable is entered last into a model. This measurement technique provides a measure of variable robustness, and relative ability to accumulate sum of squares against the other previously-entered, competing variables.

5.2 ANOVA for Ndes

Ndes was designated as the dependent variable to normalize the data to the number of gyrations to Ndes across different mix classes including E-1 (Ndes=60), E-3 (Ndes=75), and E-10 (Ndes=100). Basic statistics for the primary variables by class levels are provided in Figure 5.1. The mean density generally ranged from about 92% to 94%, with a standard deviation of about 1.4% to 2.1%.

Level of		-----ndes-----	
pg	N	Mean	Std Dev
58	84	94.1476190	1.81184165
64	36	93.7958333	1.92744149
Level of		-----ndes-----	
nmas	N	Mean	Std Dev
12	72	94.1837500	1.76030362
19	42	94.0619048	1.85237651
25	6	92.2033333	2.15305984
Level of		-----ndes-----	
source	N	Mean	Std Dev
1	72	94.1554167	1.95475364
2	48	93.8720833	1.67590681
Level of		-----ndes-----	
specgyr	N	Mean	Std Dev
60	24	93.8679167	1.35881975
75	48	94.3410417	1.77471633
100	48	93.8302083	2.10340503
Level of		-----ndes-----	
pressure	N	Mean	Std Dev
300	60	93.1590000	1.72676900
600	60	94.9251667	1.51887614
Level of		-----ndes-----	
temp	N	Mean	Std Dev
140	40	92.5817500	1.79215654
194	40	94.5882500	1.39676345
248	40	94.9562500	1.37377953

Figure 5.1 Basic Statistics for Lab Compaction Variables by Classification

There was a single E-10 25-mm NMAS mixture (the only 25-mm mix of the 30 layers) that significantly skewed the model, so it was removed. This reduced the total layers for analysis from 20 to 19 layers. Figure 5.2 provides the ANOVA output for the independent variables thought to affect the Ndes value. An important finding was that the six primary variables are able to explain about 62% of the change in density at Ndes, with pressure and temperature highly significant, while PG was marginally significant. The remaining variability was test error and other project-specific variables thought to have a significant effect on compaction, such as air voids, asphalt content, VFB, coarse-to-fine aggregate ratio, etc. These variables are obviously important, but would have confounded the ability of the analysis to investigate the stated

variables in question. Another important finding was that pressure and temperature had the largest Mean Square values and effect on lab compaction, while PG grade had a lesser Mean Square value.

Source	DF	Sum of Squares	Mean Square	F Value	Pr > F
Model	8	224.5662076	28.0707759	21.59	<.0001
Error	105	136.5163442	1.3001557		
Corrected Total	113	361.0825518			
R-Square	Coeff Var	Root MSE	ndes Mean		
0.621925	1.211236	1.140244	94.13886		
Source	DF	Type III SS	Mean Square	F Value	Pr > F
pg	1	3.7992812	3.7992812	2.92	0.0903
nmas	1	0.0668118	0.0668118	0.05	0.8211
source	1	1.0477042	1.0477042	0.81	0.3714
specgyr	2	5.5471400	2.7735700	2.13	0.1236
pressure	1	91.1021763	91.1021763	70.07	<.0001
temp	2	118.4648228	59.2324114	45.56	<.0001

Figure 5.2 ANOVA results for Lab Compaction Variables

Two-way interactions were added to the model, and resulting ANOVA output is provided in Figure 5.3. The R-squared naturally increased from 62% to 76% with more model parameters. As measured by the Mean Square, the most influential main effects were pressure and temperature. PG grade became insignificant since a majority of the variability had previously been assigned to the preceding variables in the model. There were only one significant interaction, the interaction of NMAS*specified gyrations. The NMAS*specified gyrations is the result of higher densities with 12.5mm aggregates and E-3 mix class.

Source	DF	Sum of Squares	Mean Square	F Value	Pr > F
Model	27	276.0734441	10.2249424	10.34	<.0001
Error	86	85.0091076	0.9884780		
Corrected Total	113	361.0825518			
R-Square	Coeff Var	Root MSE	ndes Mean		
0.764572	1.056123	0.994222	94.13886		
Source	DF	Type III SS	Mean Square	F Value	Pr > F
pg	1	1.5870000	1.5870000	1.61	0.2085
nmas	1	1.4966173	1.4966173	1.51	0.2219
source	1	0.1818359	0.1818359	0.18	0.6691
nmas*source	1	0.0503467	0.0503467	0.05	0.8220
specgyr	2	2.5887909	1.2943954	1.31	0.2753
nmas*specgyr	2	21.9487522	10.9743761	11.10	<.0001
source*specgyr	2	9.5207391	4.7603696	4.82	0.0104
pressure	1	76.0746061	76.0746061	76.96	<.0001
nmas*pressure	1	0.5975852	0.5975852	0.60	0.4390
source*pressure	1	0.2338546	0.2338546	0.24	0.6279
specgyr*pressure	2	1.6880076	0.8440038	0.85	0.4294
temp	2	106.6584333	53.3292167	53.95	<.0001
nmas*temp	2	1.8140794	0.9070397	0.92	0.4033
source*temp	2	0.6263543	0.3131771	0.32	0.7293
specgyr*temp	4	0.4689268	0.1172317	0.12	0.9756
pressure*temp	2	1.5006368	0.7503184	0.76	0.4712

Figure 5.3 ANOVA results for Lab Compaction Variables

Based on the preliminary ANOVA findings, the model was reduced to the three significant effects, including PG grade, temperature, and pressure. The ANOVA and estimated model parameters are provided in Appendix D (Figure D.1). The model R-square = 60% with the pressure and temperature highly significant, and PG grade marginally significant. The estimated model parameters are presented in Equation 5.1.

$$\begin{aligned}
 \text{Lab Density} &= 95.6 \\
 &+0.5*\text{PG} [1 \text{ if PG58}; 0 \text{ if PG64}] \\
 &-1.8*\text{Pressure} [1 \text{ if 300kPa}; 0 \text{ if 600kPa}] \\
 &-2.4*\text{Temp} [1 \text{ if Temp}=140^\circ\text{F}; 0 \text{ otherwise}] \\
 &-0.4*\text{Temp} [1 \text{ if Temp}=194^\circ\text{F}; 0 \text{ otherwise}] \quad (5.1)
 \end{aligned}$$

Plant-produced mixtures yielded a 95.6% density at Ndes, within 0.4% density of the lab-designed density of 96.0%. A softer PG-58 grade binder results in a mix compacted to an additional 0.5% density at Ndes. Using a baseline compaction temperature of 248°F, the compacted density was 0.4% lower density at 194°F, and 2.4% lower density at 140°F. Clearly, pressure and temperature have a pronounced effect. The model was further reduced to pressure and temperature, with resulting output in Appendix D (Figure D.2). The model R-square = 55% with the two variables; estimated model parameters derived in Equation 5.2.

$$\text{Lab Density} = 95.9$$

$$\begin{aligned}
& -1.8 * \text{Pressure [1 if 300kPa; 0 if 600kPa]} \\
& -2.3 * \text{Temp [1 if Temp=140°F; 0 otherwise]} \\
& -0.4 * \text{Temp [1 if Temp=194°F; 0 otherwise]} \qquad (5.2)
\end{aligned}$$

The model and supporting ANOVA indicate that when the pressure is reduced from 600 kPa to 300 kPa, there is a corresponding 1.8% density drop in Ndes lab compaction from 95.9% to 94.1%. There is also a density reduction from a baseline temperature in 248°F, with a 0.4% density drop at 194°F and 2.3% at 140°F.

5.3 Ndes=60 Gyration

The data were stratified by number of gyrations to Ndes for ESAL mixtures for E-1, E-3, and E-10 mixtures. The E-30 USH-41 project was pooled with the E-10 mixtures since the Ndes=100 were equivalent. This approach allowed for an individual investigation by total number of Ndes gyrations, as opposed to the pooled data from the earlier analysis. The GLM procedure was again used to understand changes in mean density gain after the mixture is compacted to a specified number of gyrations.

E-1 series mixtures use 60 gyrations to design the asphalt mixture to 4% air voids. The theory is that 1 million ESALs applied to the pavement will compact the pavement to 96% density, or 4% in-place air voids. Figure 5.4 provides the analysis of variables thought to affect the density at 60 gyrations. PG grade was omitted from the analysis since all E-1 series projects had 58-28 binder grade.

Source	DF	Sum of Squares	Mean Square	F Value	Pr > F
Model	5	36.20182500	7.24036500	20.80	<.0001
Error	18	6.26517083	0.34806505		
Corrected Total	23	42.46699583			
R-Square	Coeff Var	Root MSE	ndes Mean		
0.852470	0.628511	0.589970	93.86792		
Source	DF	Type III SS	Mean Square	F Value	Pr > F
nmas	1	0.02151111	0.02151111	0.06	0.8065
source	1	1.07467778	1.07467778	3.09	0.0959
pressure	1	11.88633750	11.88633750	34.15	<.0001
temp	2	23.19630833	11.59815417	33.32	<.0001

Figure 5.4 Ndes=60 Gyration ANOVA Results for Main Effects

Both temperature and pressure had a significant effect on the final lab-compacted density, while aggregate source had a marginal effect. Similar values for Mean Square were computed for both pressure and temperature. The measured R-square=85.2% was very high, indicating the pressure and temperature have a large influence on the density after 60 gyrations.

Interactions were tested, with ANOVA results in Figure 5.5. Only 2-way interactions were modeled to simplify the interpretation, and provide sensitivity in the F-test computation with greater degrees of freedom assigned to the denominator. The ANOVA table indicates that no interactions were significant, and that only the previous main effects of temperature and pressure were again significant. The R-Square increased slightly to 89.0%.

Source	DF	Sum of Squares	Mean Square	F Value	Pr > F
Model	13	37.81402083	2.90877083	6.25	0.0032
Error	10	4.65297500	0.46529750		
Corrected Total	23	42.46699583			

R-Square	Coeff Var	Root MSE	ndes Mean
0.890433	0.726688	0.682127	93.86792

Source	DF	Type III SS	Mean Square	F Value	Pr > F
nmas	1	0.02151111	0.02151111	0.05	0.8341
source	1	1.07467778	1.07467778	2.31	0.1595
nmas*source	0	0.00000000	.	.	.
pressure	1	4.47740833	4.47740833	9.62	0.0112
nmas*pressure	1	0.00000000	0.00000000	0.00	1.0000
source*pressure	1	0.55254444	0.55254444	1.19	0.3014
temp	2	11.37631667	5.68815833	12.22	0.0021
nmas*temp	2	0.03943889	0.01971944	0.04	0.9587
source*temp	2	0.01507222	0.00753611	0.02	0.9840
pressure*temp	2	0.91097500	0.45548750	0.98	0.4090

Figure 5.5 Ndes=60 Gyration Main Effects and Interactions

With the strong relationship of Ndes lab density with temperature and pressure, a statistical model was created to formally quantify the relationship, and provide a prediction tool for achieving a specified level of density. In this model, only the significant main effects were retained, and both NMAS and aggregate source were dropped. Appendix D (Figure D.3) provides the ANOVA table and estimated model parameters. Model diagnostic checks, including residuals versus predicted values and normality plot of residuals, concluded that the model is valid. Equation 5.3 provides the model.

$$\begin{aligned}
 \text{Lab Density} &= 96.0 \\
 &-1.8*\text{Pressure} [1 \text{ if } 300\text{kPa}; 0 \text{ if } 600\text{kPa}] \\
 &-2.3*\text{Temp} [1 \text{ if } \text{Temp}=140^\circ\text{F}; 0 \text{ otherwise}] \\
 &-0.2*\text{Temp} [1 \text{ if } \text{Temp}=194^\circ\text{F}; 0 \text{ otherwise}] \quad (5.3)
 \end{aligned}$$

The indicator variable for Temp=194°F is insignificant, suggesting no statistical difference in the final compacted density between 248°F and 194°F. This is the result of a standard of error nearly double the parameter estimate, creating a t-test value half their ratio.

When the pressure is reduced from 600 kPa to 300 kPa, there is a corresponding 1.8% density drop in lab compaction from 96.0% to 94.2%. There is also a density reduction from a baseline temperature in 248°F, with a 0.2% density drop at 194°F and 2.3% at 140°F. This change is similar to the pooled data model shown earlier.

5.4 Ndes=75 Gyration

Data for E-3 mixtures having an Ndes=75 were analyzed in a similar manner to the Ndes=60. The E-3 series mixtures use 75 gyrations to design the asphalt mixture to 4% air voids. Figure 5.6 provides the analysis of variables thought to affect the density at 75 gyrations.

Source	DF	Sum of Squares	Mean Square	F Value	Pr > F
Model	6	118.0576097	19.6762683	26.91	<.0001
Error	41	29.9744382	0.7310839		
Corrected Total	47	148.0320479			
R-Square	Coeff Var	Root MSE	ndes Mean		
0.797514	0.906323	0.855034	94.34104		
Source	DF	Type III SS	Mean Square	F Value	Pr > F
pg	1	0.89460069	0.89460069	1.22	0.2751
nmas	1	3.15005000	3.15005000	4.31	0.0442
source	1	0.25561250	0.25561250	0.35	0.5576
pressure	1	37.64791875	37.64791875	51.50	<.0001
temp	2	52.26080417	26.13040208	35.74	<.0001

Figure 5.6 Ndes=75 Gyration ANOVA Results

Both temperature and pressure had a significant effect on the final lab-compacted density, while aggregate source had a marginal effect. PG and aggregate source were not significant. The measured R-square=80% was very high, indicating the pressure and temperature have a great influence on the density after 75 gyrations.

Two-way interactions were tested, with ANOVA results in Figure 5.7. The ANOVA table indicates that only the NMAS*temperature interaction was significant. The R-Square increased slightly to 86%. NMAS and temperature were plotted in Figure 5.8 to understand the relationship.

Figure 5.8 illustrates that NMAS has a more significant effect with lower compaction temperatures, yielding lower density with 19mm and higher density with 12.5mm mixtures. The practical result is that larger 19mm aggregates have greater difficulty re-orienting in the compactor mold at lower temperatures.

Source	DF	Sum of Squares	Mean Square	F Value	Pr > F
Model	17	126.7718938	7.4571702	10.52	<.0001
Error	30	21.2601542	0.7086718		
Corrected Total	47	148.0320479			

R-Square	Coeff Var	Root MSE	ndes Mean
0.856381	0.892323	0.841826	94.34104

Source	DF	Type III SS	Mean Square	F Value	Pr > F
pg	0	0.00000000	.	.	.
nmas	1	3.15005000	3.15005000	4.45	0.0435
pg*nmas	0	0.00000000	.	.	.
source	1	0.25561250	0.25561250	0.36	0.5526
pg*source	0	0.00000000	.	.	.
nmas*source	0	0.00000000	.	.	.
pressure	1	28.94440000	28.94440000	40.84	<.0001
pg*pressure	1	0.01755625	0.01755625	0.02	0.8760
nmas*pressure	1	0.09245000	0.09245000	0.13	0.7205
source*pressure	1	0.05951250	0.05951250	0.08	0.7740
temp	2	35.18357222	17.59178611	24.82	<.0001
pg*temp	2	1.65581806	0.82790903	1.17	0.3247
nmas*temp	2	4.79500833	2.39750417	3.38	0.0473
source*temp	2	0.51413333	0.25706667	0.36	0.6988
pressure*temp	2	1.62251250	0.81125625	1.14	0.3318

Figure 5.7 Ndes=75 Gyration ANOVA Results with Main Effects and Interactions

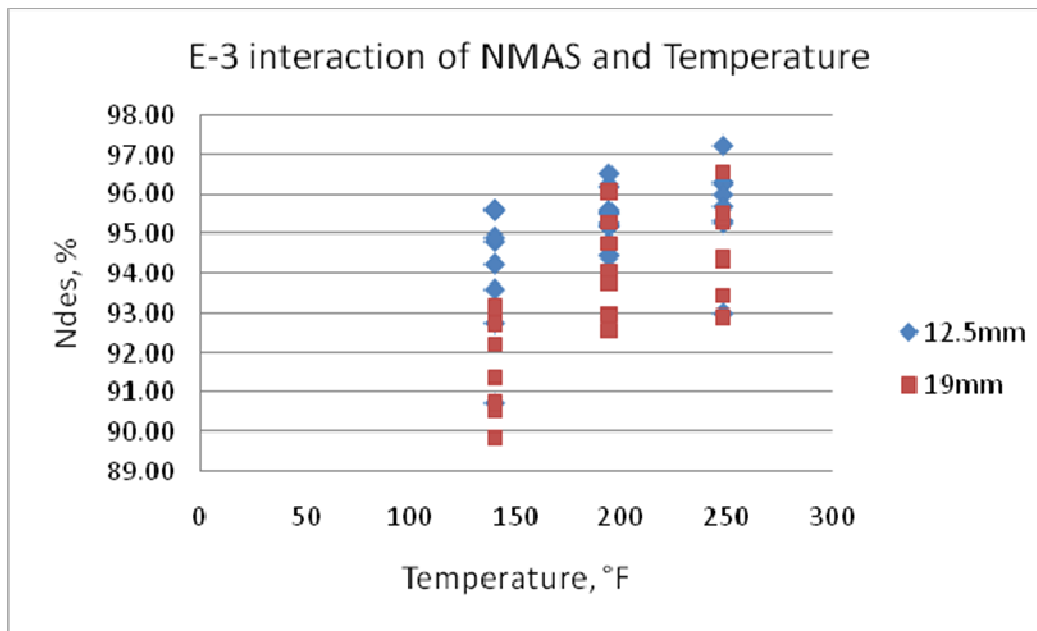


Figure 5.8 Interaction of NMAS and Temperature (Ndes=75 Gyration)

A model was created with three significant main effects: NMAS, pressure and temperature. Figure D.4 in Appendix provides the detailed ANOVA output and model parameters, and Equation 5.4 the resulting model.

$$\begin{aligned}
&\text{Lab Density} = 95.4 \\
&+1.4*\text{NMAS} [1 \text{ if } 12.5\text{mm}; 0 \text{ otherwise}] \\
&-1.8*\text{Pressure} [1 \text{ if } 300\text{kPa}; 0 \text{ if } 600\text{kPa}] \\
&-2.3*\text{Temp} [1 \text{ if } \text{Temp}=140^\circ\text{F}; 0 \text{ otherwise}] \\
&-0.2*\text{Temp} [1 \text{ if } \text{Temp}=194^\circ\text{F}; 0 \text{ otherwise}] \quad (5.4)
\end{aligned}$$

Similar to the E-1 modeled relationship, the indicator variable for Temp=194°F is insignificant, suggesting no statistical difference in the final compacted density between 248°F and 194°F. NMAS of 12.5mm provides 1.4% more density. When the pressure is reduced from 600 kPa to 300 kPa, there is a 1.8% density drop. Nearly identical to the E-1 mixes, there is also a density reduction from a baseline temperature in 248°F, with a 0.2% density drop at 194°F and 2.3% at 140°F.

A statistical model having an R-squared = 61% was created having only temperature and pressure as independent variables. Figure D.5 (Appendix D) provides the ANOVA table and estimated model parameters, and Equation 5.5 the final model.

$$\begin{aligned}
&\text{Lab Density} = 96.1 \\
&-1.8*\text{Pressure} [1 \text{ if } 300\text{kPa}; 0 \text{ if } 600\text{kPa}] \\
&-2.3*\text{Temp} [1 \text{ if } \text{Temp}=140^\circ\text{F}; 0 \text{ otherwise}] \\
&-0.2*\text{Temp} [1 \text{ if } \text{Temp}=194^\circ\text{F}; 0 \text{ otherwise}] \quad (5.5)
\end{aligned}$$

The model parameters are nearly identical to the E-1 mixtures, where a reduction in pressure from 600 kPa to 300 kPa reduces 1.8% density. A density reduction from a baseline temperature in 248°F has a 0.2% density drop at 194°F and 2.3% drop at 140°F.

5.5 Ndes=100 Gyration

E-10 mixtures having an Ndes=100 were analyzed in a similar manner. There was a single E-10 25-mm NMAS mixture (the only 25-mm in the 30 layers) that significantly skewed the model, so it was removed from the analysis. This reduced the total layers for analysis from 8 to 7 layers. Figure 5.9 provides the ANOVA table of primary independent variables explaining change in lab compaction to Ndes.

Source	DF	Sum of Squares	Mean Square	F Value	Pr > F
Model	6	112.1132119	18.6855353	12.00	<.0001
Error	35	54.5022000	1.5572057		
Corrected Total	41	166.6154119			
R-Square	Coeff Var	Root MSE	ndes Mean		
0.672886	1.326649	1.247880	94.06262		
Source	DF	Type III SS	Mean Square	F Value	Pr > F
pg	1	1.58700000	1.58700000	1.02	0.3197
nmass	1	23.36418750	23.36418750	15.00	0.0004
source	1	8.66274510	8.66274510	5.56	0.0241
pressure	1	43.02619286	43.02619286	27.63	<.0001
temp	2	43.39989048	21.69994524	13.94	<.0001

Figure 5.9 Ndes=100 Gyration ANOVA Results

Four variables were significant, including NMAS, aggregate source, pressure, and temperature. PG grade was not significant. The measured R-square=67%. Two-way interactions were tested, with ANOVA results in Figure 5.10.

Source	DF	Sum of Squares	Mean Square	F Value	Pr > F
Model	18	123.1632508	6.8424028	3.62	0.0022
Error	23	43.4521611	1.8892244		
Corrected Total	41	166.6154119			

R-Square	Coeff Var	Root MSE	ndes Mean
0.739207	1.461251	1.374491	94.06262

Source	DF	Type III SS	Mean Square	F Value	Pr > F
pg	1	0.67222222	0.67222222	0.36	0.5567
nmas	1	26.52672222	26.52672222	14.04	0.0011
pg*nmas	1	4.29355556	4.29355556	2.27	0.1453
source	1	12.36270000	12.36270000	6.54	0.0176
pg*source	0	0.00000000	.	.	.
nmas*source	0	0.00000000	.	.	.
pressure	1	19.62410824	19.62410824	10.39	0.0038
pg*pressure	1	0.14145333	0.14145333	0.07	0.7868
nmas*pressure	1	0.67050750	0.67050750	0.35	0.5572
source*pressure	1	0.23920039	0.23920039	0.13	0.7252
temp	2	30.76879471	15.38439735	8.14	0.0021
pg*temp	2	1.88275500	0.94137750	0.50	0.6140
nmas*temp	2	1.28250500	0.64125250	0.34	0.7157
source*temp	2	4.85636725	2.42818363	1.29	0.2957
pressure*temp	2	0.02170000	0.01085000	0.01	0.9943

Figure 5.10 Ndes=100 Gyration ANOVA with Main Effects and Interactions

The ANOVA table indicates no significant interactions, and only the three main effects being significant. The R-Square increased from 67% to 74%.

A model having R-squared = 69% was developed to include the three main effects (NMAS pressure and temperature), with output in Figure D.6 (Appendix D), and illustrated model shown by Equation 5.6. Source was dropped from the model since it inflated the intercept to 98.2%, and the data were unbalanced with only one of seven layers having limestone source.

$$\begin{aligned}
 \text{Lab Density} &= 97.0 \\
 &+1.4*\text{NMAS} [1 \text{ if } 12.5\text{mm}; 0 \text{ otherwise}] \\
 &-2.0*\text{Pressure} [1 \text{ if } 300\text{kPa}; 0 \text{ if } 600\text{kPa}] \\
 &-2.4*\text{Temp} [1 \text{ if } \text{Temp}=140^\circ\text{F}; 0 \text{ otherwise}] \\
 &-0.5*\text{Temp} [1 \text{ if } \text{Temp}=194^\circ\text{F}; 0 \text{ otherwise}] \qquad (5.6)
 \end{aligned}$$

The 12.5-mm mixes have 1.4% greater density than 19mm. Pressure yields 2% less density with 300kPa, similar finding with the E-1 and E-3 mixes. Temperature also had a consistent effect, with greater density reduction at 140°F (2.4% less density than at 248°F) and lesser density reduction at 194°F (0.5% less density than at 248°F).

5.6 Summary of Lab Compaction Models

Table 5.1 summarizes the developed statistical models for pooled layer data, and individual ESAL series. The plant-produced mix intercept value was within 1% density of the lab-designed 96% density. For higher-ESAL mixes, a smaller NMAS of 12.5mm will yield an increase of 1.4% density. Pressure demonstrated a consistent relationship across all E-series mixes, in which the 300 kPa pressure yields a density about 1.8% less than 600 kPa. Temperature had an equally consistent relationship, where a baseline temperature of 248°F has density reduced by about 0.4% when compacting at 194°F, and 2.4% at 140°F.

Table 5.1 Summary of Lab Compaction Analysis

Model	Intercept	NMAS 19mm default, If 12.5mm then	Pressure 600kPa default, If 300kPa then	Temperature 248°F default, If 194°F then	Temperature 248°F default, If 194°F then
(1)	(2)	(3)	(4)	(5)	(6)
Pooled, 19 layers	95.6	ns	-1.8%	-0.4%	-2.3%
E-1, 4 layers	96.0	ns	-1.8%	-0.2%	-2.3%
E-3, 8 layers	95.4	+1.4%	-1.8%?	-0.2%	-2.3%?
E-10, 7 layers	97.0	+1.4%	-2.0%	-0.5%	-2.4%

5.7 Compaction Densification Index

To put the previous compaction analysis in context, the Construction Densification Index (CDI) was computed to assess the relative compaction at varying temperatures and pressures. The CDI counts the number of gyrations to compact the loose mix from 88% to 92% density in the SGC, as shown by Equation 5.8.

$$CDI = [\text{Gyrations at 92\% Gmm, } n] - [\text{Gyrations at 88\% Gmm, } n] \quad (5.8)$$

The data were stratified by ESAL series, since a different level of compaction is necessary to reach 4% air voids for E-1, E-3, and E-10 mixtures. The CDI plots for varying levels of temperature and pressure for E-1, E-3, and E-10 mixes are shown in Figures 5.11 through 5.13.

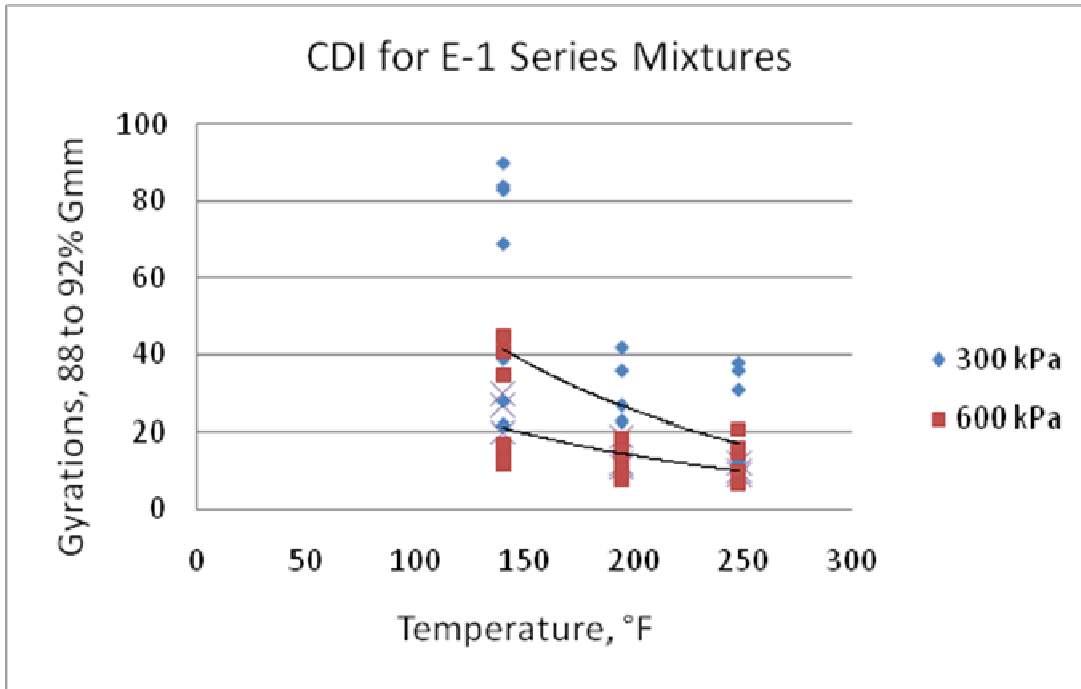


Figure 5.11 CDI for E-1 Mixtures

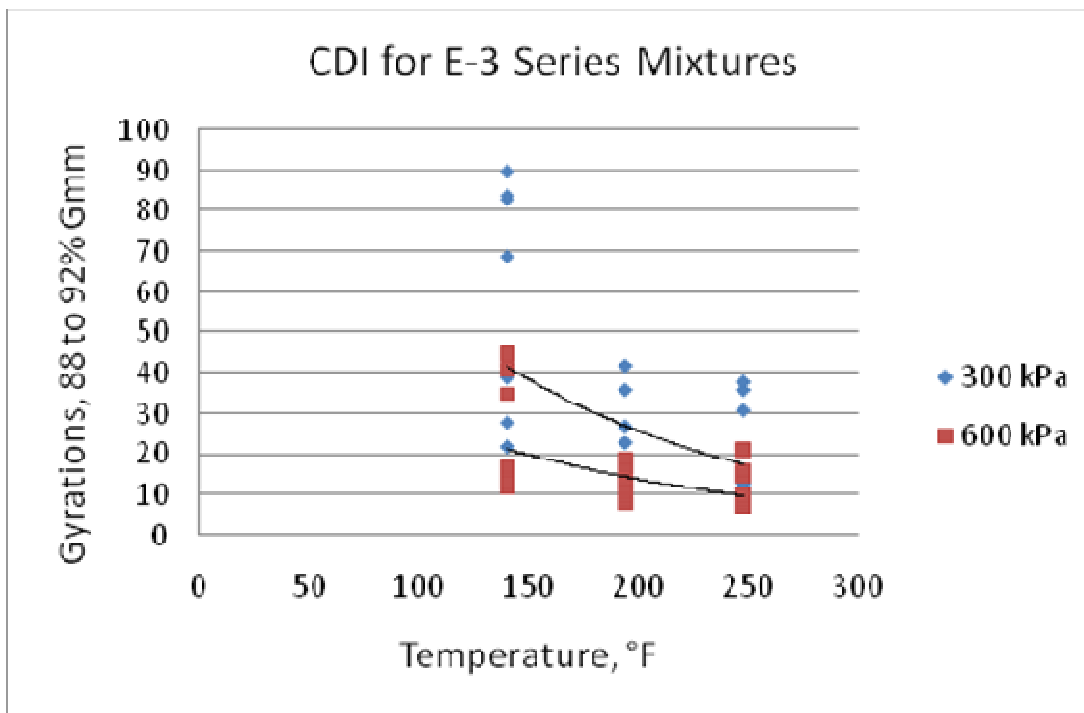


Figure 5.12 CDI for E-3 Mixtures

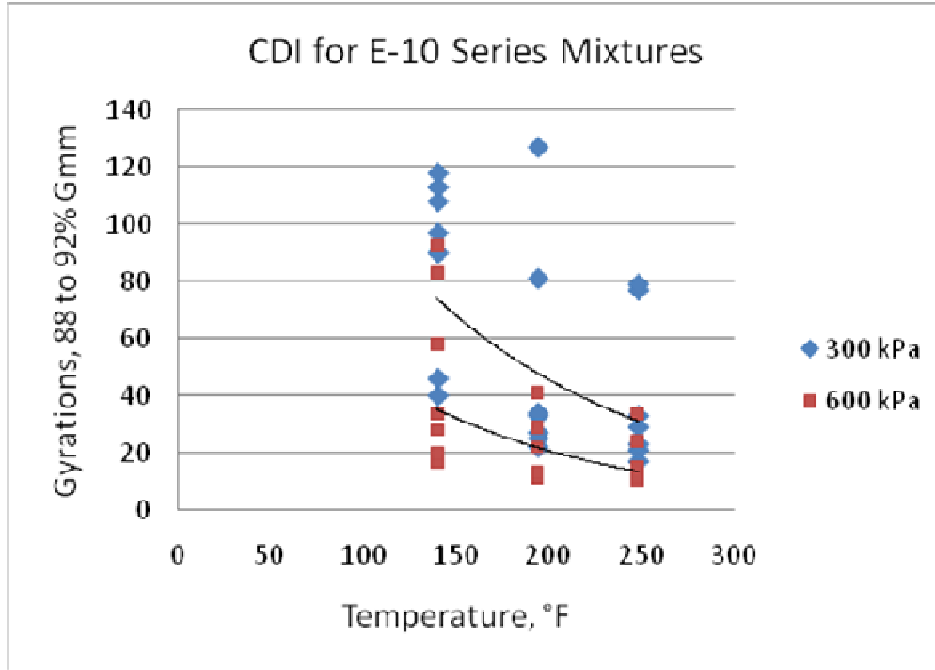


Figure 5.13 CDI for E-10 Mixtures

For all mixtures, temperature had a more pronounced effect at 300kPa than 600kPa, where it became increasingly more difficult to compact at lower temperatures. Higher pressure at 600 kPa had a lesser effect, where compaction effort at 194°F and 248°F were nearly equivalent, and more compaction needed at 140°F.

The E-10 mixture had a more dramatic effect, particularly at 140°F, where the 600 kPa pressure had a significantly higher level of compactive effort than the E-1 and E-3 mixtures. The number of gyrations for E-10 included observations ranging from 20 to 90, while the number of gyrations for E-1 and E-3 had a lower range of 10 to 45.

Aggregate source was identified as having a marginal effect on compactive effort (p-value ≈ 0.02), where gravels yielded a lower density of 1.2% when compared with limestone. This important factor was further investigated in Appendix E, by evaluating the JMF for specific aggregate properties, such as quarry/pit location, crushed face counts, percent thin and elongated pieces (by weight), and fine aggregate angularity (FAA).

5.8 Field and Lab Correlation

The relationship between lab and field compaction of plant-produced mix was investigated. Differences can occur when plant-mixed lab and field compacted specimens are subject to different temperatures and compaction pressures. These differences produce sources of variability in volumetric and mechanical testing, and can create barriers in the design and constructing an asphalt mixture. For this reason, the lab and field data sets were merged and then analyzed.

5.8.1 Merging Process

A single data set was created by merging all lab-compacted data with the field-compacted data. The merging process began by sorting the lab data by project, temperature, compaction temperature, and density, with a partial representation of the lab data set is provided in Figure 5.14.

Obs	project	temp	pressure	gyrno	density
1	8	140	300	1	79.7
2	8	140	300	2	80.9
3	8	140	300	3	81.8
4	8	140	300	4	82.6
5	8	140	300	5	83.2
6	8	140	300	6	83.7
7	8	140	300	7	84.2
8	8	140	300	8	84.6
.
53	8	140	300	53	90.0
54	8	140	300	54	90.0
55	8	140	300	55	90.1
56	8	140	300	56	90.1
57	8	140	300	57	90.2
58	8	140	300	58	90.2
59	8	140	300	59	90.2
60	8	140	300	60	90.2
61	8	140	300	61	90.3
62	8	140	300	62	90.3
63	8	140	300	63	90.4
64	8	140	300	64	90.4
65	8	140	300	65	90.5
66	8	140	300	66	90.5

Figure 5.14 Lab Compaction Data sorted by Project, Temperature, and Density

The number of gyrations at a specific density were averaged to create a single density value. The purpose was to create a sole lab density value for subsequent merging with the field data. Use of the median value was considered, but averaging provides an estimate of central tendency in the data. Figure 5.15 illustrates a partial display of gyration averaging by density. For illustration purposes, density of about 90% to 90.5% at 140°F and 300kPa are shown. An

example calculation for the four gyration values at 90.2% lab density (57, 58, 59, 60) yielded an average number of 58.5 gyrations.

Obs	project	pressure	temp	density	_TYPE_	_FREQ_	gyrno
1	8	300	140	79.7	0	1	1.0
2	8	300	140	80.9	0	1	2.0
3	8	300	140	81.8	0	1	3.0
43	8	300	140	90.0	0	2	53.5
44	8	300	140	90.1	0	2	55.5
45	8	300	140	90.2	0	4	58.5
46	8	300	140	90.3	0	2	61.5
47	8	300	140	90.4	0	2	63.5
48	8	300	140	90.5	0	2	65.5

Figure 5.15 Lab Compaction Averaging by Density and Gyration

Next, the field data were sorted by project and density, with a partial illustration shown in Figure 5.16. Temperature and total passes applied to the test section were also retained for later analysis. Note that multiple measurements at 90.3% and 90.5% density were recorded on the USH 8 project.

Obs	project	temp	totalpass	density
1	8	243	1	88.9
2	8	220	1	89.3
3	8	246	1	89.6
4	8	260	2	89.7
5	8	137	4	90.2
6	8	250	2	90.3
7	8	202	2	90.3
8	8	234	1	90.3
9	8	235	2	90.3
10	8	204	3	90.3
11	8	132	3	90.4
12	8	256	2	90.5
13	8	246	2	90.5
14	8	222	1	90.5
15	8	255	2	90.6
16	8	222	2	90.6

Figure 5.16 Field Compaction Data sorted by Project and Density

As illustrated in Figure 5.16, there are multiple density readings of equal value, many at different test sites, posing a potential problem for merging data sets. In an effort to merge multiple field densities with a unique lab density value, a single stand-alone value was needed. Thus, all temperature and passes for a particular field density value were averaged. This approach lost the ability to evaluate each density reading; however, this was the only feasible method to yield a single field density measurement for merging with lab density. Figure 5.17

illustrates this averaging. For example, the five 90.3% density readings averaged a temperature of 225°F and 2 passes.

Obs	project	density	_TYPE_	_FREQ_	temp	totalpass
1	8	88.9	0	1	243.000	1.0000
2	8	89.3	0	1	220.000	1.0000
3	8	89.6	0	1	246.000	1.0000
4	8	89.7	0	1	260.000	2.0000
5	8	90.2	0	1	137.000	4.0000
6	8	90.3	0	5	225.000	2.0000
7	8	90.4	0	1	132.000	3.0000
8	8	90.5	0	3	241.333	1.6667
9	8	90.6	0	2	238.500	2.0000

Figure 5.17 Lab Compaction Averaging by Density and Gyration

The final step in the merging process was to align the modified lab and field data sets by density, as shown partially in Figure 5.18. For certain lab density values, there may have been no field density values (and vice versa), so those observations were deleted. After merging, a total of 2,786 observations were created for analysis.

Obs	project	density	labtemp	pressure	gyrno	fieldtemp	totalpass
1	8	89.3	140	300	40.0	220.000	1.00000
2	8	89.3	194	300	8.0	220.000	1.00000
3	8	89.3	248	300	7.0	220.000	1.00000
4	8	89.3	140	600	7.0	220.000	1.00000
5	8	89.3	194	600	5.0	220.000	1.00000
6	8	89.6	140	300	45.5	246.000	1.00000
7	8	89.6	248	600	5.0	246.000	1.00000
8	8	89.7	140	300	47.0	260.000	2.00000
9	8	89.7	194	300	9.0	260.000	2.00000
10	8	89.7	248	300	8.0	260.000	2.00000
11	8	89.7	140	600	8.0	260.000	2.00000
12	8	90.2	140	300	58.5	137.000	4.00000
13	8	90.3	140	300	61.5	225.000	2.00000
14	8	90.3	194	300	11.0	225.000	2.00000
15	8	90.3	194	600	7.0	225.000	2.00000
16	8	90.4	140	300	63.5	132.000	3.00000
17	8	90.4	248	300	10.0	132.000	3.00000
18	8	90.4	140	600	10.0	132.000	3.00000
19	8	90.5	140	300	65.5	241.333	1.66667
20	8	90.5	194	300	12.0	241.333	1.66667
21	8	90.5	248	600	7.0	241.333	1.66667

Figure 5.18 Merged Lab and Field Compaction Data

To develop a perspective on the merged data, simple statistics were computed, and are shown in Figure 5.19. These fundamental statistics also provided an assessment of any potential outliers created in the data, which none were found.

Variable	N	Mean	Std Dev	Minimum	Maximum
density	2786	90.90345	2.05064	80.9	96.8
pressure	2786	437.50897	149.50584	300.0	600.0
labtemp	2786	191.22828	44.03133	140.0	248.0
gyrno	2786	41.26813	31.30342	1.0	160.0
fieldtemp	2786	179.69484	38.52305	105.0	261.0
totalpass	2786	4.65188	2.72468	1.0	17.0

Figure 5.19 Simple Statistics of Merged Data

5.8.2 Data Analysis - Correlations

The merged data set created a unique opportunity to understand any relationship between lab and field compaction, along with any associated variables. A correlation matrix was prepared for each combination of variables, with output in Figure 5.20. The correlation coefficient is a numerical measure that quantifies the strength of linear relationships, where coefficients near 1.000 indicate a strong relationship.

Pearson Correlation Coefficients, N = 2786 Prob > r under H0: Rho=0						
	density	pressure	labtemp	gyrno	fieldtemp	totalpass
density	1.00000	0.15597 <.0001	0.18461 <.0001	0.47456 <.0001	-0.42715 <.0001	0.50846 <.0001
pressure	0.15597 <.0001	1.00000	-0.06756 0.0004	-0.18515 <.0001	-0.04026 0.0336	0.07179 0.0001
labtemp	0.18461 <.0001	-0.06756 0.0004	1.00000	-0.24473 <.0001	-0.07992 <.0001	0.10775 <.0001
gyrno	0.47456 <.0001	-0.18515 <.0001	-0.24473 <.0001	1.00000	-0.19832 <.0001	0.39555 <.0001
fieldtemp	-0.42715 <.0001	-0.04026 0.0336	-0.07992 <.0001	-0.19832 <.0001	1.00000	-0.65117 <.0001
totalpass	0.50846 <.0001	0.07179 0.0001	0.10775 <.0001	0.39555 <.0001	-0.65117 <.0001	1.00000

Figure 5.20 Correlation Matrix of Merged Data

Correlations between the lab measures (pressure, lab temperature, gyrations) and field measures (field mat temperature, total passes) are the principal focus of the analysis. Two of the higher correlations between the lab and field were: (1) lab gyrations vs. total field passes, and (2) lab gyrations vs. field temperature. First, a fairly strong correlation of 39.6% was measured between lab gyrations and total field passes to achieve the same mutual density value. This is an expected finding since it suggests that lab mixtures requiring more compaction will require more field passes, for the same density level. A simple plot in Figure 5.21 was prepared to help

illustrate the relationship between number of gyrations and total passes to achieve equivalent density.

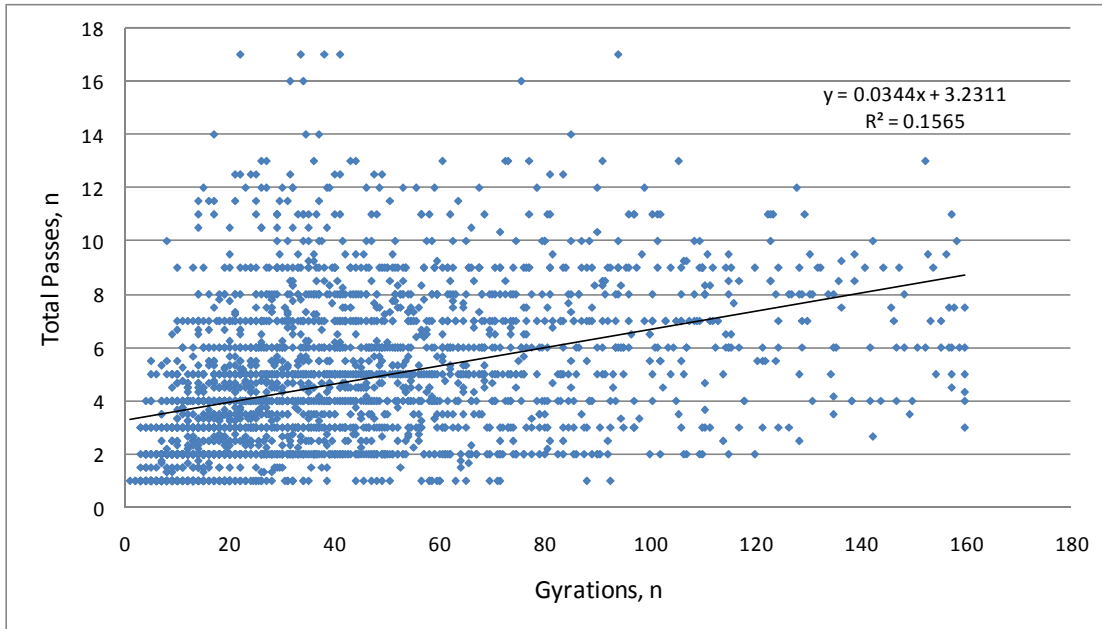


Figure 5.21 Correlation of Lab Gyration with Roller Passes

No strong trend can be observed with the concentrated cluster at lower gyrations and passes, so the data were truncated. Figure 5.22 illustrates the correlation with the reduced data sets. The plot of gyrations ≤ 40 was selected to identify any trend. A slight relationship was measured with the linear model, where each 10 gyrations require an additional roller pass; however, this model is very weak.

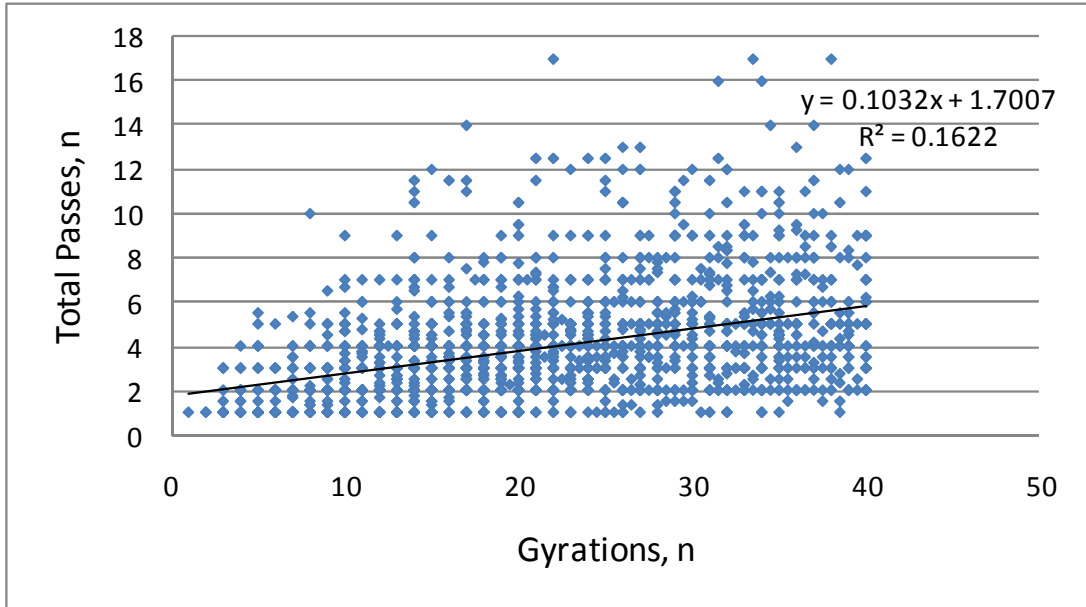


Figure 5.22 Correlation of Lab Gyration with Roller Passes

To further understand the relationship of field passes and lab gyrations, the data were stratified by gyratory pressure at 300 kPa and 600 kPa. Figure 5.23 illustrates the upward trend between gyrations and passes, where greater pressure at 600 kPa requires less gyrations for total cumulative roller passes.

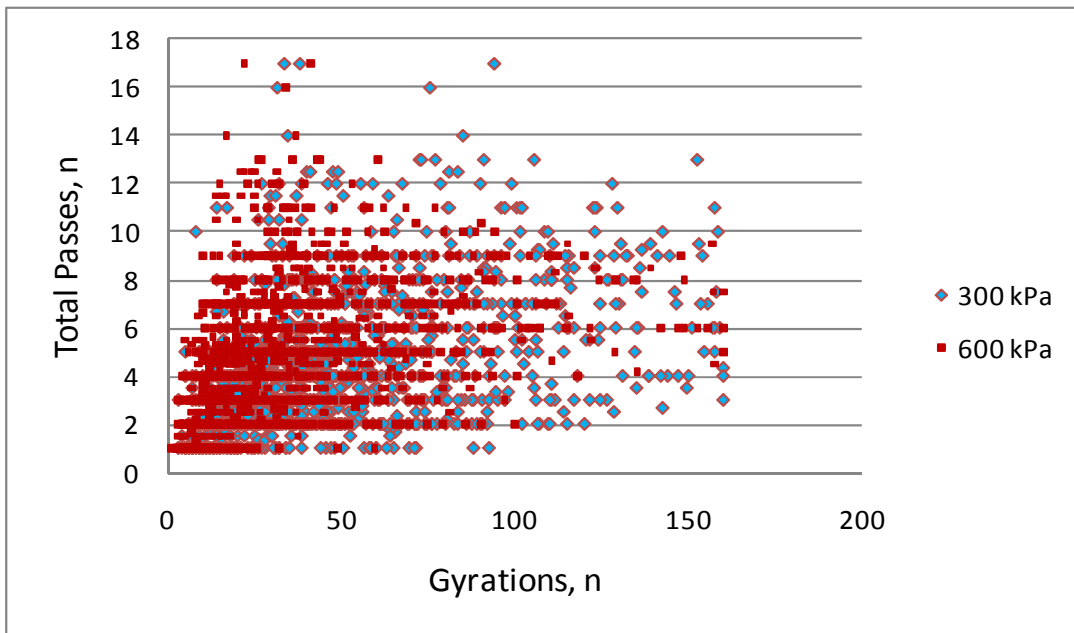


Figure 5.23 Effect of Pressure on Lab Gyration with Roller Passes

Since the 600 kPa pressure is used for lab design and plant-produced mix production, the data were reduced to 600 kPa pressure only. Figure 5.24 illustrates the 600 kPa data only, where a strong upward trend existed between the gyrations and passes. It must be noted that the linear model for the relationship does not meet the assumption of normally and independently distributed residuals.

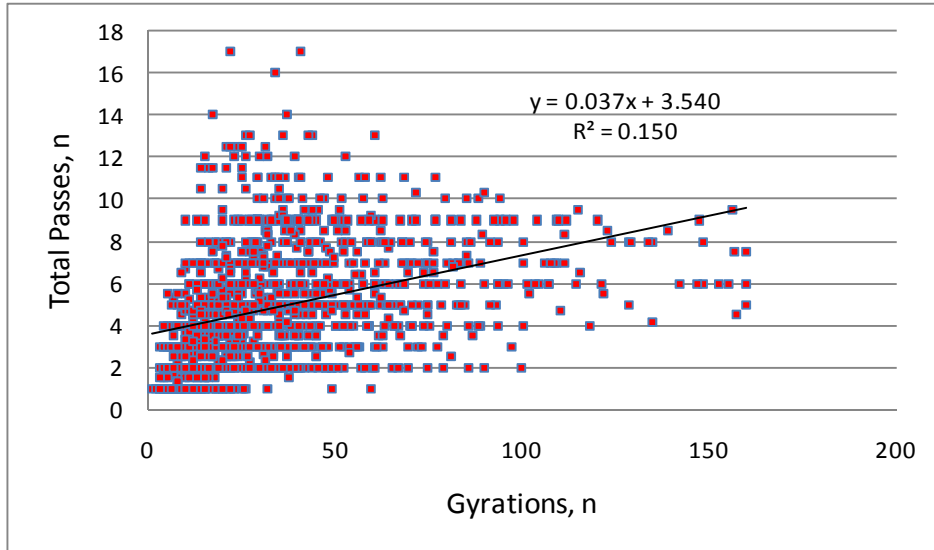


Figure 5.24 600 kPa Pressure for Lab Gyrations and Roller Passes

The 600 kPa pressure data were stratified by temperature, as shown in Figure 5.25. The fanning appearance in the data are illustrated by the temperature readings to achieve the mutual density values between lab and field compaction.

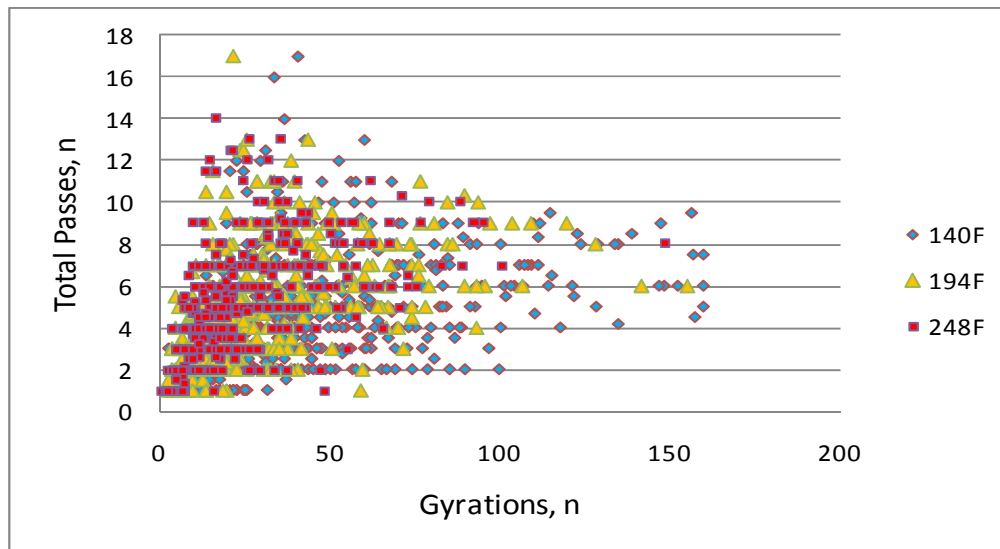


Figure 5.25 Temperature at 600 kPa Pressure for Lab Gyrations and Roller Passes

Second, a lower correlation of 19.8% was measured between lab gyrations and field temperature. Figure 5.26 plots the number of gyrations and field mat temperature. As the number of gyrations increases, the mat temperature decreases. This relationship may suggest that higher Ndes mixes required additional compactive effort, in some cases compaction occurring at lower temperatures.

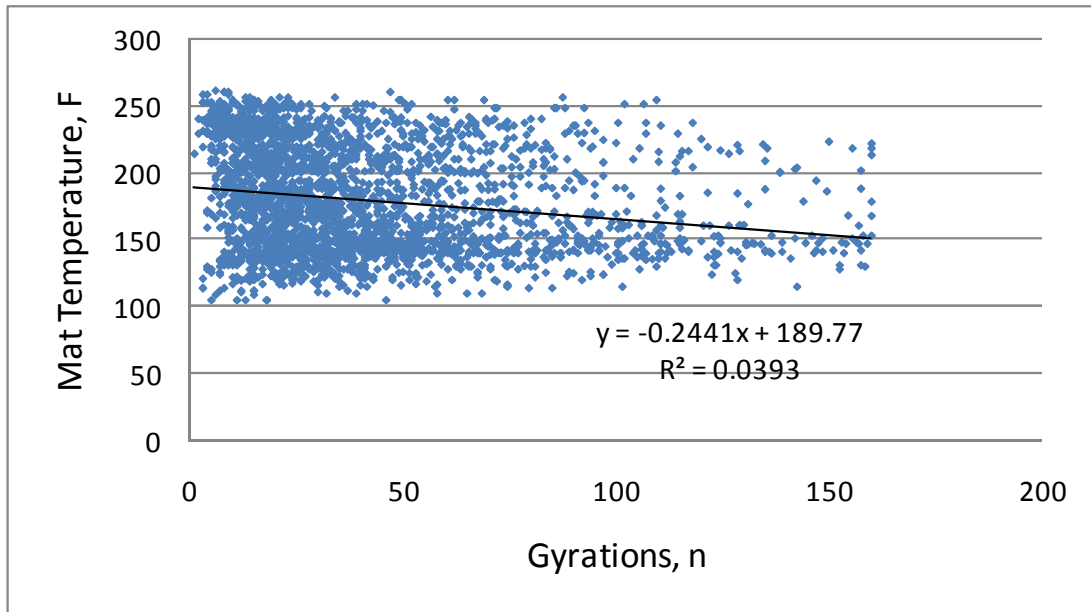


Figure 5.26 Correlation of Lab Gyration with Field Mat Temperature

CHAPTER 6 WARM MIX ASPHALT

6.1 Introduction

Recently, there have been significant laboratory and field research efforts related to assessment of the impact of Warm Mix Asphalt (WMA) Technologies in terms of constructability, performance, and energy demand to construct roads. The focus of these research efforts was to determine if application of WMA is feasible and to quantify its environmental impacts. In September 2008 an opportunity arose to supplement the research study to include an initial evaluation of Warm Mix Asphalt using the previously defined laboratory and field compaction parameters. This chapter will present the results of the laboratory and field analysis, and how the findings from the warm mix field demonstration relate to the objectives of this study.

6.2 Lab Investigation

6.2.1 Data Collection and Comparison to QC Data

The aim of the field project was to evaluate the ability of a surfactant-based WMA additive to allow a conventional HMA mix to be placed at lower compaction temperatures, and allow for use of higher amounts of Recycled Asphalt Pavement (RAP) in the mix design. It is expected that these changes in compaction temperature and mix design components will achieve the same in-place density as a conventional HMA mix. The laboratory component of the WMA evaluation is focused on comparison of the WMA mixes to the HMA in terms of mixture workability. Mixture workability and temperature sensitivity are evaluated using %Air Voids at the design level of gyrations and the previously defined Construction Densification Index (CDI). The HMA mix design was a 12.5-mm E1 mix using 20% RAP, samples of the HMA mix were collected from the site. The mix design was modified to include the WMA additive and incorporate RAP Percentages of 30%, 35%, and 40%. Unfortunately, the QC technician was only able to collect mix samples of the WMA 30% RAP and WMA 40% RAP mixes during production. A summary of the mix proportions and JMF properties are provided in Tables 6.1 and 6.2.

Table 6.1 Summary of Mix Proportions

Aggregate	HMA	WMA - 30%	WMA-40%
3/4" Crushed Gravel	50%	35%	35%
5/8" Screened Sand	30%	35%	25%
RAP	20%	30%	40%
Opt AC	0.5%	4.7%	4.7%
% Gmm Design	2.53	2.543	2.545
% Gmm Measured	2.549	2.540	2.545

Table 6.2 Summary of Job Mix Properties

Summary of Mix Properties						
Source	3/4" Crushed Gravel	5/8" Screened Sand	RAP	JMF HMA	JMF WMA - 30%	JMF WMA 40%
Percent Passing						
3/4"	100.0%	100.0%	100.0%	100.0%	100.0%	100.0%
1/2"	90.0%	100.0%	95.0%	94.0%	95.0%	94.5%
3/8"	70.0%	97.0%	90.0%	82.1%	85.5%	84.8%
#4	42.0%	87.0%	74.0%	61.9%	67.4%	66.1%
#8	28.0%	81.0%	64.0%	51.1%	57.4%	55.7%
#16	21.0%	77.0%	57.0%	45.0%	51.4%	49.4%
#30	16.0%	59.0%	47.0%	35.1%	40.4%	39.2%
#50	12.0%	18.0%	28.0%	17.0%	18.9%	19.9%
#100	8.0%	3.0%	13.0%	7.5%	7.8%	8.8%
#200	5.8%	1.5%	8.0%	5.0%	5.0%	5.6%
Crushed 1 Face	100.0%	32.0%	82.0%	90.6%		
Crushed 2 Face	99.0%	30.0%	80.0%	89.3%		
Flat and Elongated	1.4%	1.0%	0.7%	1.2%		
FAA				41.30		
Water Abs	1.4%	0.5%	1.0%	1.1%		

One item of note in the previously provided information is the difference in maximum specific gravity (Gmm) between the HMA Mix Design provided on the project and the value measured using the field sample collected. In subsequent analysis, the Gmm measured for the UW laboratory sample was used.

Table 6.3 provides design data for the HMA mix and quality control data from the WMA-30% and WMA 40% mixes. Table 6.3 also provides a comparison of the HMA design data to the field sample collected.

Table 6.3 Summary of Field QC Data

Aggregate	HMA - Design	HMA - UW	WMA - 30% QC	WMA-40%
Compaction Temp (F)	275	275	215	221
Nini - 7	91.2%	90.4%	92.0%	93.8%
Ndes - 60	96.1%	95.4%	97.0%	98.3%
Nmax- 75	96.6%	95.8%	N/A*	N/A*
VMA	14.10	12.86	12.30	11.00
*WMA QC samples were compacted to Ndes.				

Comparison of the HMA data from the field sample collected to the mix design show variations in air voids of approximately 0.7% between the densification data provided in the mix design and laboratory compacted values. Furthermore, the QC data from the WMA samples show that even with a ~50°F reduction in temperature and 10-20% additional RAP the densification of the mix exceeds that of the HMA mix design used on the project. The laboratory portion of the study will investigate the densification characteristics of the WMA and HMA mixes and their dependence on compaction temperature and pressure further.

6.2.3 Experimental Design

The focus of the laboratory study was to assess the impacts of the WMA additives and mix design changes on densification behavior and its dependence on compaction temperature and pressure. Mixes were compacted at three temperatures ranging from 194°F to 275°F and compaction pressures of 300 kPa and 600 kPa. The experimental design and summary of compactions is provided in Table 6.4.

Table 6.4 Experimental Design – Evaluation of WMA

Mix	Compaction Temperature (F)	Compaction Pressure	
		300	600
HMA	194	X	X
	230	X	X
	275	X	XX
WMA 30% RAP	194	XX	XX
	230	XX	XX
	275	X	XX
WMA 40% RAP	194	XX	XX
	230	XX	XX
	275	X	XX
Total Samples		13	16

The letter “X” denotes a compacted sample; due to lack of materials, two replicates for each temperature/pressure combination could not be prepared. The total mixes compacted at each level of pressure are also provided in the table. Mixes were compacted using the Pressure Distribution Analyzer (PDA) plate developed by UW Madison (Faheem and Bahia 2004) to measure the resistive forces of the mix during compaction. Previous research defined an index to assess workability, the Construction Force Index (CFI), which measures the force required to densify the mix from 88% Gmm to 92% Gmm. The rapid densification of the E1 mix did not allow for an adequate number of data points to be collected to calculate the workability index. Therefore, the CFI was eliminated as a potential evaluation criteria for mixture workability in this particular study. Instead, comparison of mixture behavior was conducted using the previously defined evaluation parameters of air voids at the design number of gyrations (N=60) and the construction densification index (CDI), which is defined in Equation 5.8. Consistent with the procedures previously detailed in this report, the significance of these parameters will be evaluated using general linear models to perform ANOVA analysis.

6.2.4 Results and Analysis

Comparison of the air voids at 60 gyrations, the design compactive effort for E-1 level mixes for compaction pressures of 300kPa and 600kPa over the range of previously defined compaction temperatures are provided in Figures 6.1 and 6.2, respectively.

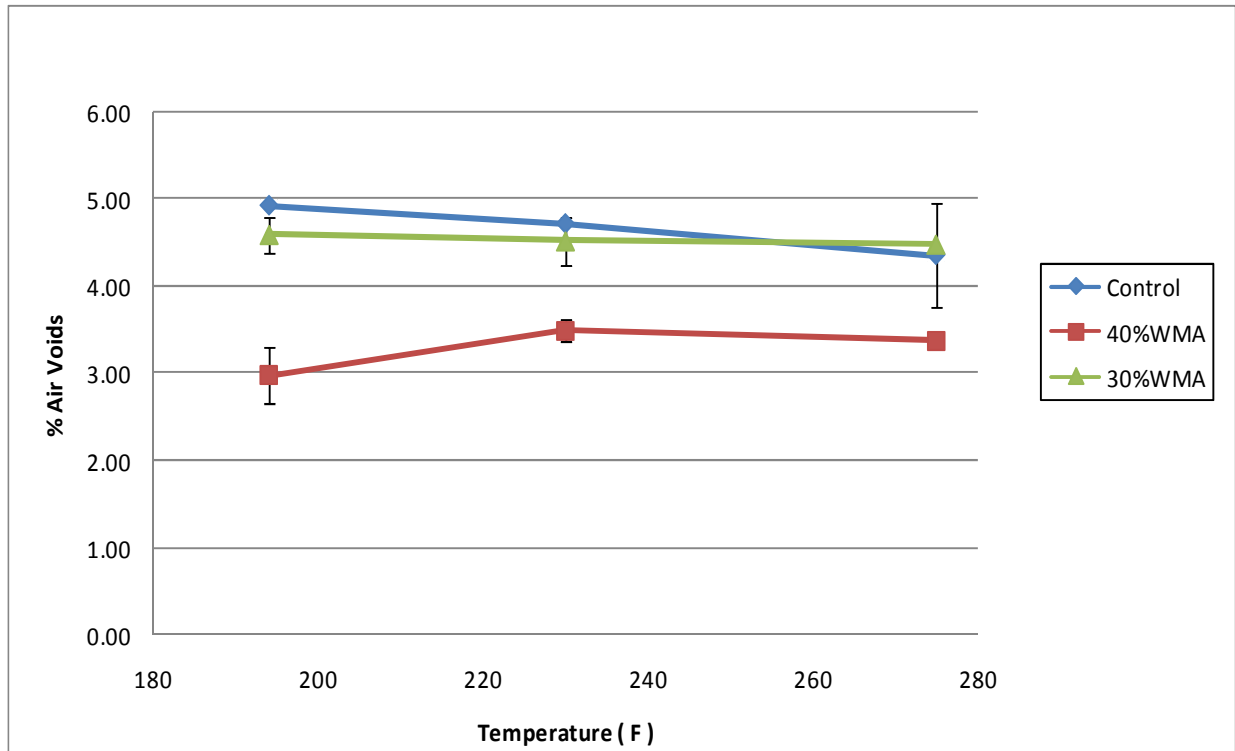


Figure 6.1 Air Voids vs. Temperature – Ndes = 60 gyrations at 300kPa

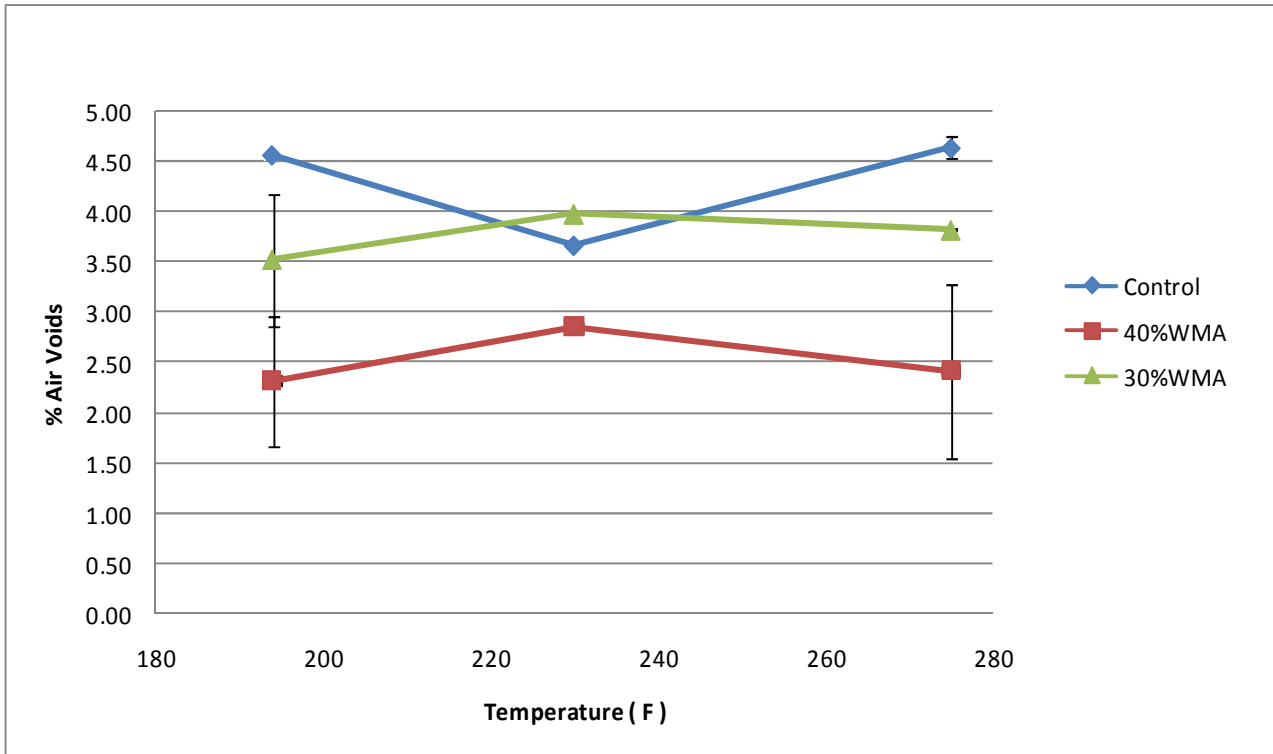


Figure 6.2 Air Voids vs. Temperature – Ndes = 60 gyrations at 600kPa

At both compaction pressures, the three mixes behaved similarly in terms of ranking. The HMA mix is defined as “Control” in these and subsequent figures. For both compaction pressures, the HMA mix and the WMA 30% RAP mixes vary by no more than approximately 1% air voids with the 40% WMA mix at lower air void levels across all compaction temperatures. Both the HMA and 30% WMA mix approach the specification limit of 4% air voids at Ndes. The deviation of the 40% WMA mix from the target air void level is consistent with the previously presented QC results and is hypothesized to be caused by the added amount of P200 in the mix caused by increasing RAP percentages. In-place quantities were insufficient to modify the JMF to achieve design density with the 40% RAP mix. Furthermore, the mixes show little temperature sensitivity across the approximately 80°F temperature range tested. This finding is consistent with Equation 5.3, which specifies a 0.2% adjustment to predicted Air Voids for a compaction temperature of 194°F. ANOVA analysis at a 95% confidence level was used to determine if the performance of these mixes are statistically different and the significance of pressure and temperature. Results of this analysis are provided in Table 6.5.

Table 6.5 ANOVA Analysis – Air Voids at Ndes

Source	DF	Seq SS	Adj SS	Adj MS	F	P
Mix Type	2	15.327	13.800	6.899	76.93	0.00
Pressure	1	3.263	2.953	2.953	32.92	0.00
Temperature	2	0.188	0.021	0.011	0.12	0.89
Mix Type*Pres	2	0.109	0.072	0.036	0.40	0.68
Mix * Temp	4	0.954	0.901	0.225	2.51	0.10
Pres*Temp	2	0.199	0.173	0.086	0.96	0.41
Mix*Pres*Temp	4	0.312	0.312	0.078	0.87	0.51
Error	11	0.987	0.987	0.090		
Total	28	21.338				
R -Squared	95.38%					

Results of the ANOVA analysis indicate that mix type and compaction pressure are the only two factors that significantly affect the level of air voids in the mix at Ndes. These results confirm the previously stated observation that the mixes did not appear to be sensitive to temperature changes at either compaction pressure. Insensitivity to temperature could be due to a combination of two factors: the E-1 mix design being relatively easy to compact since it is intended for lower traffic, and the range of compaction temperatures evaluated in the lab being too narrow to see significant changes in densification. The Tukey Pairwise Comparison test was used to evaluate if the behavior of the three mix designs was statistically different at a 95% confidence level. Based on data presented in the previous figures, it could be assumed qualitatively that the WMA-40% mix behaved differently than the HMA and WMA-30%, however, differences between the HMA and WMA-30% were not easily observed. The Tukey Test provides a quantitative method to further evaluate these differences. Results are provided in Table 6.6.

Table 6.6 Results of Tukey Pairwise Comparison Test

Mix	Difference of Means	SE	T-Value	Adj P-Value
WMA - 30% - HMA	-0.5610	0.1497	-3.7500	0.0083
WMA - 40% - HMA	-1.7440	0.1497	-11.6500	0.0000
WMA - 30% - WMA-40%	-1.1830	0.1321	-8.9610	0.0000

Results of the pairwise comparison show quantitatively that the HMA and WMA-30% mixes are statistically different. However, differences between these two mixes are considerably smaller than differences observed in comparisons with the WMA-40% mix. The differences are negative for the comparisons of WMA minus HMA, indicating the WMA mixes are undergoing significantly more compaction for a given temperature and level of compactive effort.

The second evaluation parameter was the Construction Densification Index (CDI). The CDI was used to indicate the level of compactive effort required for the mix to densify from 12%

to 8% air voids. In the field, this parameter relates to the densification experienced by the mix during compaction by the breakdown and finish rollers. The CDI for the 300 kPa and 600 kPa compaction pressures are provided in Figures 6.3 and 6.4, respectively.

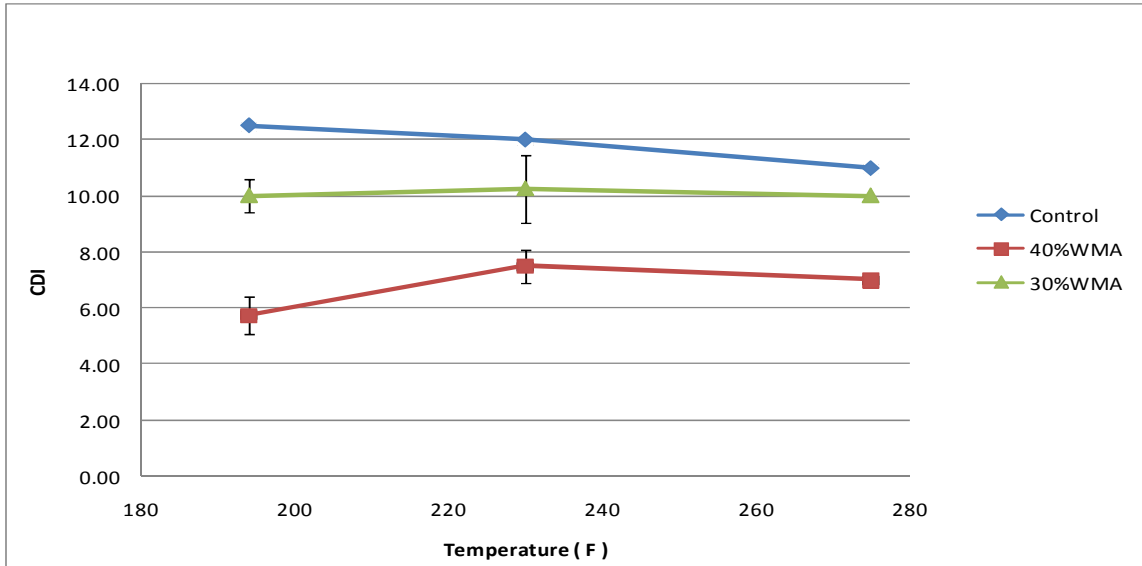


Figure 6.3 CDI vs. Temperature at 300kPa

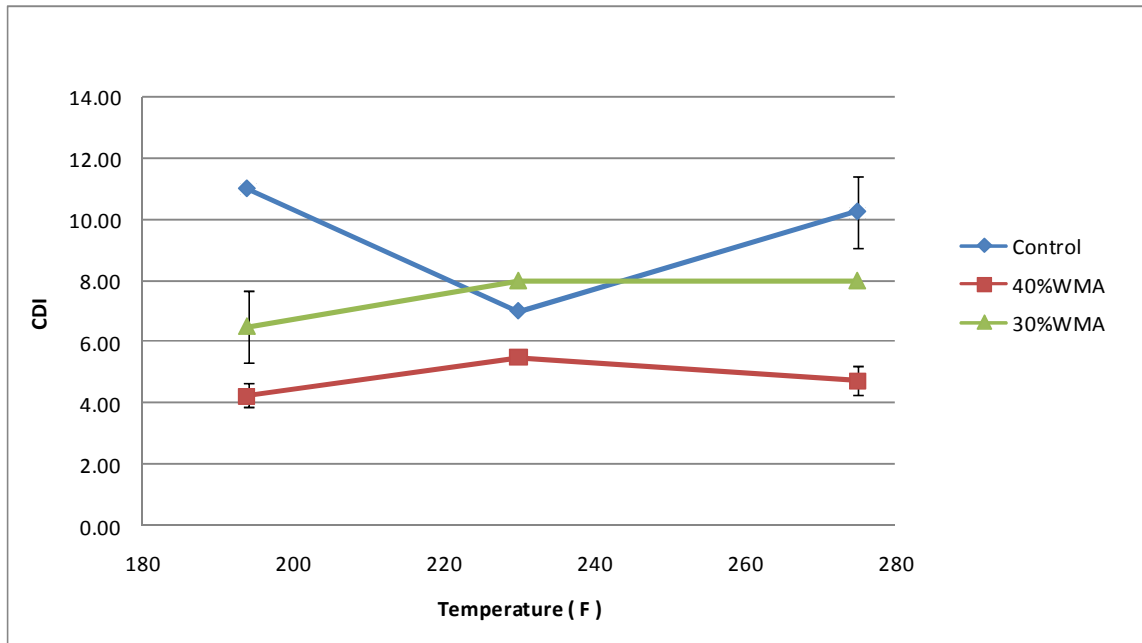


Figure 6.4 CDI vs. Temperature at 600kPa

As expected, the results for CDI are very similar to those provided in the comparison of Air Voids at Ndes with the HMA and WMA-30% mixes exhibiting similar behavior with the

WMA-40% mix showing significantly lower CDI values across all compaction temperatures. At 300 kPa, all three mixes show very little sensitivity having consistent rank for all three compaction temperatures. This trend is also shown in the WMA mixes compacted at 600 kPa, however the HMA mix shows more fluctuation in CDI across the compaction temperatures with a range of approximately 3 gyrations. This general behavior was also demonstrated to a lesser extent in the air voids at Ndes for the HMA sample in Figure 6.2. Tenderness could partly be the cause, however further investigation is needed to identify the reason for this behavior. The ANOVA results and Tukey pairwise comparisons are provided in Tables 6.7 and 6.8, respectively.

Table 6.7 ANOVA Analysis – CDI

Source	DF	Seq SS	Adj SS	Adj MS	F	P
Mix Type	2	15.327	13.800	6.899	76.93	0.00
Pressure	1	3.263	2.953	2.953	32.92	0.00
Temperature	2	0.188	0.021	0.011	0.12	0.89
Mix Type*Pres	2	0.109	0.072	0.036	0.40	0.68
Mix * Temp	4	0.954	0.901	0.225	2.51	0.10
Pres*Temp	2	0.199	0.173	0.086	0.96	0.41
Mix*Pres*Temp	4	0.312	0.312	0.078	0.87	0.51
Error	11	0.987	0.987	0.090		
Total	28	21.338				
R -Squared	95.38%					

Table 6.8 Results of Tukey Pairwise Comparison Test – CDI

Mix	Difference of Means	SE	T-Value	Adj P-Value
WMA - 30% - HMA	-1.8330	0.4667	-3.92	0.01
WMA - 40% - HMA	-4.7500	0.4667	-10.16	0.00
WMA - 30% - WMA-40%	-2.9170	0.4125	-7.07	0.00

Results for CDI using ANOVA and pairwise comparison to identify differences between mixture behavior are similar to those provided for air voids at Ndes. The ANOVA analysis identified mix type and compaction pressure as the only two significant factors, confirming that these mixes are not sensitive to change in temperature. The pairwise comparison showed significant differences between all mixes, the difference between WMA-30% and HMA was smaller relative to the other combinations. Furthermore, CDI was significantly reduced for both WMA mixes relative to the HMA, indicating that the use of the WMA additive results in more workability, even with the addition of higher percentages RAP.

In conclusion, the results of the laboratory evaluation demonstrate that the use of the WMA additive allowed for an increased amount of RAP in the mix without a significant

detriment to mixture workability as shown using the CDI. Both the HMA and WMA 30% mixes approached the Superpave criteria of 4% air voids at Ndes over all compaction temperatures, the air void levels in the WMA 40% were considerably lower than the 4% target, this result was consistent with the field QC data collected and was due to increased P200 in the mix. Although these results are promising, one project is not sufficient to draw any firm conclusions. A more rigorous evaluation of the impacts of a variety of warm mix additives and processes on workability and relationships between the laboratory and field is recommended. Evaluation of workability should also include mixes designed for higher traffic levels, varying in gradation, and using modified binders. A control mix is needed in subsequent field sections in which the only change in the mix design is the addition of a WMA additive. If possible, this section should also be compacted at warm mix temperatures to provide a means of comparison for in-place density and field performance. Field sections should also be of adequate size to allow for measurement of emissions and energy consumption to quantify the environmental benefits of WMA relative to HMA.

6.3 Field Investigation

A field evaluation of WMA was conducted on the same E-1 mixture, paved in Adams County, County Highway E, on September 5, 2008. On this project, both a traditional hot-mix asphalt (HMA) and WMA with varying levels of RAP were paved within the same day.

6.3.1 Data Collection

A field evaluation of WMA was conducted on an E-1 mixture, County Highway E in Adams County, paved on September 5, 2008. WMA having three different levels of RAP and a traditional hot-mix asphalt (HMA) were paved within the same day. Density data were collected from a total of 39 test sites, with a breakdown provided in Table 6.9.

Table 6.9 Test Site Summary

Mixture Type (1)	Number of Test Sites (2)	Gmm (3)
WMA with 30% RAP	12	2.540
WMA with 35% RAP	3	2.543
WMA with 40% RAP	6	2.545
HMA with 20% RAP	18	2.549
Total	39	---

Nuclear readings of 15 seconds in duration were taken between roller passes with the contractor’s QC gauge. A minimum of 2 readings were taken after each roller pass, then averaged to yield a single density value for each test site. No cores were sampled and actual QC density values were adjusted to the owner/consultant (QA) gauge for analysis. A comparison was made with a QA gauge, and it was determined that the QC gauge was reading an average of

2.5% lower density than the QA gauge due to calibration to a different set of blocks. Based on this calibration offset, all QC nuclear density readings had 2.5% density added to the raw readings. Maximum specific gravity (G_{mm}) changed by mixture type, and the appropriate lab values were used to compute density.

Figure 6.5 shows the heat gun reading of 235°F as the Warm Mix Asphalt exits the mixing drum, and Figure 6.6 measures the mat temperature of 195°F behind the paver. A single breakdown roller in the vibratory mode (Ingersoll-Rand DD110), and a single cold roller operating primarily in the vibratory mode (Svedala Dynapac CC422), were used to compact the mat.



Figure 6.5 Warm Mix Temperature Reading at Drum Discharge



Figure 6.6 Warm Mix Temperature Reading behind Paver

6.3.2 Data Analysis – WMA versus HMA during Compaction

Data analysis methods were similar to the 30 layers presented earlier. Both the traditional density value and the new ‘Density Delta’ measure were designated as the dependent variable, and independent variables were mixture type (WMA or HMA), temperature, passes between density readings, total passes, and difference between actual density and 96% Gmm (‘dens96’).

A fundamental question was whether a similar range of density can be measured behind the rollers for both WMA and HMA mixtures. To formally test if a difference exists, an Analysis of Variance (ANOVA) using the Generalized Linear Model (GLM) approach was conducted among all density values behind roller passes. Figure 6.7 provides the output, where there was no statistical difference between WMA and HMA (p-value = 0.776). The average density readings behind the roller were nearly identical with 91.2% and 91.3% for WMA and HMA, respectively. The standard deviation of WMA was higher because of decreasing density values as the amount of RAP increased (analyzed later in this section).

Source	DF	Sum of Squares	Mean Square	F Value	Pr > F
Model	1	0.2967837	0.2967837	0.08	0.7760
Error	97	353.5428122	3.6447713		
Corrected Total	98	353.8395960			
R-Square	Coeff Var	Root MSE	density Mean		
0.000839	2.151853	1.909128	88.72020		
Level	-----density-----				
	N	Mean	Std Dev		
1 WMA	50	91.1666000	2.13021126		
2 HMA	49	91.2755102	1.65322042		

Figure 6.7 GLM for Density Readings between WMA and HMA

Next, the mean density gain between passes, ‘Density Delta’, was used to compare WMA and HMA. Figure 6.8 provides the GLM output, where no statistical difference was found between density gains among the two mixture types. On average, the density gain in WMA was 3.2% density, while HMA was 2.8% density. Standard deviation measures were very similar.

Source	DF	Sum of Squares	Mean Square	F Value	Pr > F
Model	1	3.2123657	3.2123657	0.37	0.5441
Error	97	840.8442000	8.6684969		
Corrected Total	98	844.0565657			
R-Square	Coeff Var	Root MSE	densdelta Mean		
0.003806	99.20997	2.944231	2.967677		
Level	-----densdelta-----				
	N	Mean	Std Dev		
1 WMA	50	3.14600000	2.88388981		
2 HMA	49	2.78571429	3.00457984		

Figure 6.8 GLM for Delta Density between WMA and HMA

The other independent variables and 2-way interactions were added to the model to assess their relative effect on density gains. Figure 6.9 illustrates the output for Type III Sum of Squares, where the variable is entered last into the model; this is a more robust assessment of variables than Type I Sum of Squares where the variable is entered first.

Source	DF	Sum of Squares	Mean Square	F Value	Pr > F
Model	10	460.4778000	46.0477800	10.56	<.0001
Error	88	383.5787656	4.3588496		
Corrected Total	98	844.0565657			
R-Square	Coeff Var	Root MSE	densdelta Mean		
0.545553	70.35085	2.087786	2.967677		
Source	DF	Type III SS	Mean Square	F Value	Pr > F
wmahma	1	0.21519059	0.21519059	0.05	0.8247
temp	1	18.06255534	18.06255534	4.14	0.0448
temp*wahma	1	4.03043887	4.03043887	0.92	0.3389
totalpasses	1	3.20546498	3.20546498	0.74	0.3935
totalpasses*wahma	1	1.90722847	1.90722847	0.44	0.5100
temp*totalpasses	1	39.45910643	39.45910643	9.05	0.0034
dens96	1	3.15865791	3.15865791	0.72	0.3969
dens96*wahma	1	9.26100023	9.26100023	2.12	0.1485
temp*dens96	1	0.01502829	0.01502829	0.00	0.9533
totalpasses*dens96	1	5.77096748	5.77096748	1.32	0.2530

Figure 6.9 GLM for Delta Density Main Effects and Interactions

No main effect or interaction involving WMA versus HMA were significant, and only the temperature main effect and temperature*totalpasses interaction were significant. As concluded earlier, temperature has a significant impact on the ability to achieve density gains, and a declining temperature interacts with the increasing number of passes.

6.3.3 Data Analysis – WMA versus HMA Final Density

A fundamental question concerning Warm Mix Asphalt is whether a final resultant density can be achieved similar to traditional Hot Mix Asphalt, given the compaction effort is nearly equal. To address this question, the final density readings among WMA and HMA were compared using a formal statistical analysis, with GLM output in Figure 6.10.

Source	DF	Sum of Squares	Mean Square	F Value	Pr > F
Model	1	0.05863248	0.05863248	0.03	0.8709
Error	37	81.01111111	2.18948949		
Corrected Total	38	81.06974359			
R-Square	Coeff Var	Root MSE	density Mean		
0.000723	1.608316	1.479692	92.00256		
Level	-----density-----				
	N	Mean	Std Dev		
1 WMA	21	91.9666667	1.90613046		
2 HMA	18	92.0444444	0.70060665		

Figure 6.10 GLM for Final Density between WMA and HMA

The total degrees of freedom were 38, one less than the sample size of 39 test sites. A total of 21 WMA test sites were compared with 18 HMA test sites. The result of the hypothesis test for mean final density between WMA and HMA concluded no statistical difference. Means for WMA and HMA were nearly identical, when rounded to 92.0%. Variability in WMA final density was larger by a factor of 2.5 for the standard deviation, which was the result of different RAP levels in the mix (analyzed in the next section).

Figure 6.11 plots the final density versus number of passes for both mix types. Warm Mix had much more variability, ranging from 89% to 96%, while the Hot Mix was much more consistent between 90.5% and 93.5% density. This variability may be attributed to changes in the job mix proportions (i.e., bin percentages, asphalt metering, etc.). It is recommended that additional controlled experiments be conducted to assess whether this feature can be found on other projects.

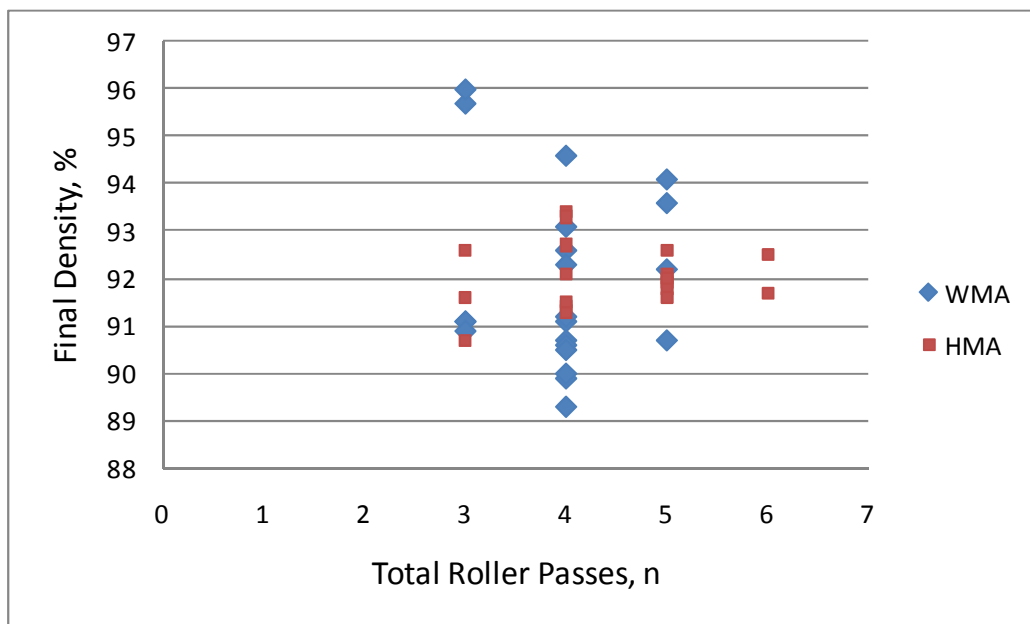


Figure 6.11 Final Density Comparison for WMA and HMA

6.3.4 Data Analysis – WMA at Varying RAP

The final portion of the analysis compared the varying RAP percentages with final density. Test sites and corresponding sample sizes for the three RAP levels (30%, 35%, and 40%) were unbalanced, with $n = 12, 3,$ and $6,$ respectively. During plant production, the mix was transitioned from 30% to 40% RAP within a few truckloads, primarily corresponding to the 35% RAP test sections. Because of this short transition period and small sample size, the 35% RAP data was removed from the dataset. A formal analysis of variance for 30% and 40% RAP was conducted with output in Figure 6.12.

Source	DF	Sum of Squares	Mean Square	F Value	Pr > F
Model	1	26.35111111	26.35111111	10.33	0.0054
Error	16	40.80666667	2.55041667		
Corrected Total	17	67.15777778			

R-Square	Coeff Var	Root MSE	density Mean
0.392376	1.733778	1.597002	92.11111

Level of rap	N	Mean	Std Dev
30	12	92.9666667	1.87438879
40	6	90.4000000	0.65726707

Figure 6.12 GLM for Varying RAP Levels in WMA

The means of the 12 30% RAP test sites were compared with six 40% RAP test sites. The mean at 30% RAP was 93.0%, while the 40% RAP was 90.4%, and strong statistical difference was determined (p-value < 0.006). Variability in 30% RAP was much higher by a factor of 3.

Figure 6.13 plots the final density versus number of passes for both RAP contents. For similar compaction levels of 3 and 4 passes, the 30% RAP mixture achieved a consistently higher density. Several explanations for this include more traditional asphalt binder to heat at a lower WMA mixing temperature, gradation characteristics of the different RAPs, and compactibility characteristics of the RAP portion of the mixture. Based on this analysis, lower RAP levels are recommended for WMA mixtures to achieve higher density levels. However, this recommendation is based upon a single project; additional research is needed to investigate this relationship.

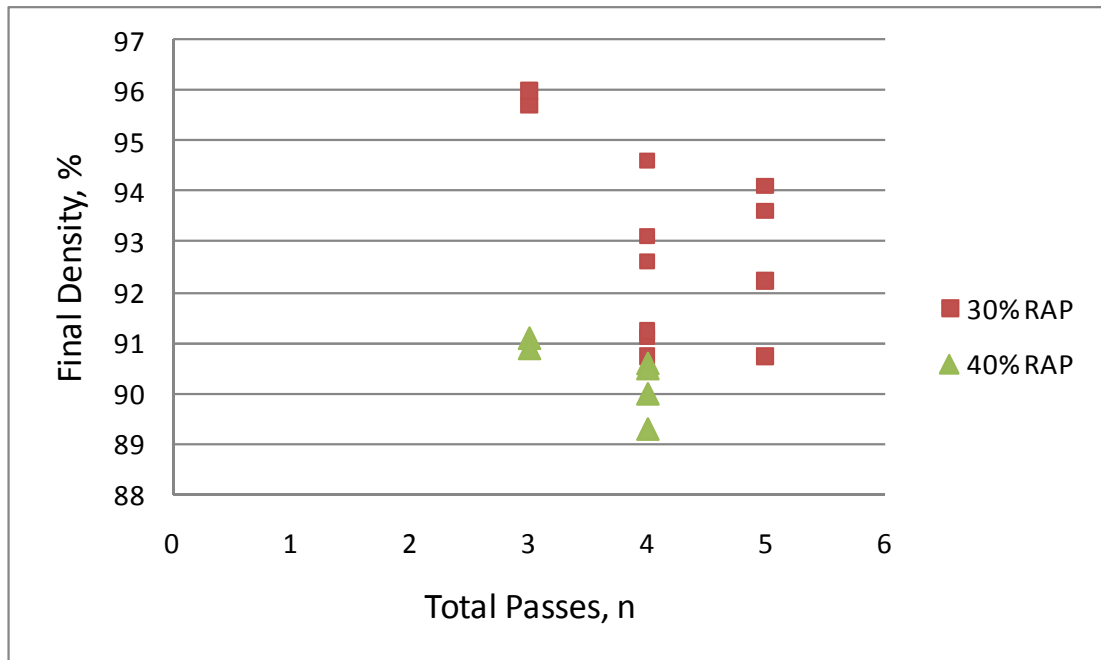


Figure 6.13 Final Density Comparison for RAP Contents

CHAPTER 7 Development of Permeability and Density Criteria

7.1 Introduction

A primary objective in this study is to measure how as-built density and permeability affect asphalt pavement performance in Wisconsin. To achieve this objective, an as-built construction database must be created to provide comparison with actual performance after a period of several years. Since it will require several years to measure actual performance, this study is limited to creating the as-built construction database. This effort largely required the integration of several databases. The integration process involved an understanding of several elements including data types and formats to be collected and managed, location referencing, database structures and relationships, and software requirements.

7.2 Location Referencing Based on Reference Point System

A single database system modeled after the Meta-Manager system was created. It consists of individual spreadsheets in Microsoft Excel™ format for each of the 29 construction projects paved in 2007, where all project data were furnished by WisDOT and/or the contractor. Approximately 80 projects having 10,000 tons or more were paved in 2007; however, data were only provided for 29 of these projects.

The basic location reference database is founded on the WisDOT reference point (RP) system. This involved the conversion of construction projects termini, as well as the start and end locations of all test lots/sublots in terms of the WisDOT reference point system. Once this was accomplished, construction data measures for as-built density, JMF, and material properties associated with particular lots/sublots for given reference point interval were aligned with future performance data.

Figure 7.1 provides a schematic of overlaying databases for the purpose of assigning data attributes to pavement segments based on the Reference Point System. In this figure, performance data are identified by sequence numbers, while design, traffic, and environmental data are continuous across the given constructed segment. Construction data for the contractor's Job Mix Formula (JMF) and IRI ride data overlay the entire project. Where there was a JMF change during construction, the date and subplot of the change were recorded and applied to the RP. Construction mix properties and density required the actual as-built test values, where mix properties were in the individual subplot test result, and density was the average of 7 nuclear density tests per 750-ton lot. Because of the relatively large standard deviation associated with determining density, at this time it is recommended that the average for the lot be used in assigning an as-built density to the appropriate RP and sequence number. Further research is recommended to determine the appropriate assignment of as-built construction data to a given location reference.

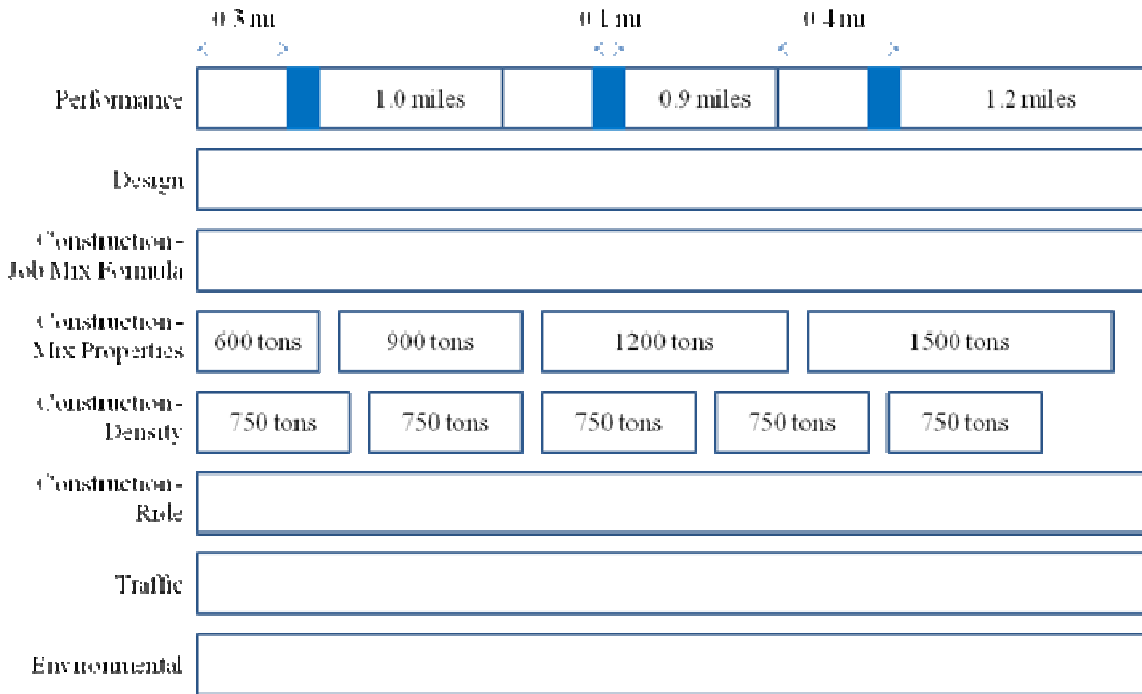


Figure 7.1 Overlay of Databases using Reference Point System

7.3 Conversion of Construction Stationing to Reference Point

At the present time, WisDOT does not have a defined procedure for relating construction stationing to the reference point system. In order to complete the alignment and integration of applicable HMA databases to model pavement performance over time, construction plan sets and field data were necessarily obtained. Plan sets for each pavement project, formatted as PDF files, were obtained via email or an ftp website (<ftp://ftp.dot.state.wi.us/pub/>) used by WisDOT, depending upon the method preferred by each regional office.

Using the existing reference point system, an overlay of the project stationing with the pre-existing reference point system was completed for several sample projects. In order to measure the PDI, an automated performance survey is taken continuously from an intersection or some other distinguishable feature, such as a bridge or county line. The recorded length begins 0.3 miles from a reference point for a length of 0.1 miles; therefore, as depicted by the shaded areas in Figure 7.2, the performance is recorded between 0.3 to 0.4 miles after a pre-determined point.

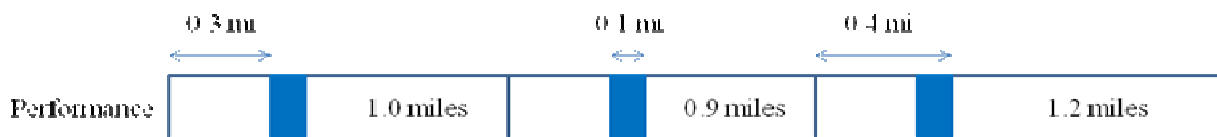


Figure 7.2 Ride Quality Measurement Methodology.

A sample overlay is displayed in Table 7.1 for USH 18 in Iowa County. Here, the sequence number, depicted as the name for the RP used in the PDI measurement, was matched up with the stationing of the project. The *Length* column is the length between sequence numbers. The *Beg STA* column is the beginning project stationing from the plan sets. The *Start 0.3 – 0.4* column is the *Beg STA* column with 1,584 feet added (number of feet to reach 0.3-mile starting point). The *End 0.3 – 0.4* column is the *Beg STA* column with 2,112 feet added (number of feet to reach 0.4 miles). In this example, any data obtained between station 1040+02 and 1045+30 can be correlated with the PDI sequence number of 20820 to determine the performance of the HMA pavement over time.

Table 7.1 Sequence Number/Project Stationing Overlay (USH 18, Project I.D. 1660-04-73)

Sequence Number (1)	Length, mile (2)	Intersection (3)	Beg STA, ft. (4)	Start 0.3 - 0.4, ft. (5)	End 0.3 - 0.4, ft. (6)
20820	1.47	GRANT-IOWA CO LN	102418.0	104002.0	104530.0
20830	1.51	CTH XX INT R	110188.3	111772.3	112300.3
20840	1.02	ANDERSON LA INT	118170.1	119754.1	120282.1
20850	1.00	VICKERMAN RD INT	123523.8	125107.8	125635.8
20860	1.01	STH 80N & CTH G L	128831.6	130415.6	130943.6
20870	0.72	CTH J INT R	134135.7	135719.7	136247.7
20880	1.26	WHITSON RD INT R	137927.5	139511.5	140039.5
20890	1.01	STH 39E INT R	144617.9	146201.9	146729.9
20900	0.94	SUNNY SLOPE RD R	149949.9	151533.9	152061.9
20910	1.09	BETHLEHEM RD INT	154922.5	156506.5	157034.5
20920	1.00	CTH Q (BERG RD) R	160658.7	162242.7	162770.7
20930	0.90	TN OF DODGEVILLE	165938.7	167522.7	168050.7
20940	1.26	CTH Q (SURVEY RD)	171084.3	172668.3	173196.3
20950	0.78	USH 18W INT L	177737.1	179321.1	179849.1

7.4 Assignment of Construction Data to Sequence Numbers

The alignment of construction data measures with PDI sequence numbers is necessary to determine the effects each asphaltic concrete property has on the durability of road sections over time. Construction data measures included in the alignment were aggregate gradation, aggregate blend, bitumen data, mixture data, optimum asphalt content properties, and JMF properties. For each of the properties, field and design data was included if available.

7.4.1 Job Mix Formulas

JMF data were obtained from the contractor for the project. An example of a portion of the JMF data overlay table is displayed in Table 7.2.

Table 7.2 Sequence Number/JMF Data Overlay (USH 45, Project I.D. 9847-03-60)

Sequence Number	Date Placed	Daily Average, 1/2"	Daily Average, 3/8"	Daily Average AC Calc	JMF, 1/2"	JMF, 3/8"	JMF AC Calc	JMF Pbe	JMF P _{0.075} /Pbe	JMF Plant Mix Temp.
(1)	(2)	(3)	(4)	(5)	(6)	(7)	(8)	(9)	(10)	(11)
61760	8/9/07	93.4	82.5	5.07	91.3	81.9	5.10	4.64	0.87	280-320
61770	8/9/07	93.4	82.5	5.07	91.3	81.9	5.10	4.64	0.87	280-320
61780	8/9/07 & 8/6/07	92.8	82.0	5.13	91.3	81.9	5.10	4.64	0.87	280-320
61790	8/6/07 & 8/2/07	91.6	81.3	5.20	90.7	80.9	5.20	4.70	0.81	280-320
61800	8/2/07	91.3	81.2	5.19	90.7	80.9	5.20	4.70	0.81	280-320
61810	8/2/07	91.3	81.2	5.19	90.7	80.9	5.20	4.70	0.81	280-320
61820	8/2/07	91.3	81.2	5.19	90.7	80.9	5.20	4.70	0.81	280-320
61830	8/2/07	91.3	81.2	5.19	90.7	80.9	5.20	4.70	0.81	280-320

The data displayed under the heading column heading *JMF* are the optimum values for each of the sieve sizes as designed; these values were obtained directly from the documents provided by the contractor, B.R. Amons & Sons, Inc. However, the *Daily Average* values that are displayed were calculated. Each day, anywhere from two to five different samples was taken, and a moving average calculated for the four most recent test results. In order to obtain the *Daily Average* for these cells, a weighted average was taken utilizing the daily average from each day. This weighted average was then input to Table 7.2. The *Daily Average* calculation methodology for the 1/2" sieve for Sequence Number 61780 is as follows: four samples were taken on 8/9/07, which had a daily average of 93.4, and three samples were taken on 8/6/07, which had a daily average of 91.9. These averages were then weighted, as shown by Equation 7.1, to provide the *Daily Average* value that was entered into Table 7.2.

$$DailyAverage_{1/2"} = \frac{4 * 93.4 + 3 * 91.9}{7} = 92.8 \quad (7.1)$$

7.4.2 Density

Density data was also obtained from the documents provided by the contractor. A sample of this data is provided in Table 7.3.

Table 7.3 Sequence Number and Density Data Overlay (USH 45, Project I.D. 9847-03-60)

Sequence Number (1)	Date Placed (2)	Density Lower Lift (3)	Density Upper Lift (4)
61760	8/9/07	-	93.2
61770	8/9/07	-	92.9
61780	8/9/07 & 8/6/07	-	93.1
61790	8/6/07 & 8/2/07	-	93.3
61800	8/2/07	-	93.4
61810	8/2/07	-	92.6
61820	8/2/07	-	93.5
61830	8/2/07	-	93.7

Determining the density for the upper and lower lifts follows the same calculation procedure as the *Daily Average* described earlier, depending upon whether the lift was placed in one or two days. For this project, only a wedge and single surface layer were paved.

7.4.3 Mix Properties

Multiple mix properties were given in the documents provided by the contractor. A sample of the data provided is given in Table 7.4.

Table 7.4 Sequence Number and Mix Properties Overlay (USH 45, I.D. 9847-03-60)

Sequence Number (1)	Date Placed (2)	Daily Average Gmm (3)	Daily Average Gmb (4)	Daily Average Voids (5)	Daily Average VMA (6)	Opt. Gmm (7)	Opt. Gmb (8)	Opt. Voids (9)	Opt. VMA (10)
61760	8/9/07	2.509	2.420	3.5	14.7	2.516	2.416	4.0	14.8
61770	8/9/07	2.509	2.420	3.5	14.7	2.516	2.416	4.0	14.8
61780	8/9/07 & 8/6/07	2.509	2.416	3.7	14.9	2.516	2.416	4.0	14.8
61790	8/6/07 & 8/2/07	2.510	2.410	4.0	15.1	2.513	2.413	4.0	15.0
61800	8/2/07	2.510	2.410	4.0	15.1	2.513	2.413	4.0	15.0
61810	8/2/07	2.510	2.410	4.0	15.1	2.513	2.413	4.0	15.0
61820	8/2/07	2.510	2.410	4.0	15.1	2.513	2.413	4.0	15.0
61830	8/2/07	2.510	2.410	4.0	15.1	2.513	2.413	4.0	15.0

Data that are not displayed in Table 7.4, but are included in the spreadsheet, were design aggregate blend, bitumen data, mixture data, and aggregate data. The *Daily Average* columns were again calculated as described earlier, and the *Optimum* values were recorded directly from the documents provided by the contractor.

7.5 Assignment of Permeability Data to Sequence Numbers

Air and water permeability were measured on 30 layers during the 2007 paving season; 15 of the construction projects had testing performed on the surface layer. After the pavement cooled, water and air permeability testing occurred on five (5) of the 20 test sites per layer. The NCAT permeameter was filled and the drop in water height was recorded per unit time. The ROMUS air permeameter was used to collect data for a comparative analysis, with test locations offset 6 to 12 inches longitudinally to avoid the wet pavement surface. A complete discussion of the test procedures and data collection is provided in Chapter 3.

Figure 7.3 provides an aggregate test site comparison of equivalent water permeabilities measured by the ROMUS device versus NCAT device across all projects. Air permeameter values had a higher order of magnitude than the water permeameter, by a factor of approximately 5. Except for a few outliers, the water permeability was generally less than 300×10^{-5} cm/sec, and air permeability was generally less than $1,500 \times 10^{-5}$ cm/sec.

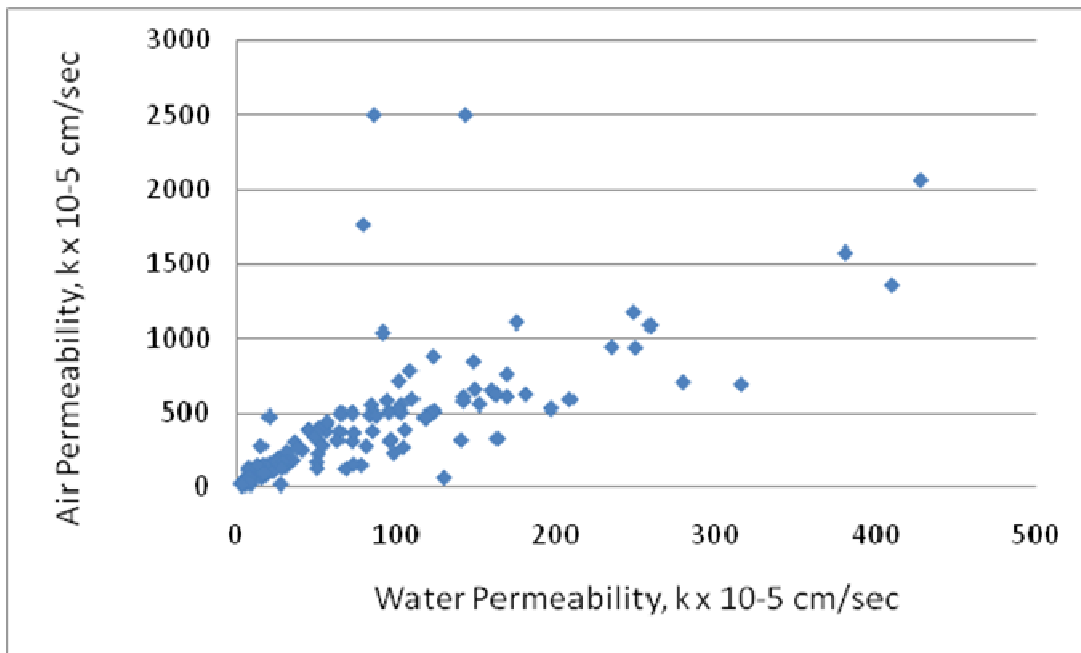


Figure 7.3 Comparison of Permeability Methods

Figures 7.4 and 7.5 provides an aggregate test site comparison for core density and both air and water permeability, respectively. In general, there was a slight downward trend, where an increase in density caused a decrease in permeability. By comparison, the 2002 WHP permeability-density study found that no trend existed for fine-graded gravel-source mixes, but a trend was observed for fine-graded limestone-sourced mixes (Russell et al. 2004). Also by comparison, NCHRP 9-27, a comprehensive density-permeability study that evaluated 37 mixtures, found that variability of permeability among mixtures was very high with some more

permeable at 90 to 92% density and others not (Brown et al. 2004). Both studies concluded that the permeability-density relationship is mixture specific with respect to as-constructed pavement density, say in the range of 90% to 93%.

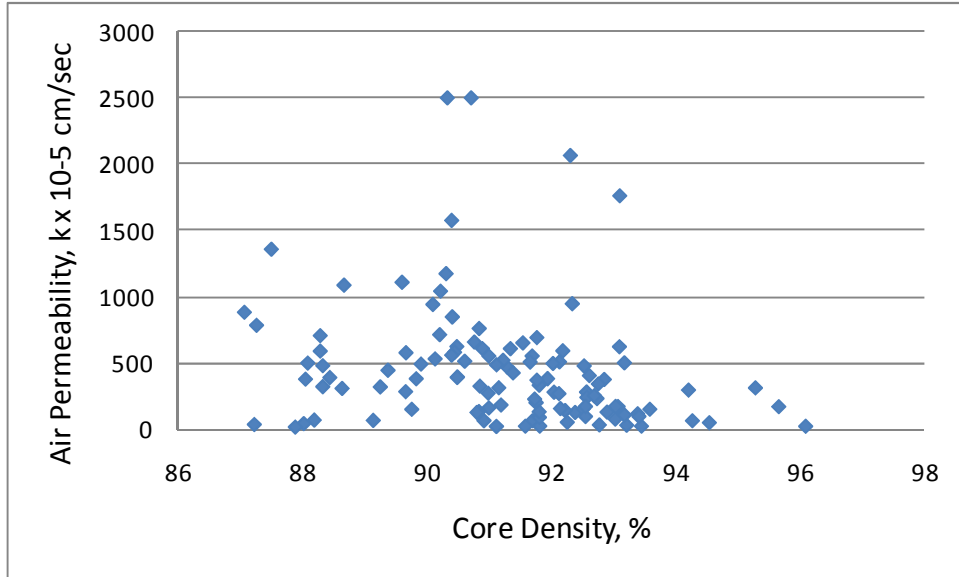


Figure 7.4 Comparison of Air Permeability and Core Density

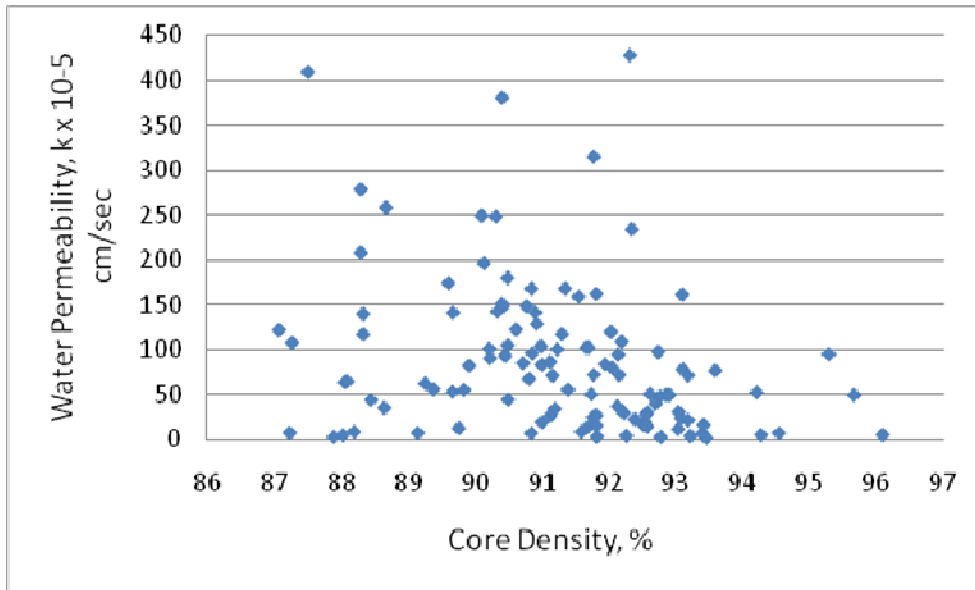


Figure 7.5 Comparison of Water Permeability and Core Density

Air and water permeability measures from the tested layers were assigned to the performance data set. Only 15 of the construction projects had testing performed on the surface layer. Since it was not feasible to conduct permeability testing within each Sequence Number segment, a modeling approach was developed to estimate permeability based on core densities. This process included developing a regression equation between permeability and cores, estimating permeability for a range of density values using the equation, then assigning the permeability to specific density values within each Sequence Number. There is variability in this process, especially with only 5 cores per project; however, this approach provides the most scientifically defensible approach for determining the relationship between permeability and density. The statistical models are provided in the created performance data set.

7.6 Performance-Construction Data Set

A stand-alone spreadsheet file merging construction data with Sequence Number is included as a separate attachment to this report. Table 7.5 summarizes the 31 project segments paved in 2007 where plan sets and as-built construction data were collected. Unfortunately, it was not possible to collect data from each project paved in 2007 having more than 10,000 tons of HMA, which totaled about 80 projects. A combination of donated time from WisDOT and contractors to compile data, along with warranted pavement projects having no formal QC/QA testing, were major factors impacting data collection. On a majority of projects, no surface permeability tests were conducted; these projects were either not included in the 30 layers or where permeability testing occurred on the lower layers. Beginning around 2011, this spreadsheet is to be used to develop performance models.

Table 7.5 Sequence Number and Mix Properties Overlay

Project ID	Route ID	Route No.	Termini	County	Region	Beginning Sequence Number	Ending Sequence Number	Sequence Sections with Data	Permeability Measurements
1610-40-60	STH	13	FIFIELD - PARK FALLS	PRICE	NC	14500	14501	2	None
1146-22-71	STH	15	APPLETON - NEW LONDON	OUTAGAMIE	NE	60960	60990	3	None
2200-10-70	USH	18	WEST BLUE MOUND ROAD	MILWAUKEE	SE	21860	21870	2	Surface layer
1660-04-73	USH	18	MONTFORT - DODGEVILLE ROAD	IOWA	SW	20820	20950	13	Surface layer
4085-22-71	STH	32	GREENLEAF - DEPERE	BROWN	NE	39220	39290	6	Surface layer
9130-08-71	STH	32	TOWNSEND - NCL	OCONTO	NE	39980	40020	5	None
3240-05-72	STH	32	SHERIDAN ROAD	KENOSHA	SE	38070	38080	1	Lower layer, 19mm
5121-09-71	STH	33	LA CROSSE-CASHTON/CT F-KIRSCHNE	LA CROSSE	SW	40980	41040	7	Lower layer, 19mm
1160-00-74	IH	39	STEVENS POINT - MOSINEE	PORTAGE	NC	49160	49180	3	None
1160-00-75	IH	39	STEVENS POINT - MOSINEE	PORTAGE	NC	49200	49260	7	None
1166-04-76	IH	39	PLAINFIELD - STEVENS POINT	PORTAGE	NC	49740	49860	12	Lower layer, 12.5mm
1166-04-79	IH	39	WESTFIELD - PLAINFIELD	WAUSHARA	NC	48820	48920	11	None
1166-04-80	IH	39	COLUMBIA COUNTY LINE - WESTFIELD	MARQUETTE	NC	48670	48760	10	Lower layer, 12.5mm
9847-03-60	USH	45	SUMMIT LAKE - ONEIDA COUNTY LINE	LANGLADE	NC	61760	61830	8	None
4110-15-71	USH	45	S CNTY LINE - OSHKOSH	WINNEBAGO	NE	60620	60670	6	None
4660-07-71	STH	47	APPLETON RD, CITY MENASHA	WINNEBAGO	NE	63170	63190	2	None
6990-04-60	STH	54	PLOVER - WAUPACA	PORTAGE	NC	75080	75240	16	None
5730-05-65	STH	56	GENOA-VIROQUA	VERNON	SW	77860	77950	10	None
1381-02-70	STH	57	MEQUON ROAD (STH 57/STH 167)	OZAUKEE	SE	78500	78520	3	None
2230-01-70	STH	59	GREENFIELD AVE	MILWAUKEE	SE	81330	81340	2	Lower layer, 19mm
2310-02-60	STH	60	Commerce Blvd	WASHINGTON	SE	82950	82970	3	None
9000-10-71	STH	64	OREGON ST - FOSTER ST	LINCOLN	NC	87160	87170	1	None
9160-12-71	STH	64	VILLAGE OF POUND	MARINETTE	NE	87940	87940	1	None
6280-03-73	STH	66	POLONIA TO ROSHOLT	PORTAGE	NC	88800	88860		None
9090-03-60	STH	70	EAGLE RIVER - ALVIN	VILAS	NC	92330	92430	11	Surface layer
6517-08-71	STH	76	STEPHENSVILLE - SHIOCTON	OUTAGAMIE	NE	96040	96070	4	None
9260-03-71	STH	77	MELLEN - HURLEY ROAD	ASHLAND	NW	97130	97160	4	Surface layer
1510-01-73	STH	96	FREMONT - OUTAGAMIE CO LINE	WAUPACA	NC	6100	6100	1	Surface layer
4075-14-71	STH	96	APPLETON - LITTLE CHUTE	OUTAGAMIE	NE	112870	112870	1	None
6190-12-71	STH	116	WINNECONNE - USH 45	WINNEBAGO	NE	117760	117760	1	None
2140-08-71	STH	181	NORTH 76TH STREET	MILWAUKEE	SE	132690	132700	1	Surface layer

CHAPTER 8 CONCLUSIONS AND RECOMMENDATIONS

Field testing and loose-mix sampling occurred on 23 unique construction projects, totaling 30 unique layers of HMA during the 2007 paving season, and a single Warm Mix project during the 2008 paving season. Loose-mix samples from the construction projects were compacted in the Superpave Gyratory compactor at two pressure settings, 300 kPa and 600 kPa; and at three temperatures of 248, 194, and 140°F. The following sections describe conclusions and recommendations from the field and lab work.

8.1 Conclusions from Field Compaction

Multiple regression models for each of the 30 layers yielded the following project-specific conclusions:

- 1) Higher temperatures yield greater increases in density.
- 2) Roller type has an inconsistent effect across a range of projects.
- 3) Vibratory ON setting yields greater density increases.
- 4) As the density approaches 96% Gmm, the density gain decreases.

When all projects are pooled together:

- 1) 60% of the change in density during compaction can be explained by PG grade, vibratory setting (ON or OFF), mat temperature, successive passes between QC tests, cumulative passes, and density approaching 96% Gmm.
- 2) The factors affecting density gain in rank order were mat temperature, number of passes, roller type, density approaching 96% Gmm, vibratory setting, and PG grade.
- 3) The remaining 40% of variability would be explained by testing error, changes in lab air voids, AC%, base rigidity, aggregate angularity, numerous other variables presented earlier in this report, and other project specific factors.
- 4) Density growth from screed to the first successive passes of the breakdown roller was about 8%, typically increasing from 80% after the screed to 88% after 2 passes.
- 5) When all QC tests are taken into account, including breakdown rolling, intermediate rubber-tired rolling, and finish rolling, the average density gain between QC tests was computed at 3.2%.
- 6) Breakdown roller had the greatest density increases; however, the test of least squares means (Figure 6.10) found no statistical difference at the 5% level with the pneumatic roller. This is because, on average, the breakdown had an increase of approximately 6% per measurable pass, but the standard deviation was equally high at 4%. This was caused from high initial compaction on the first passes, and less on the subsequent passes. The pneumatic roller had a much smaller mean increase of 1%, but the standard deviation was also much smaller at 1%, indicating more consistent growth. Thus, when considering the covariate of the mean for the breakdown and pneumatic rollers, no mean difference was detected.
- 7) Negative density increases after roller passes was the result of testing error with the nuclear gauge, or the reduction in density from displacement during final rolling, or a combination of both.

- 8) Temperature had an effect on density with the greatest density gains made above 170F with the breakdown roller. Density gains with the finish roller are possible with temperatures as low as 120°F, but there was negative scatter as well (from testing error and/or shoving).
- 9) PG grade has an effect on density gain at lower temperatures with both the intermediate rubber-tired roller and finish roller.
- 10) Interactions occurred for Passes*Roller and Totalpasses*Roller, primarily since the finish roller recorded a higher number of cumulative passes.
- 11) The interaction Totalpasses*Temperature indicates that as total passes increases, temperature decreases.
- 12) An interaction for density from 96% Gmm * roller type would be the breakdown roller compacting at levels further from 96% Gmm, and the finish roller compacting at levels closer to 96% Gmm.
- 13) The interaction of total passes and density approaching 96% Gmm is simply a total cumulative number of passes are recorded as the density approaches 96% Gmm.

Breakdown roller findings include:

- 1) 68% of the variation in breakdown density growth is explained by vibratory setting, temperature, successive passes, cumulative passes, and approaching 96% density.
- 2) Vibratory setting is important, with the ON setting providing added density gain.
- 3) Temperature is equally important, and in fact, more density gain is explained by temperature than vibratory setting.
- 4) Passes are very important. The cumulative number of passes with the breakdown roller outweighs the effects of all other factors combined.
- 5) The greater the mat density (relative to 96% of Gmm), the more difficult it is to achieve density gains.
- 6) PG grade does not have an effect on density gain with the breakdown roller. This finding suggests that a similar density gain can be expected from PG58-series and PG64-series unmodified asphalt binders with breakdown rolling.

Pneumatic intermediate roller findings include:

- 1) 17% of the density gain is found with the main effects of PG grade, vibratory setting, mat temperature, successive passes between QC tests, cumulative passes, and density approaching 96% Gmm. Adding interactive effects is able to capture 28% of variation.
- 2) Average density gain per successive roller passes is about 1%.
- 3) Unexplained gains and error in density growth account for about 70% to 80% in the data.
- 4) Total passes and the interaction of totalpasses*temperature have the greatest influence in density gain. It is more beneficial for a contractor to use the rubber-tired roller at a higher temperature, and with a greater number of initial passes.
- 5) PG*Temperature interaction indicates that binder dynamic viscosity and its relationship to temperature are influential in density gains with intermediate rolling.
- 6) Higher temperatures yield greater density gains.
- 7) Passes up to n=4 provide the greatest initial densification, and a greater number of passes provide diminishing return on effort investment.

Finish “cold” roller findings include:

- 1) The collected data were only able to explain 23% of the variation in density growth with these variables in rank order of significance: cumulative passes, vibratory setting, density approaching 96% Gmm, successive passes between QC tests, PG grade, and mat temperature.
- 2) A typical observation on all projects was the finish roller operating in either a vibratory or static setting at lower mat temperatures, generally in the range of 170°F down to 120°F.
- 3) Average density gain from successive finish roller passes (typically 1 or 2) is about 0.9%.
- 4) All main effects were significant in density gain, including PG grade, vibratory setting, temperature, passes, cumulative passes, and density approaching 96% Gmm.
- 5) The largest accounting of the growth is found with total cumulative passes.
- 6) Temperature has minimal effect on achieving density with the cold roller.
- 7) Interactions occur for temperature*totalpasses (decrease in temp with more passes) and passes*totalpasses,
- 8) Moderate significance is found with the interactions of PG*vib and passes*dens96. This suggests that in order to achieve gains in density, it is necessary to increase the cumulative number of passes at a higher temperature, setting the vibratory amplitude and frequency with respect to binder grade, and number of successive passes as 96% Gmm is approached.
- 9) Intelligent Compaction research should be capable of modeling these effects.
- 10) A vibratory setting ON yields 0.5% more density gain after successive roller passes.
- 11) A mat temp that is 10F warmer, will yield a 0.05% density increase - a negligible change.
- 12) Passes are where the greatest gains are made with a finish roller. More successive passes, more density gain. A multiplier of 0.3 is multiplied by each successive pass to predict density gain. For example, an application of 2 successive passes would achieve a 0.6% density gain.
- 13) More cumulative passes provides diminishing return on density gain. A total of 6 to 8 passes should be sufficient. But, this brings in the question of trying to achieve density gains with the cold roller at lower temperatures, when the breakdown (and pneumatic) have the greatest impact.

Warm Mix Asphalt

- 1) A lab and field evaluation of a single Warm Mix Asphalt (WMA) E-1 mixture determined that the average final density for WMA and tradition Hot Mix Asphalt were nearly identical, at 92.0% density.
- 2) The results of the laboratory evaluation demonstrate that the use of the WMA additive allowed for an increased amount of RAP in the mix without a significant detriment to mixture workability as shown using the CDI. Both the HMA and WMA 30% mixes approached the Superpave criteria of 4% air voids at Ndes over all compaction temperatures, the air void levels in the WMA 40% were considerably lower than the 4% target, this result was consistent with the field QC data collected.
- 3) Variability in WMA field density was larger by a factor of 2.5 for the standard deviation, which was the result of different RAP levels in the mix.

- 4) For a similar number of roller passes, 30% RAP content averaged 2.6% greater density values than 40% RAP content. Variability (standard deviation) in 30% RAP was much higher by a factor of 3.

8.2 Conclusions from Lab Compaction

Pooled data findings from 19 layers, [4] E-1, [8] E-3, [7] E-10:

- Lab compacted density at Ndes averages 95.6% at Ndes.
- 600 kPa pressure has 1.8% higher density than 300 kPa.
- 248°F has the highest compacted density at Ndes, with a reduction of 0.4% for 194°F, and 2.3% lower for 140°F.

E-1 mixes, 4 layers:

- R-squared = 58% with temperature and pressure in model.
- Lab compacted density averages 96.0% at Ndes.
- Pressure has an effect with 600kPa having 1.8% higher density.
- 248°F has the highest density at Ndes, 0.2% lower for 194°F, and 2.3% lower for 140°F.

E-3 mixes, 8 layers:

- R-squared = 77% with NMAS, temperature, and pressure in model.
- Lab compacted density averages 95.4% at Ndes.
- Pressure has an effect with 600kPa having 1.8% higher density.
- 248°F has the highest density at Ndes, 0.2% lower for 194°F, and 2.3% lower for 140°F.

E-10 mixes, 7 layers:

- R-squared = 62% with NMAS, temperature, and pressure in model.
- A single 25-mm NMAS mix was removed from the model.
- Lab compacted density averages 97.0% at Ndes.
- Pressure has an effect with 600kPa having 1.9% higher density
- 248°F has the highest density at Ndes, 0.5% lower for 194°F, and 2.4% lower for 140°F.

8.3 Recommendations for Achieving Field Density

Based on the data analyzed in this project, the following roller setup is recommended:

Breakdown Roller

- More cumulative passes are the most effective tool to increase density. For example, 4 passes are more important than 2 passes during breakdown compaction.
- A minimum of 4 passes across all areas of the mat are recommended.
- Vibratory setting ON.
- Compact at highest temperatures possible.

Pneumatic Roller

- Roll the mat at the highest possible temperature.
- Minimum of 4 initial passes. Multiple coverage is key. Excessive rolling (say, n=8 passes) has diminished returns. So, at a minimum, roll all areas with at least 4 passes with the warmest temperatures, then move on to the next rolling zone.

Finish Roller

- More cumulative passes are the most effective tool to increase density, but there will be minimal gain with the cold roller. If density is needed, 2 passes should provide 0.6% density gain. Four passes should yield 1.2% density gain.
- Vibratory setting ON.

Warm Mix Asphalt

- WMA final density is nearly equivalent to HMA final density for similar number of roller passes.
- Based on a single project, lower RAP levels are recommended for WMA mixtures to achieve higher density levels. In this project, 30% RAP content averaged 2.6% greater density values than 40% RAP content.

8.4 Recommendations for Continued Research – Evaluation of Warm Mix Asphalt

A more rigorous evaluation of the impacts of a variety of warm mix additives and processes on workability and relationships between the laboratory and field is recommended. Evaluation of workability should also include mixes designed for higher traffic levels, varying in gradation, and using modified binders. A control mix is needed in subsequent field sections in which the only change in the mix design is the addition of a WMA additive. If possible, this section should also be compacted at warm mix temperatures to provide a means of comparison for in-place density and field performance. Field sections should also be of adequate size to allow for measurement of emissions and energy consumption to quantify the environmental benefits of WMA relative to HMA.

8.4.1 Warm Mix Asphalt Field Experiment

Findings from the field investigation provide important considerations for evaluating Warm Mix Asphalt technology. From this study, field data are pointing to those controllable factors affecting density gain. Specifically, the following considerations are put forth:

1. Temperature. Temperature has an effect on the ability to densify the mat at higher temperatures, say above 170°F. Lower temperature (170°F and below) have minimal effect on densification. Since WMA is mixed at lower temperatures, it is critical that the mat be densified as quickly as possible. It is not known whether the temperature threshold where density can no longer be achieved is lower for WMA. In the lab, there are significant differences between WMA and HMA at 90°C for E-10 mixes, but it is unclear how that translates to field. The data in this study strongly indicate that initial breakdown rolling and intermediate rubber-tire rolling density gains are temperature dependent. Finish rolling density gains are not temperature dependent. Temperature band cutoffs should be investigated (240°F, 220°F, 200°F, 180°F, 160°F) in increments within the available study resources.
2. Passes. This is the most important factor affecting density growth. More passes, more density. Thus, the densification profiles must be measured in the WMA experiment as more compaction energy is applied. Specifically, in the lab, use the usual height measures from successive SGC gyrations, Construction Densification Index (area of the under the densification curve), and/or the resistive energy measured by the PDA to develop SGC compaction profiles. Compact and compare the profiles of a standard PG-series binder and a WMA-additive binder. Try 2 gradations if resources allow; this would yield 4 combinations, 2 binders x 2 gradations = 4. Perform hypothesis testing for profile differences for non-linear and/or linear slopes, and other model parameters. This will anticipate what may happen in the field.
3. PG Grade. PG grade does not have an affect on achieving density at higher temperatures with the breakdown roller, however, it begins to have an effect with the intermediate and finish rollers at lower temperatures. Thus, the effects of PG grade vs WMA must be investigated at the lower temperatures. Contrary to the field data, lab compaction results

from this study show PG grade does not have a significant affect. This investigation needs to be extended to PG70-series or other PG grades that require use of modified asphalts. Use at least one modified and unmodified binder to get a more clear idea of PG-densification profile. This will increase the number of test combinations, but provide important data for consideration in actual field compaction. Balance data with available resources.

4. Temperature vs Passes Interaction. Obviously, as the number of passes is added, the temperature drops. Therefore, incorporate this interaction into the lab experimental design. This will be captured by the temperature-gyration profiles when compacting the standard PG and WMA-additive mixes at the temperature increments specified above.
5. Field Experiment. Before conducting a field evaluation, a controlled experiment in the lab will simulate field compaction by varying the number of gyrations, simulating number of passes, simulating temperature bands, and altering PG grade. Since all combinations of these lab variables will not be possible in the field, several should be investigated. Vary the initial breakdown passes and cumulative passes within 20°F increment temperature bands and develop density-temperature profiles. This study has found more cumulative passes are beneficial, so vary these in the field (2, 4, 6, etc) to see if WMA-additive mixes are consistent with typical PG grades used in this study Evaluate vibratory ON and OFF settings in the field to compare against findings in this study.
6. Validate. Once the initial investigation occurs this summer on a handful of projects, assess the data and develop a strategy for validating the models next summer. Use older data to predict newer data and beyond. Also, perform a mini validation by developing a model with half the data (randomly chosen) and then measuring the ability to predict the remaining data.

8.4.2 Warm Mix Asphalt Lab Experiment

Based upon the data and findings in this study, the following recommendations are put forth for WMA lab-related research:

- Test higher Ndes mixes, such as E-3 and E-10.
- Do not use 25mm NMAS aggregate. Use either 12.5mm or 19mm NMAS aggregate. Suggest only one size to eliminate multiple levels in factorial design.
- Pressure has a significant effect, with about 2% more density from 600kPa. It is recommended that WMA additives be investigated under 2 levels of pressure loading to understand if this effect is similar for traditional binders and those with WMA additives.
- Temperature has a more pronounced effect below 194°F (90°C). Test whether this relationship applies to WMA. If resources allow, include new midpoints 105°C (221°F) 75°C (167°F) to understand whether the temperature-density relationship is linear or non-linear.

8.4.3 Density and Permeability Criteria

If criteria are to be established, the data set created in this study will truly relate as-built construction properties with performance. The data set should also have the capability to be stratified by unique indigenous materials and project characteristics within various regions of the state, and yield consistent results for design criteria. For example, the data may find that a minimum as-built density of 93% is needed during construction to ensure a certain performance level at 10 years of pavement age (say, a target PDI = 30). This relationship would better predict maintenance intervention during the life of the pavement, and aid in more accurate life-cycle cost analysis. Contractors may want to consider the findings in this study to assist in achieving the compaction. Current Ndes levels could be calibrated against the in-service density at 4, 7, or 10 years of age (data currently suggest that the levels are sufficient).

An example was illustrated in the Phase I report where as-built density of 91.5% is triggered for the target PDI/year of 4.0 with a corresponding expected water permeability of 0.60×10^{-5} cm/s (Schmitt et al. 2007). A density of 91.8% is also required to achieve the desired PDI/year of 4.0. Hence, the controlling density to satisfy permeability and PDI requirements is the latter value (91.8%), which is the greater of the two.

It is recommended that the conceptual framework developed in the Phase I study (Schmitt et al. 2007) be used to develop permeability and density criteria. A database has been created with the potential capability of producing performance models robust to a broad range of projects, that in turn will establish specific criteria to be published in construction and materials specifications. The framework presented in this report will assist in determining the specific thresholds. This effort will require a long-term study of about 5 years in duration.

The following specific components are recommended for the experimental design and work plan approach, by year:

2009 (time=2 years)

1. Collect performance data from PIF database and begin performance monitoring. A request would be made more frequent performance testing as necessary.
2. Collect MetaManager traffic data.
3. By 2009, WisDOT may have a full-integrated HMA database relating design, construction, environmental, traffic, and performance data. The conceptual database, now named the Pavement Performance Analysis System (PPAS), has been developed by UW-Platteville in cooperation with WisDOT through the Midwest Regional University Transportation Center (Schmitt et al. 2007).

2011 (time=4 years)

1. Measure in-service density on each project segment using nuclear density gauge, and offset nuclear readings with 5 cores. (Patched core holes from 2007 will help confirm test segment location). Also, conduct a manual performance distress survey. Water permeability tests will not be conducted since this study has confirmed there is minimal permeability after pavement is placed in service. These activities will require traffic control, and a plan should be developed to minimize traffic control costs with county highway departments, or an alternate means.

2. Collect performance data from PIF database and begin performance monitoring.
3. Collect MetaManager traffic data.
4. Conduct initial performance modeling to density and permeability criteria.
5. Perform a fatigue analysis on cores for those projects having significantly more distress (rutting, cracking, raveling, etc.). Consider new advancements in indirect tensile strength procedures to more realistically characterize pavement fatigue.
6. Model the data to determine density and permeability criteria.

In summary, performance modeling will require considerable time and resources. However, the scope of this work will allow WisDOT and partners to develop true criteria across a broad range of HMA paving projects. Since this state does not have full-scale testing facilities such as MnRoads, WesTrack, or the NCAT Test Track, this study provides an alternate means by using in-service pavements as the laboratory. This approach will allow the state to move towards true performance-based criteria for HMA pavement research and development, and other tangential benefits as the research progresses.

REFERENCES

- Christensen, D., and Bonaquist, R. (2005). Rut Resistance and Volumetric Composition of Asphalt Concrete Mixtures”, *Journal of the Association of Asphalt Paving Technologists*, Vol. 74, pages 485-518, 2005.
- Cooley, L.A. Jr. (2006). “Evaluation of HMA Lift Thickness”, Mississippi Department of Transportation, <http://rip.trb.org/browse/www.bcdgeo.com>, Accessed October 2007)., October 1, 2006.
- Cooley, L.A. Jr., Brown, E.R., and Maghsoodloo, S. (2001). “Developing Critical Field Permeability and Pavement Density Values for Coarse-Graded Superpave Pavements”, *Transportation Research Record No. 1761*, page 41-49, 2001.
- Decker, D. (2006). “State-of-the-Practice for Cold-Weather Compaction of Hot-Mix Asphalt Pavements”, *Transportation Research E-Circular*, E-C105, Washington, D.C., pages 27-33, September 2006, <http://onlinepubs.trb.org/onlinepubs/circulars/ec105.pdf>. (Accessed October 2007).
- Delgadillo, R., and Bahia, H. (2008). “Effects of Temperature and Pressure on Hot Mixed Asphalt Compaction : Field and Laboratory Study”, *Journal of Materials in Civil Engineering*, American Society of Civil Engineers, Reston, VA, 2008, vol. 20, no6, pp. 440-448.
- Diefenderfer, S., McGhee, K., and Donaldson, B. (2007). “Installation of Warm Mix Asphalt Projects in Virginia”, FHWA/VTRC Report #07-R25, http://www.virginiadot.org/vtrc/main/online_reports/pdf/07-r25.pdf (accessed October 2007), April 2007.
- El Halim, A., El Halim, O.A., Mostafa, A. (2006). “Asphalt multi-integrated rollers and steel drum compactors: Evaluating effect of compaction on permeability of asphalt pavements”, *Transportation Research Record No. 1967*, Washington, D.C., pages 173-180, 2006.
- Faheem, A.F., Kamel, N., and Bahia, H.U. (2007). Compaction and Tenderness of HMA Mixtures: A Laboratory Study, Proceedings of the *Transportation Research Board 86 th Annual Meeting*, Washington, D.C., 2007.
- Faheem, A.F.F., and Bahia, H.U. (2004). *Using the Gyrotory Compactor to Measure Mechanical Stability of Asphalt Mixes*, Final Report No. 05-02, Wisconsin Department of Transportation, Wisconsin Highway Research Program, Madison, WI.
- Hanna, A.S., Bahia, H.U., Russell, J.S., Schoenfelder, S., and Loh, S-W (2002). “Determining a Temperature-Density Relationship After Completed Rolling of HMA”, WHRP Report No. 02-001, <http://www.dot.wisconsin.gov/library/research/docs/finalreports/00-06temperaturredensity-f.pdf>. (Accessed October 2007), January 2002

- Huh, J.D., and Nam, Y.K. (2000). "Study of Compaction Density in Closed Form", *Transportation Research Record No. 1712*, pages 66-73, 2000.
- Kearney, E. (2006). "Oscillatory Compaction of Hot-Nix Asphalt", *Transportation Research E-Circular*, E-C105, <http://onlinepubs.trb.org/onlinepubs/circulars/ec105.pdf>. (Accessed October 2007), Washington, D.C., pages 49-53, September 2006.
- Klaus, D. (2003). Asphalt Flow Improvers – A New Technology for Reducing Mixing Temperature of Asphalt Concrete Mixes with High-Resistance against Permanent Deformation", *Proceedings of the XXIIInd PIARC World Road Congress*, October 2003.
- Mahoney, J.P., Muench, S.T., Pierce, L.M., Read, S.A., Jakob, H., and Moore, R. (2000). "Construction-Related Temperature Differentials in Asphalt Concrete Pavement: Identification and Assessment", *Transportation Research Record No. 1712*, pages 93-100, 2000.
- Nose, Y., "Vibratory Pneumatic Tire Roller", *Transportation Research E-Circular*, E-C105, <http://onlinepubs.trb.org/onlinepubs/circulars/ec105.pdf>. (Accessed October 2007), Washington, D.C., pages 54-68, September 2006.
- Russell, J.S., Bahia, H.U., Kanitpong, K., Schmitt, R.L., and Croveti, J.C. (2005). *The Effect of Pavement Thickness on Superpave Mix Permeability and Density*, Final Report No. 05-05, Wisconsin Department of Transportation, Wisconsin Highway Research Program, Madison, WI.
- Scherocman, J., "Compaction of Stiff and Tender Asphalt Concrete Mixes", *Transportation Research E-Circular*, E-C105, <http://onlinepubs.trb.org/onlinepubs/circulars/ec105.pdf>. (Accessed October 2007), Washington, D.C., pages 69-83, September 2006.
- Schmitt, R.L., S. Owusu-Ababio, S., J. Croveti, and L.A. Cooley, Jr. (2007), *Development of In-Place Permeability Criteria for HMA Pavements in Wisconsin*, Final Report No. 06-15, Wisconsin Highway Research Program, Madison, WI, March 1, 2007.
- Starry, D. (2006). "How Temperature Impacts Compaction", *Pavement*, Vol. 21 (6), pages 30-33, August 2006
- Transportation Research Board, "Factors Affecting Compaction of Asphalt Pavements", *Transportation Research E-Circular*, E-C105, <http://onlinepubs.trb.org/onlinepubs/circulars/ec105.pdf>. (Accessed October 2007), Washington, D.C., September 2006.
- Willoughby, K. (2004). "Elimination of temperature and density differentials: the cycle density specification", Washington State Department of Transportation, Report #OCLC 55688302, April 2004.
- Willoughby, K. (2003). "Construction-Related Variability in Pavement Mat Density due to Temperature Differences", *Transportation Research Record No. 1849*, pages 166-173, 2003.

Willoughby, K.A., Mahoney, J.P., Pierce, L.M., Uhlmeyer, J.S., and Anderson, K.W. (2002). "Construction-Related Asphalt Concrete Pavement Temperature and Density Differentials", *Transportation Research Record No. 1813*, pages 68-76, 2002.

Willoughby, K.A., Mahoney, J.P., Pierce, L.M., Uhlmeyer, J.S., Anderson, K.W., Read, S.A., Muench, S.T., Thompson, T.R., and Moore, R. (2001). "Construction-Related Asphalt Concrete Pavement Temperature Differentials and the Corresponding Density Differentials", Report No. WA-RD 476.1, Washington State Department of Transportation, <http://www.wsdot.wa.gov/research/reports/fullreports/476.1.pdf>. (Accessed October 2001), July 2001.

Appendix A Breakdown Roller Plots

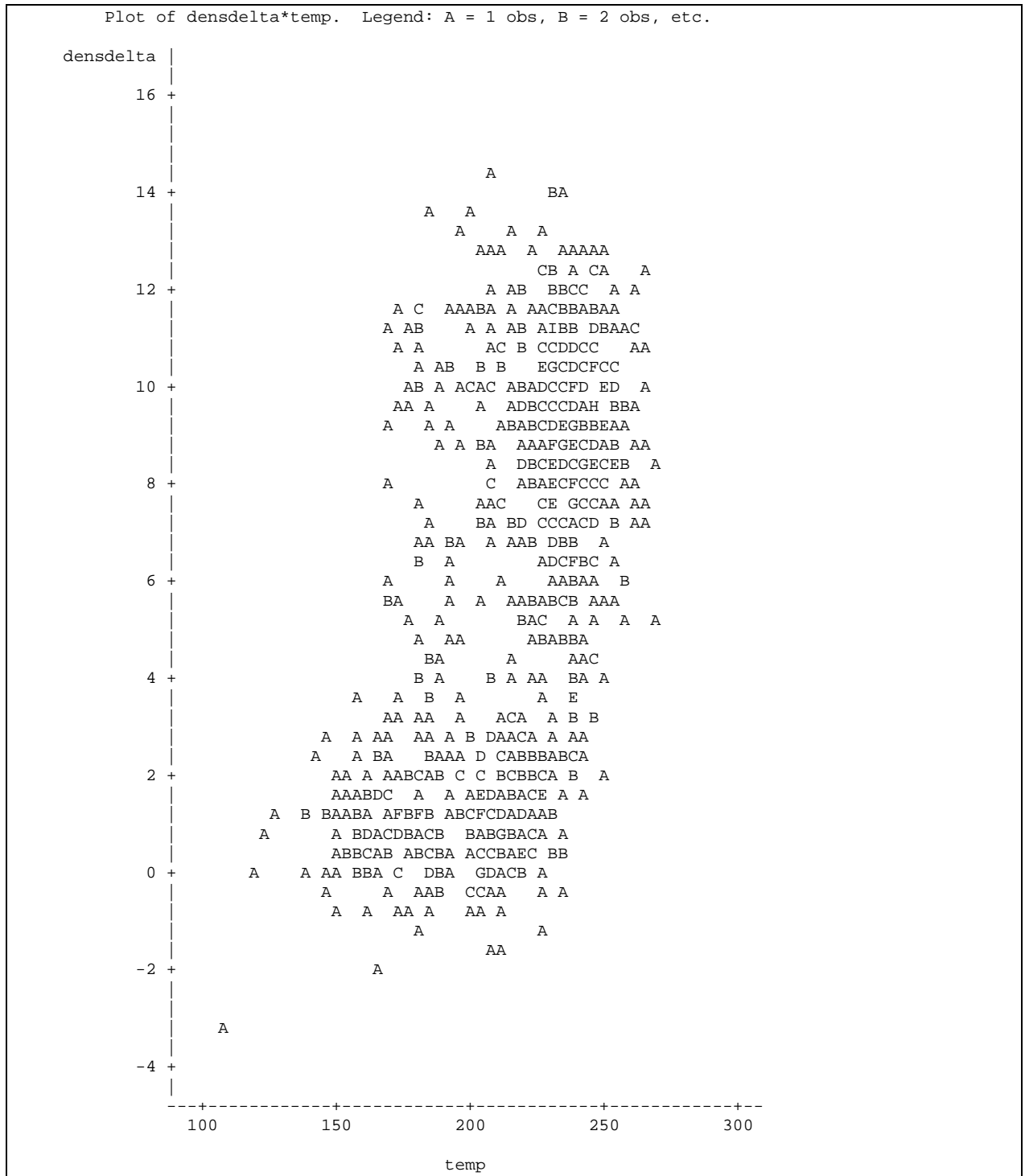


Figure A.1 Breakdown Roller – Density Gain versus Temperature

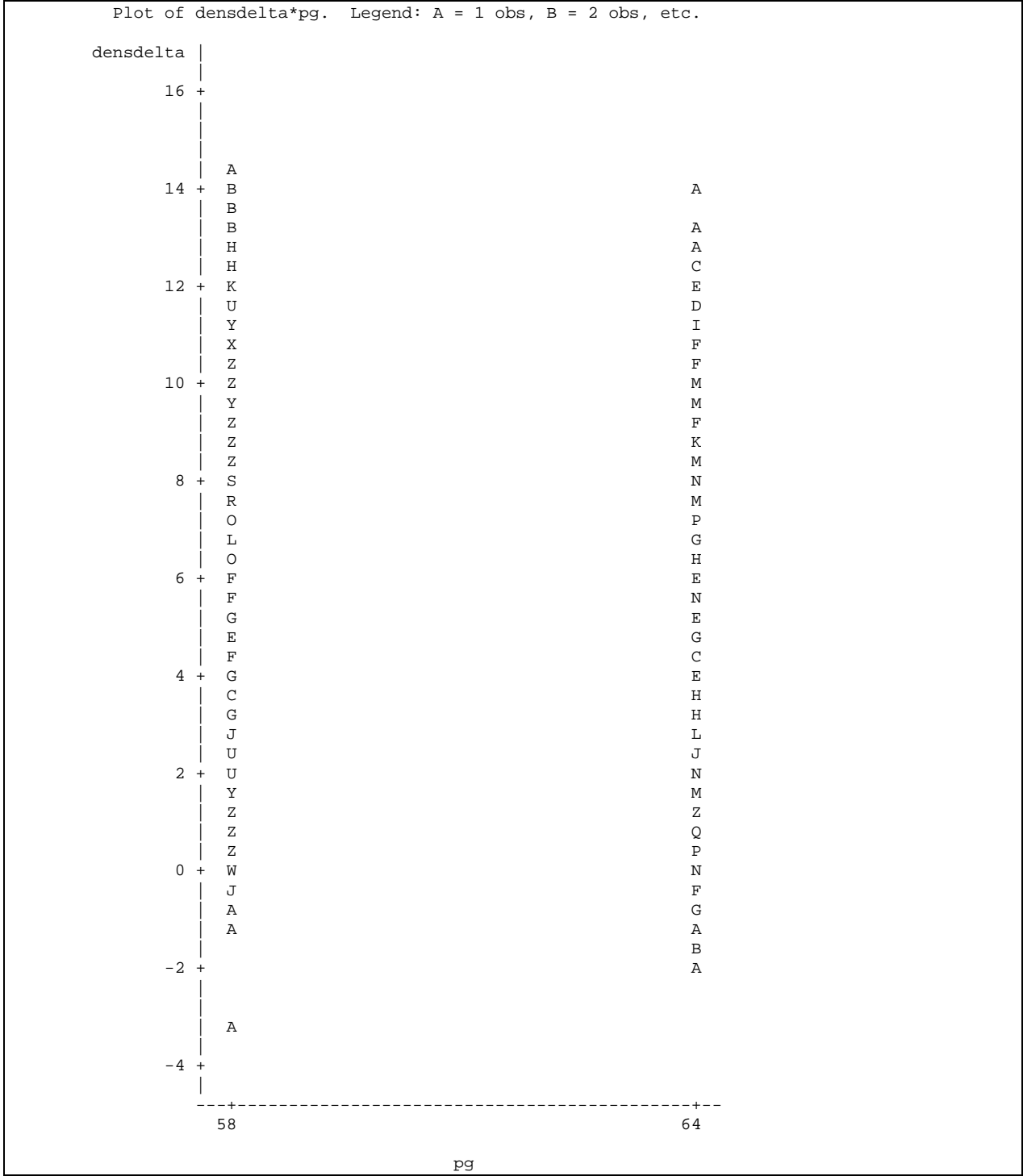


Figure A.2 Breakdown Roller – Density Gain versus PG Grade

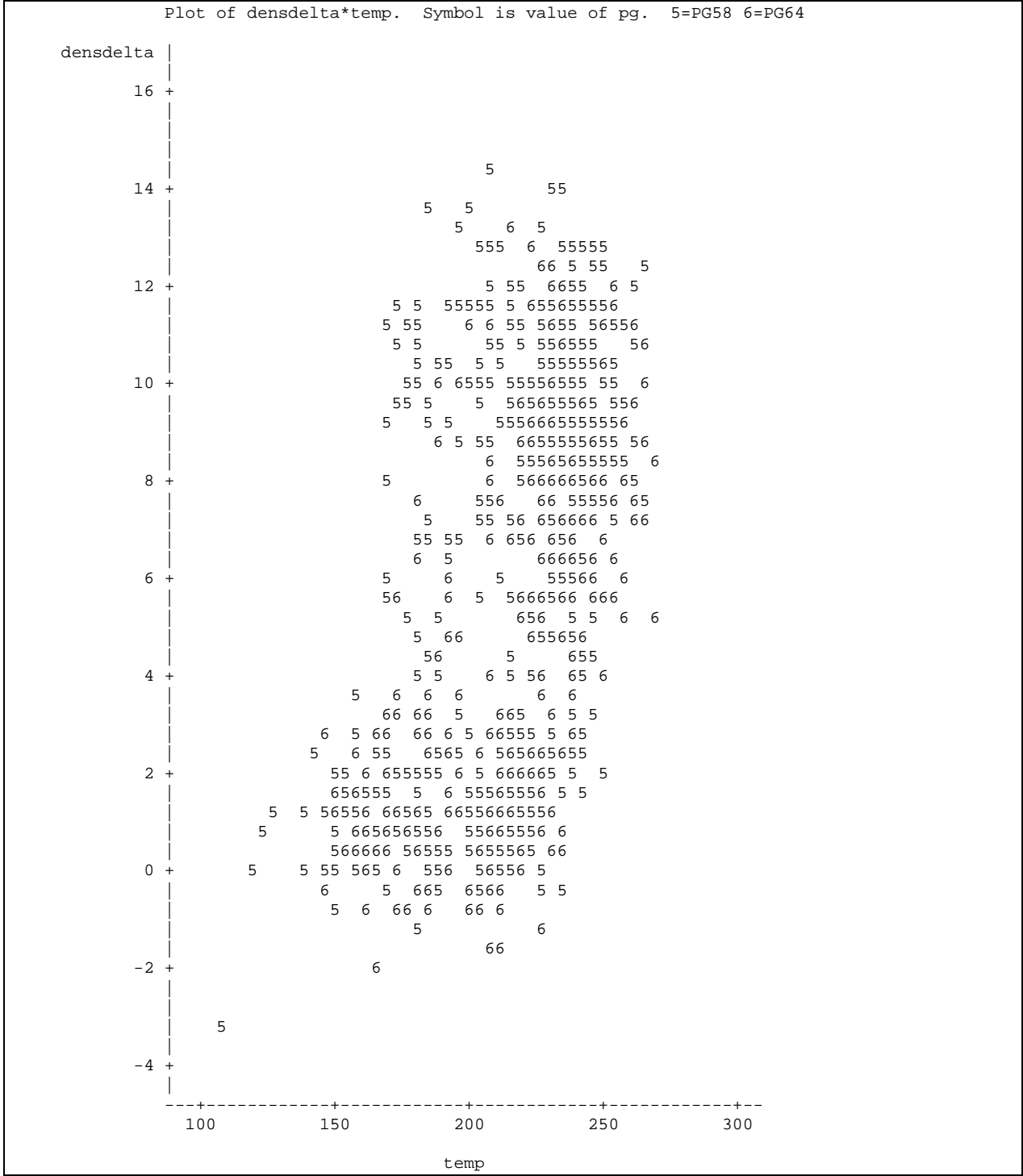


Figure A.3 Breakdown Roller – Density Gain versus Temperature by PG Grade

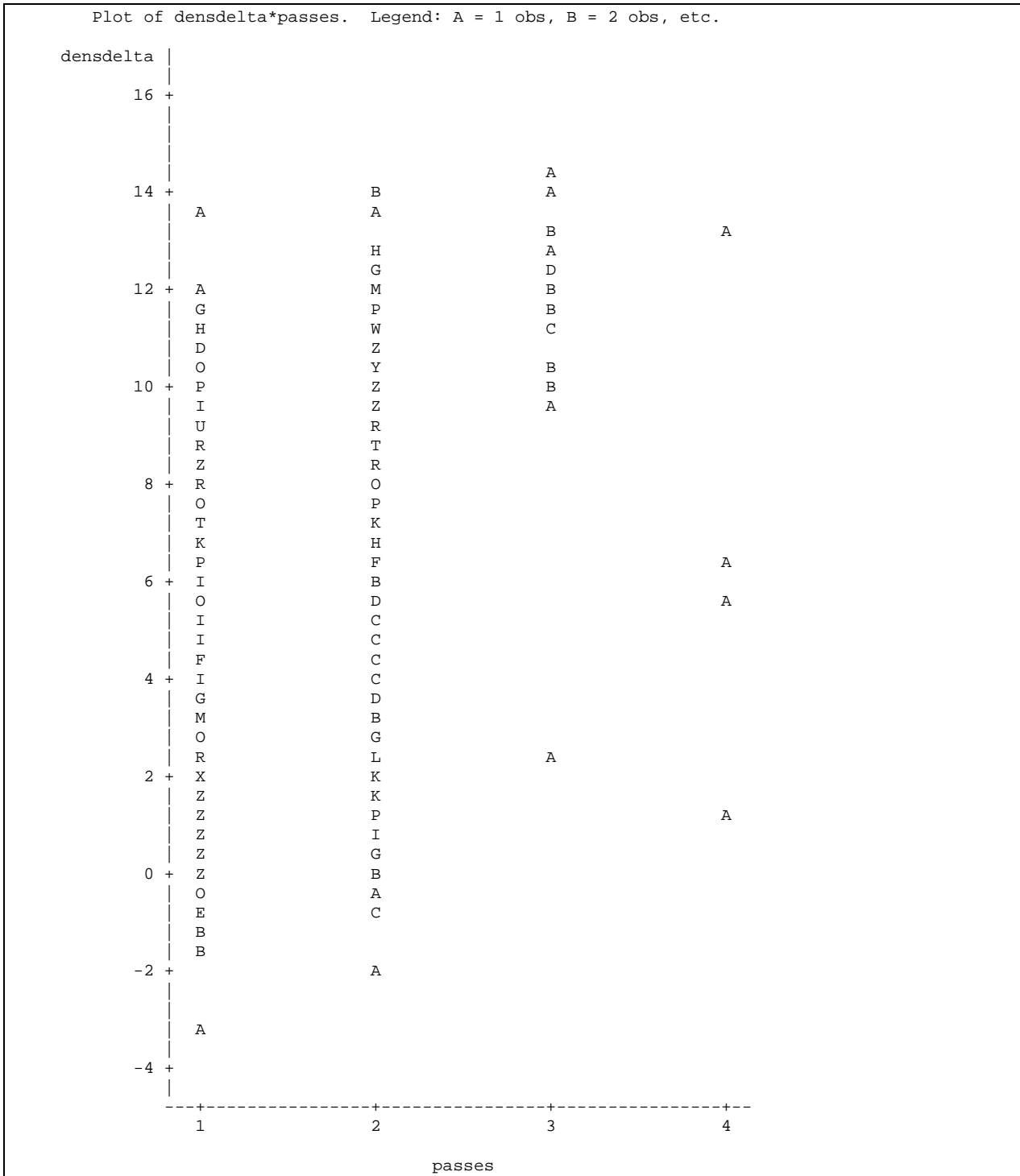


Figure A.4 Breakdown Roller – Density Gain versus Successive Passes

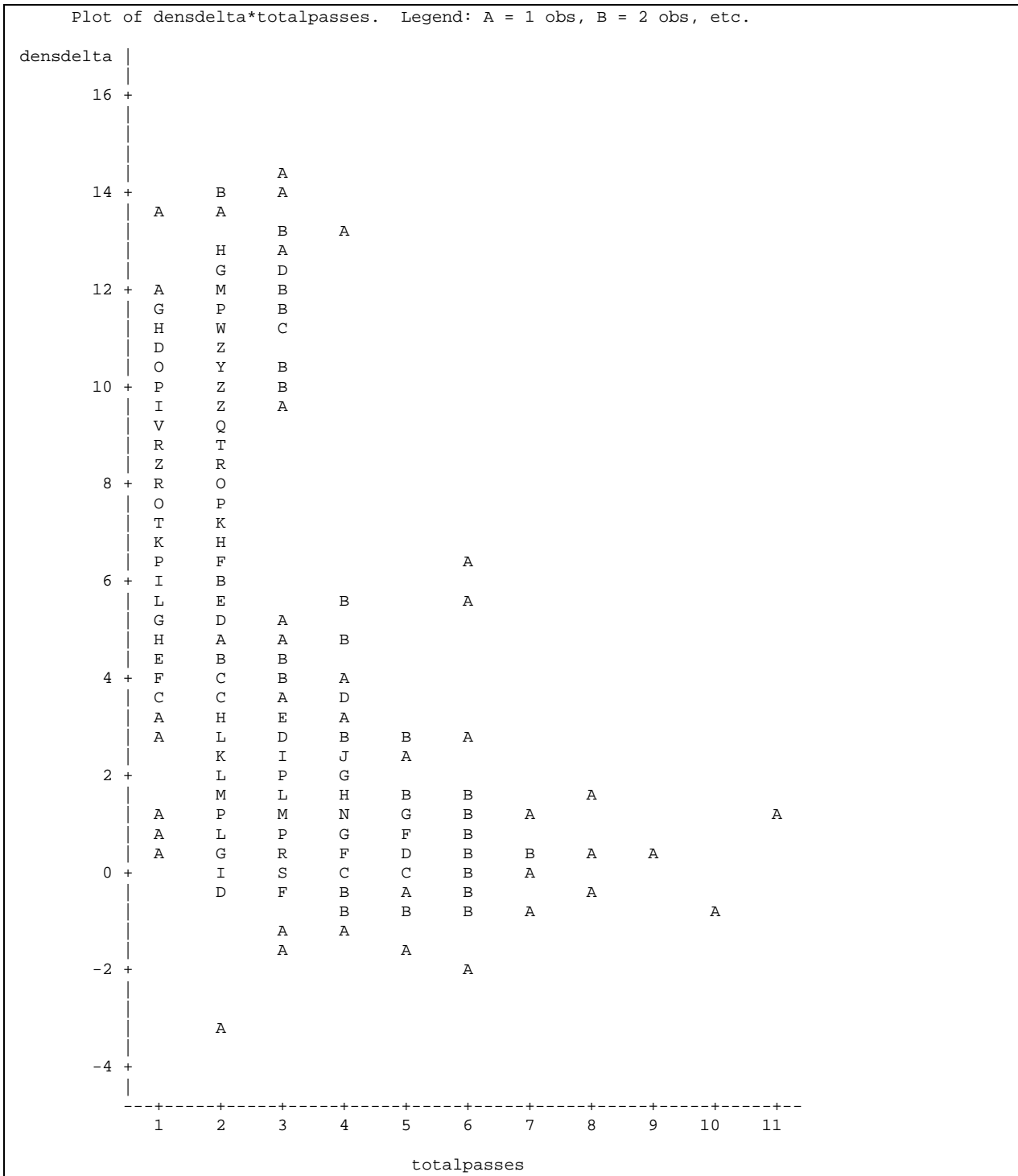


Figure A.5 Breakdown Roller – Density Gain versus Cumulative Passes

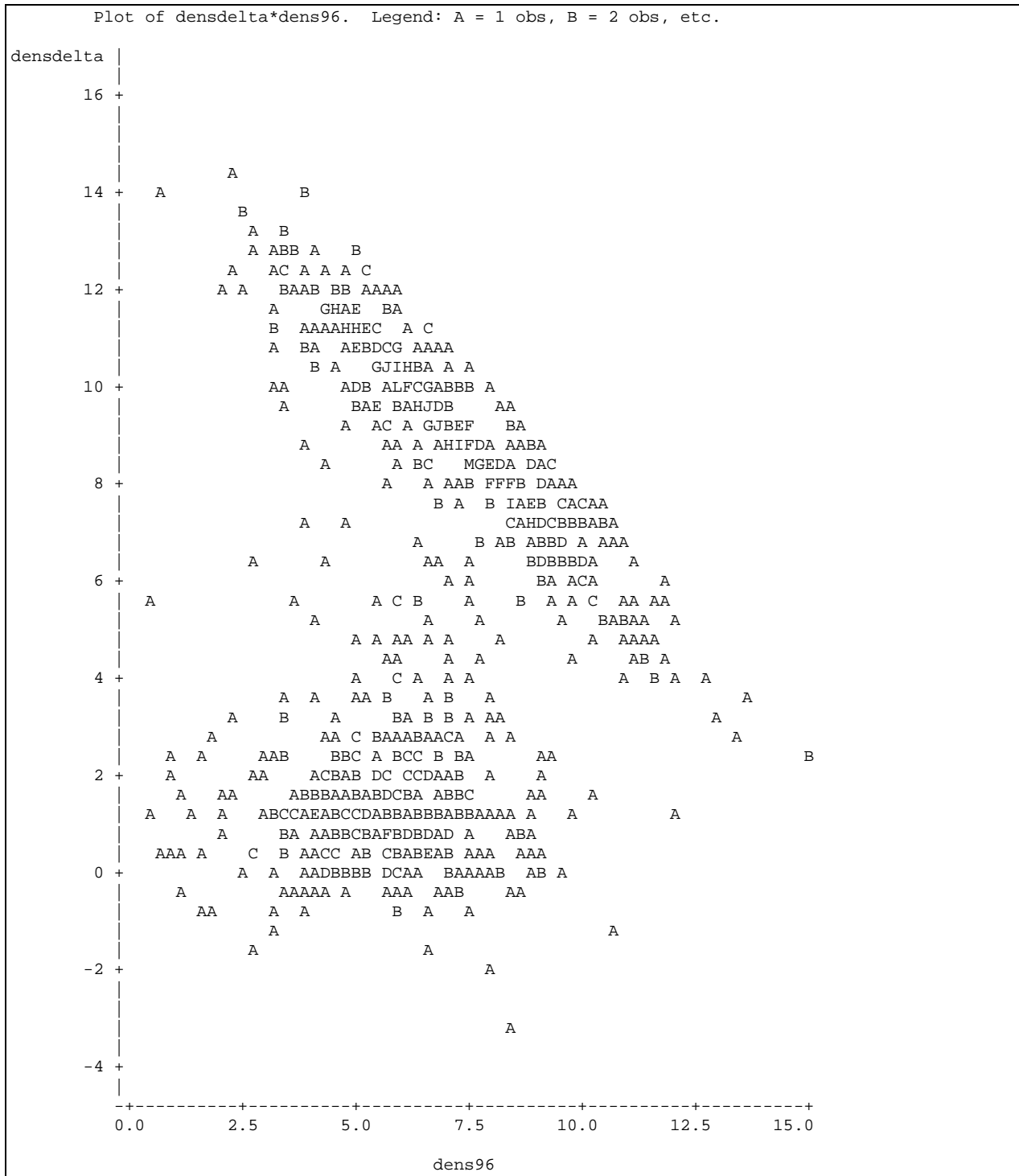


Figure A.6 Breakdown Roller – Density Gain versus Density from 96% Gmm

Appendix B Intermediate Pneumatic Roller Plots

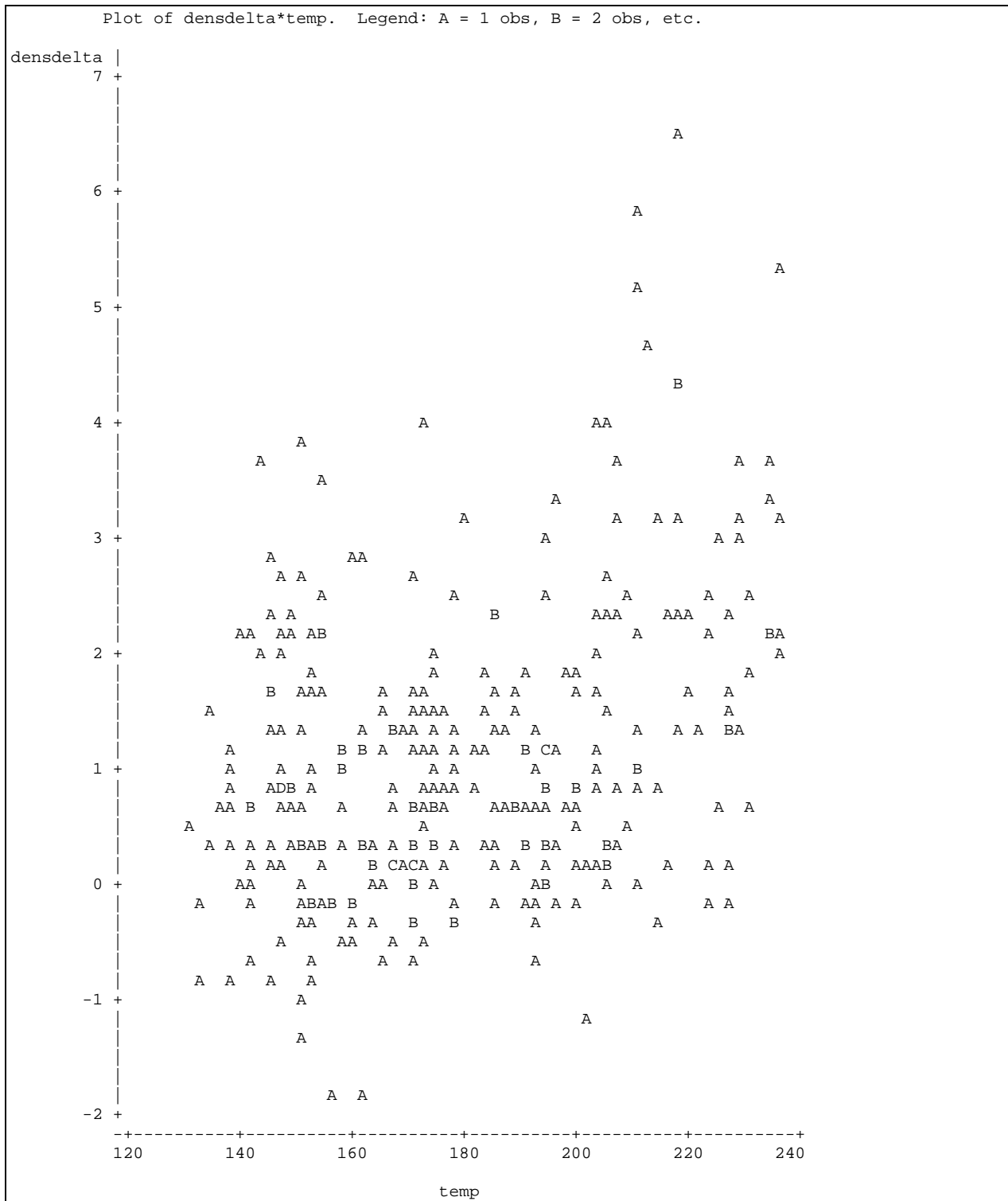


Figure B.1 Pneumatic Roller – Density Gain versus Temperature

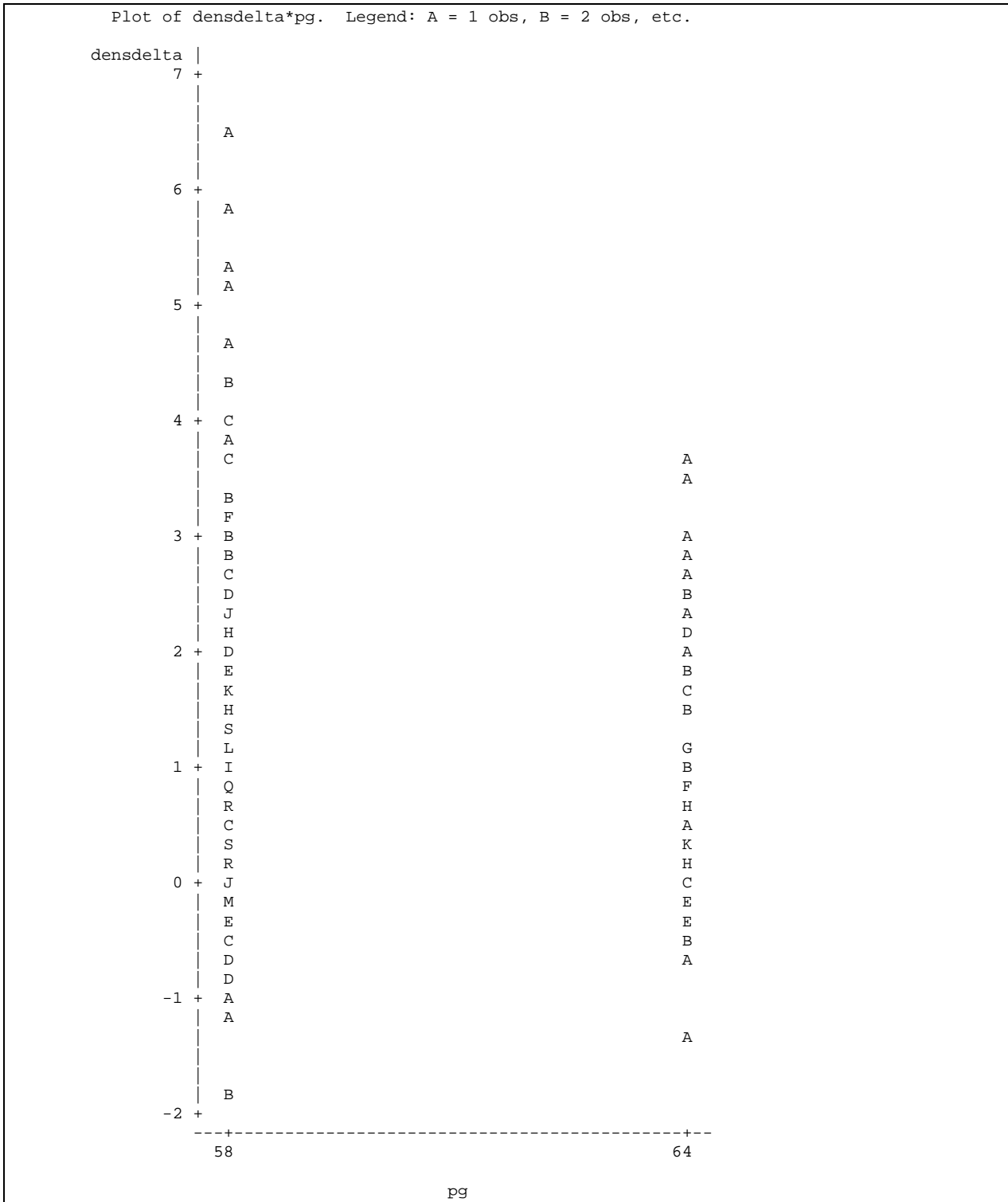


Figure B.2 Pneumatic Roller – Density Gain versus PG Grade

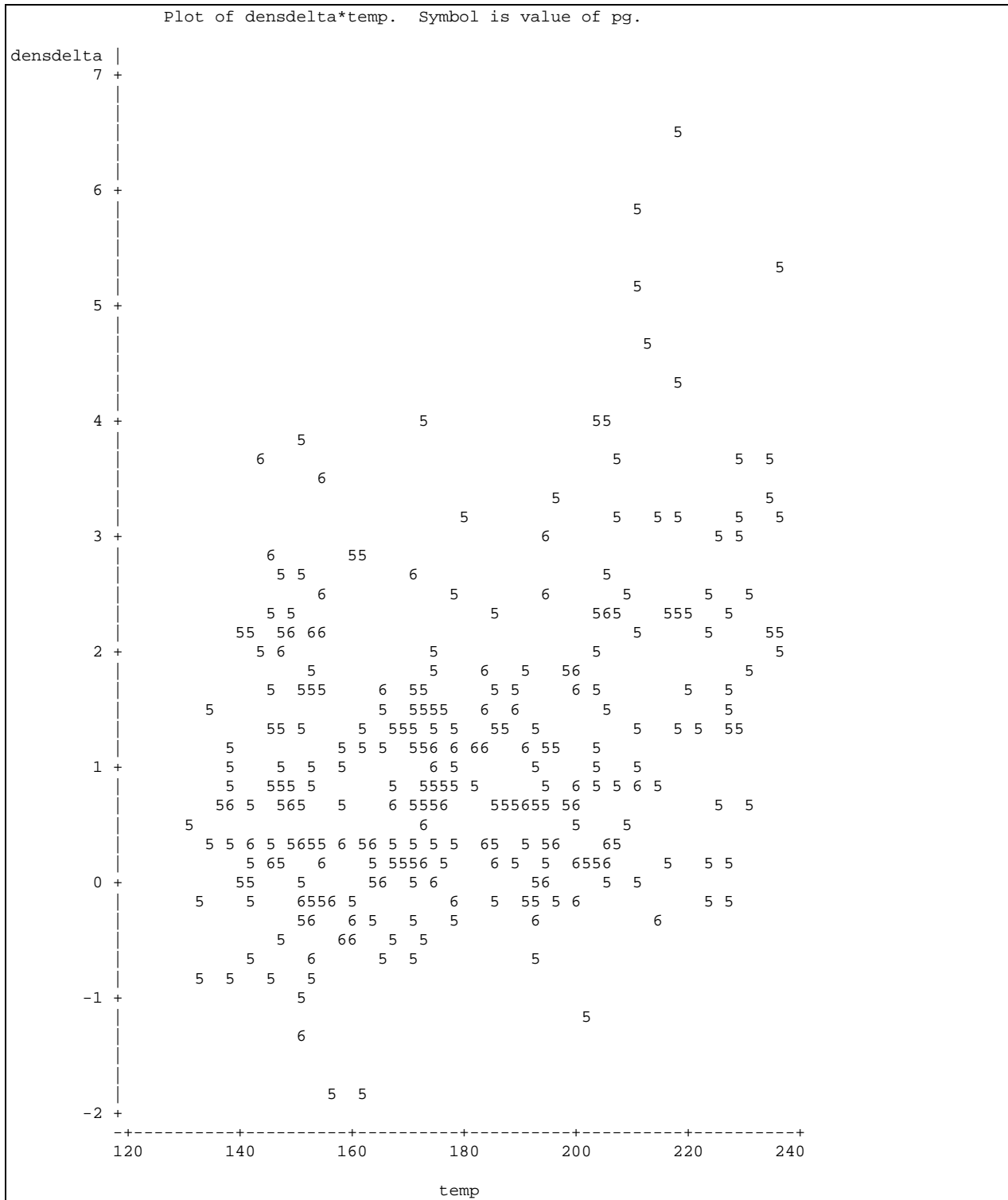


Figure B.3 Pneumatic Roller – Density Gain versus Temperature by PG Grade

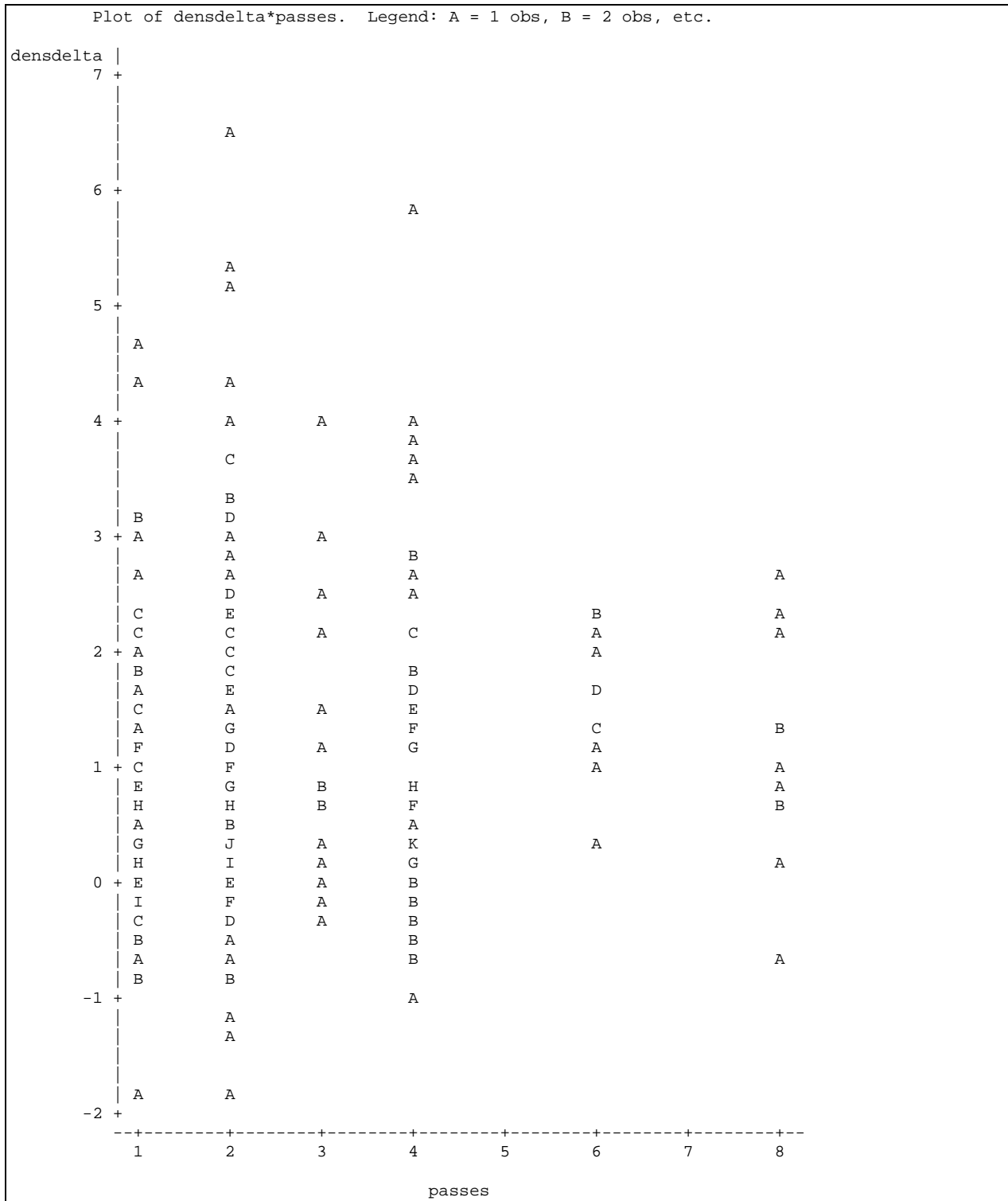


Figure B.4 Pneumatic Roller – Density Gain versus Successive Passes

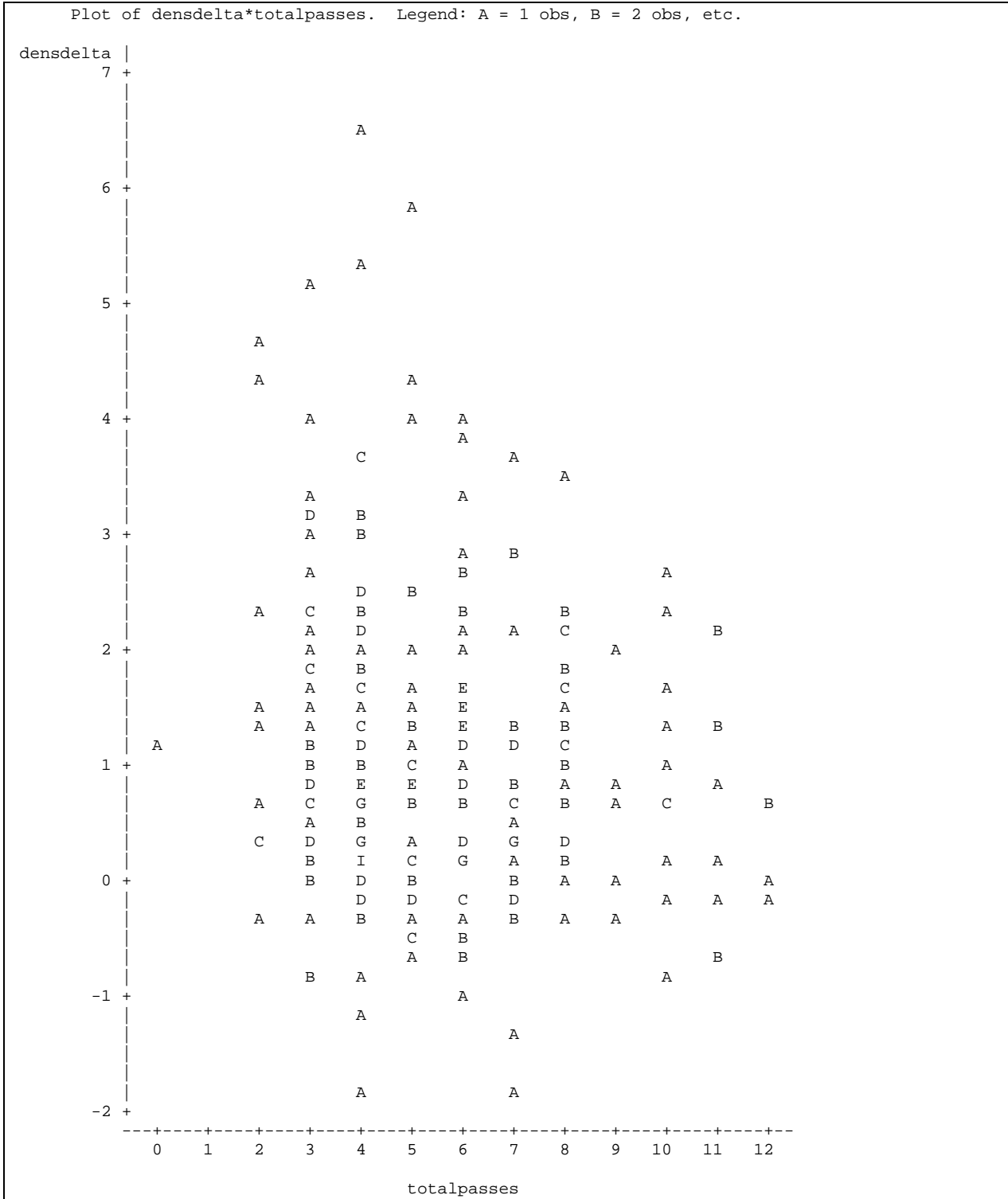


Figure B.5 Pneumatic Roller – Density Gain versus Total Passes

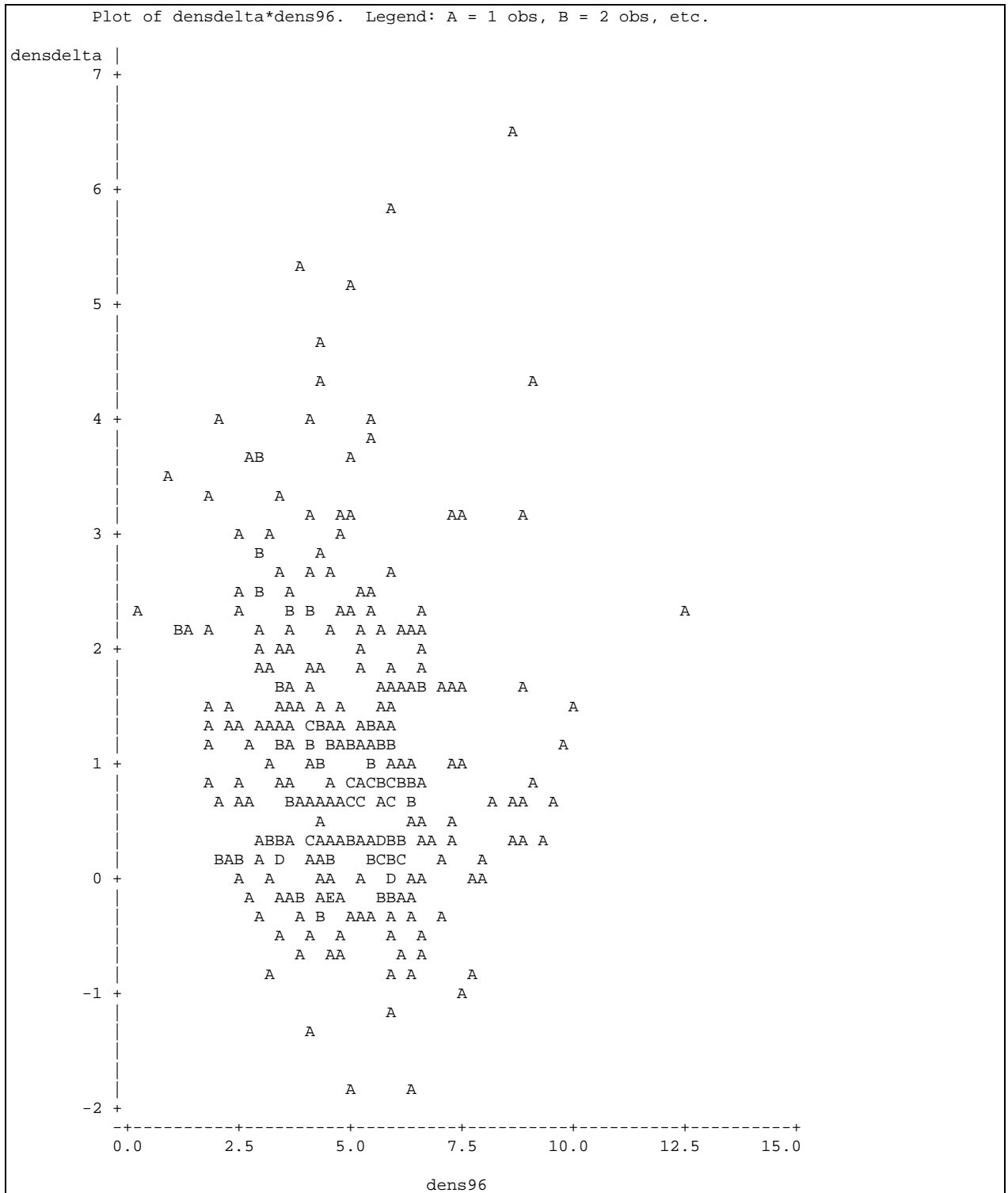


Figure B.6 Pneumatic Roller – Density Gain versus Difference with 96% Gmm

Appendix C Finish Roller Plots

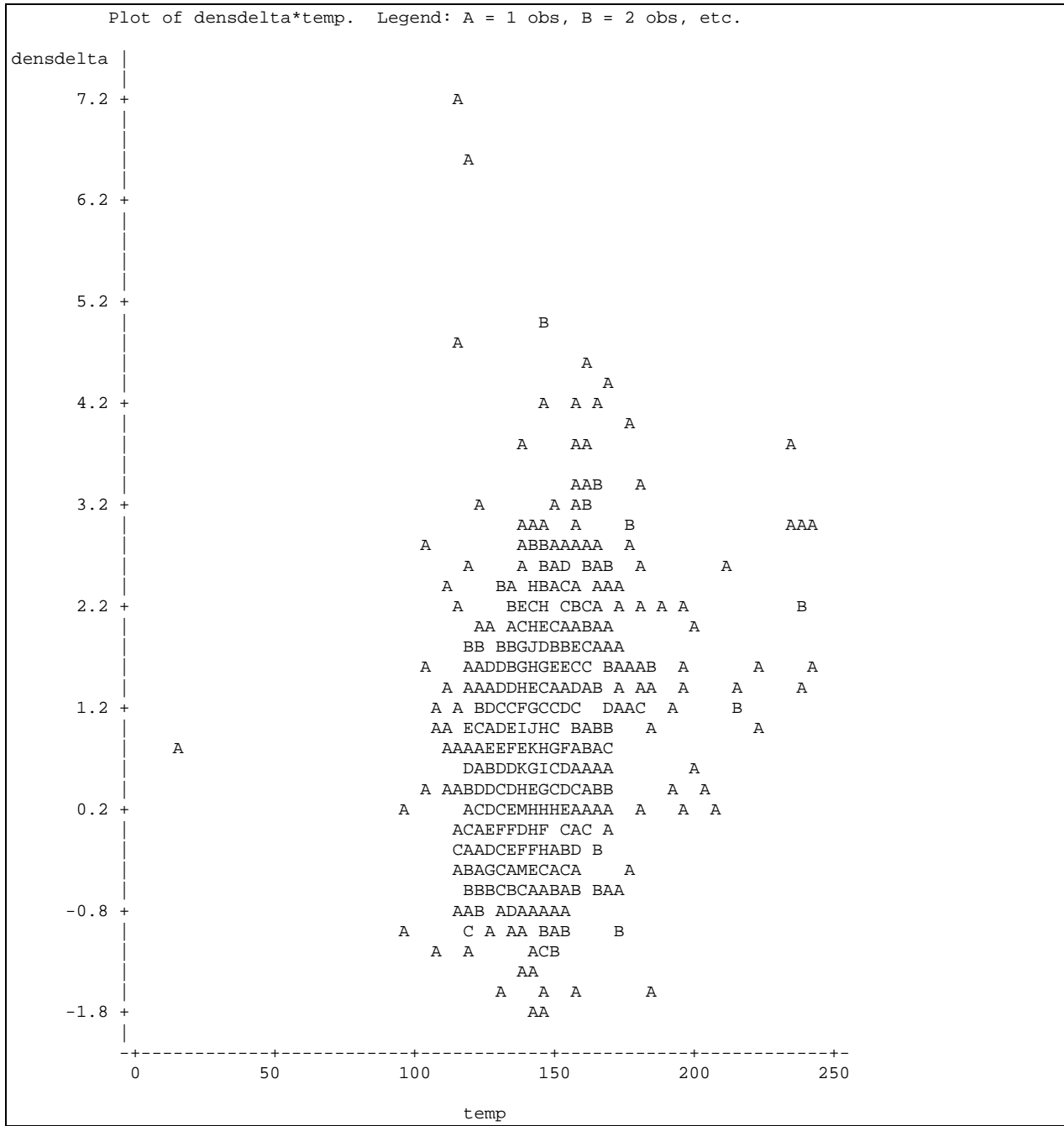


Figure C.1 Finish Roller – Density Gain versus Temperature

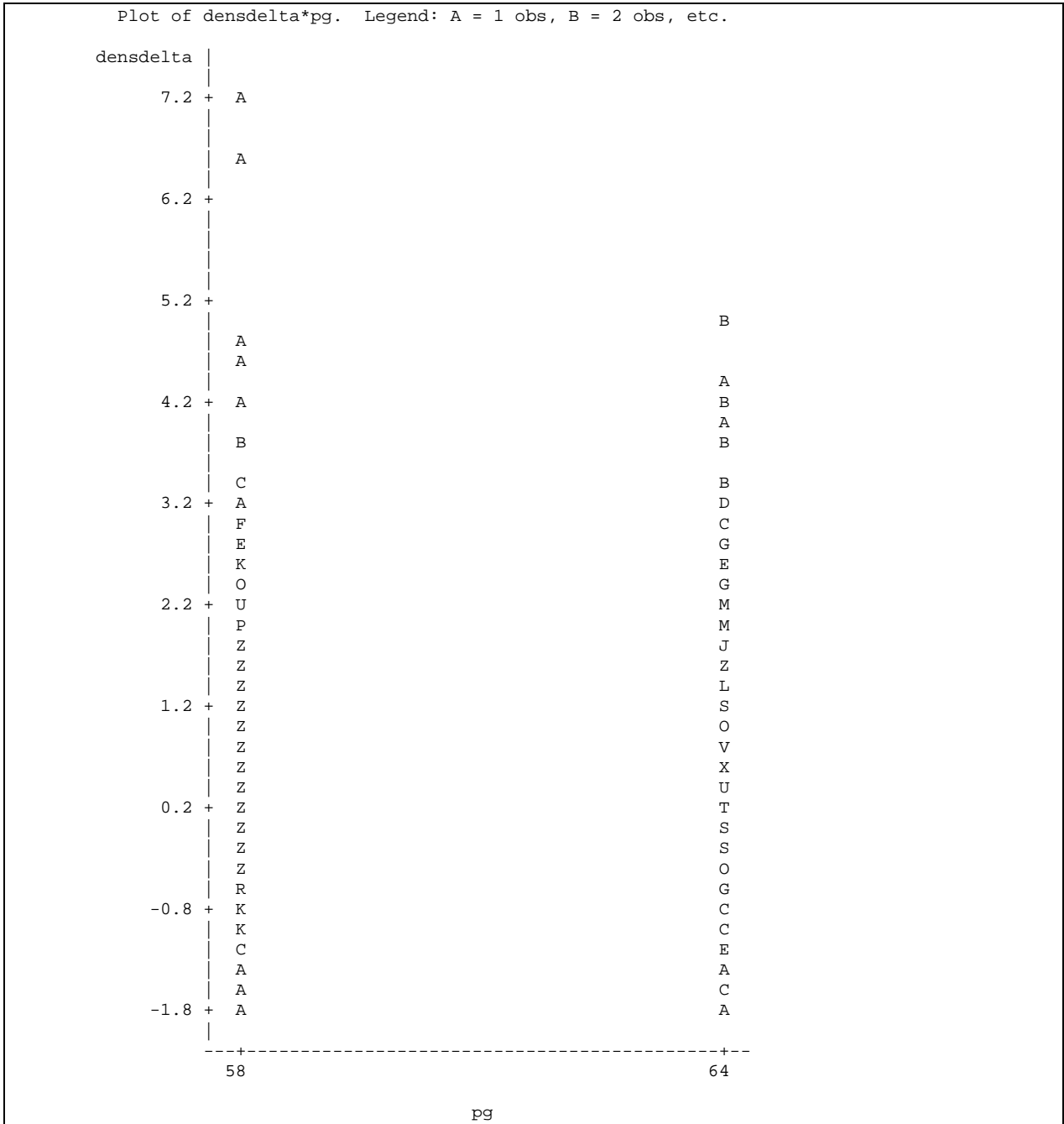


Figure C.2 Finish Roller – Density Gain versus PG Grade

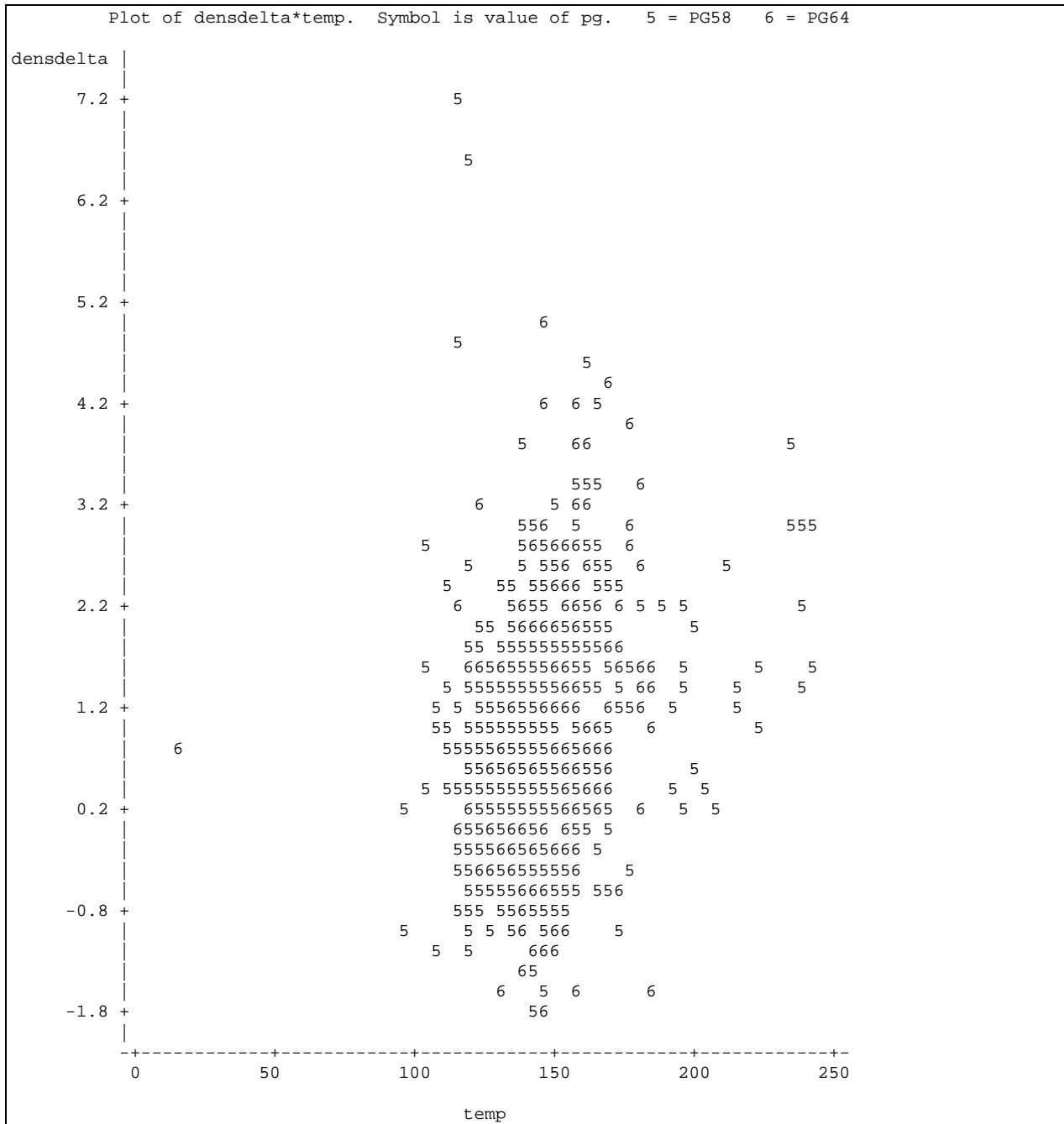


Figure C.3 Finish Roller – Density Gain versus Temperature by PG Grade

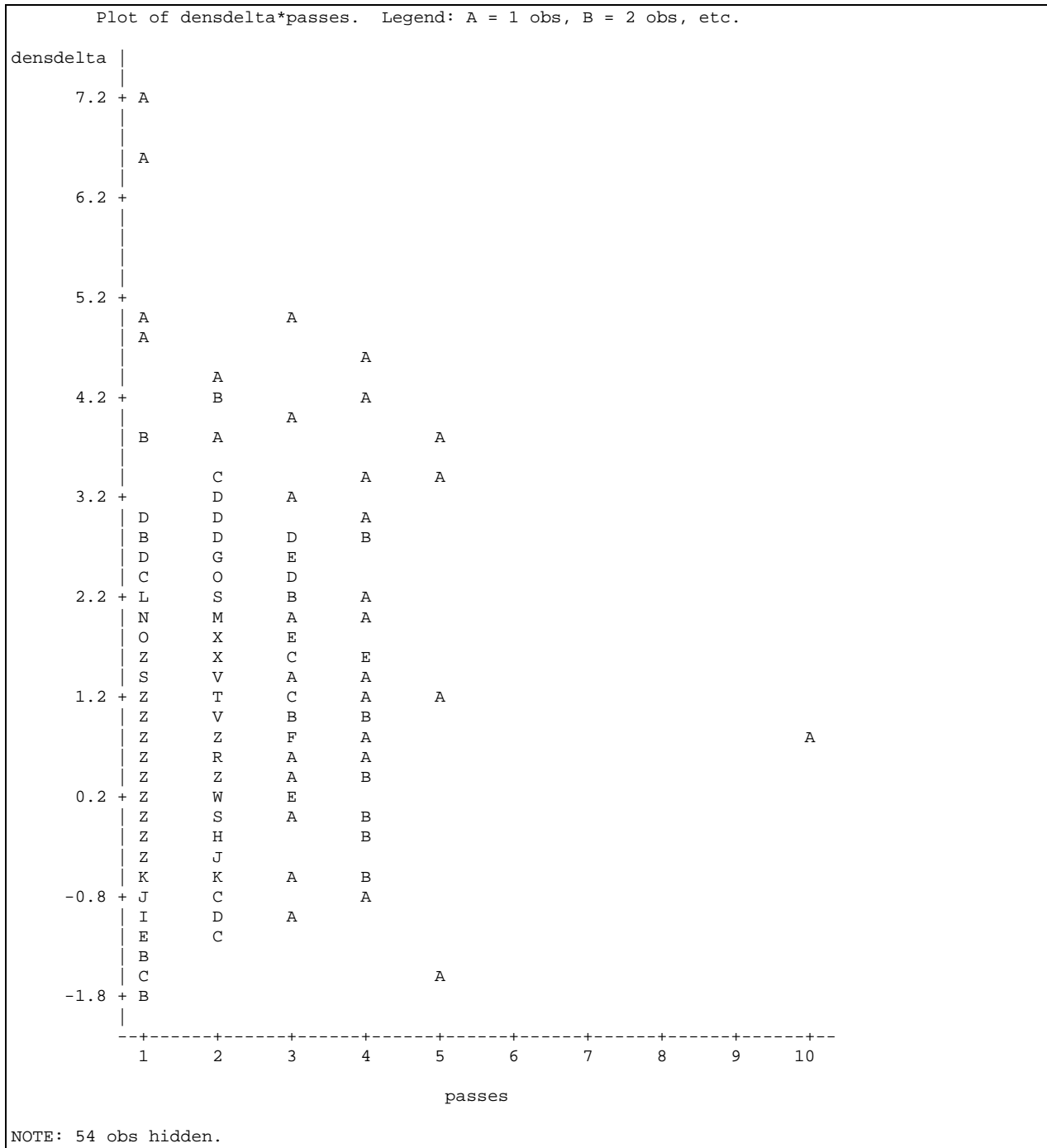


Figure C.4 Finish Roller – Density Gain versus Successive Passes

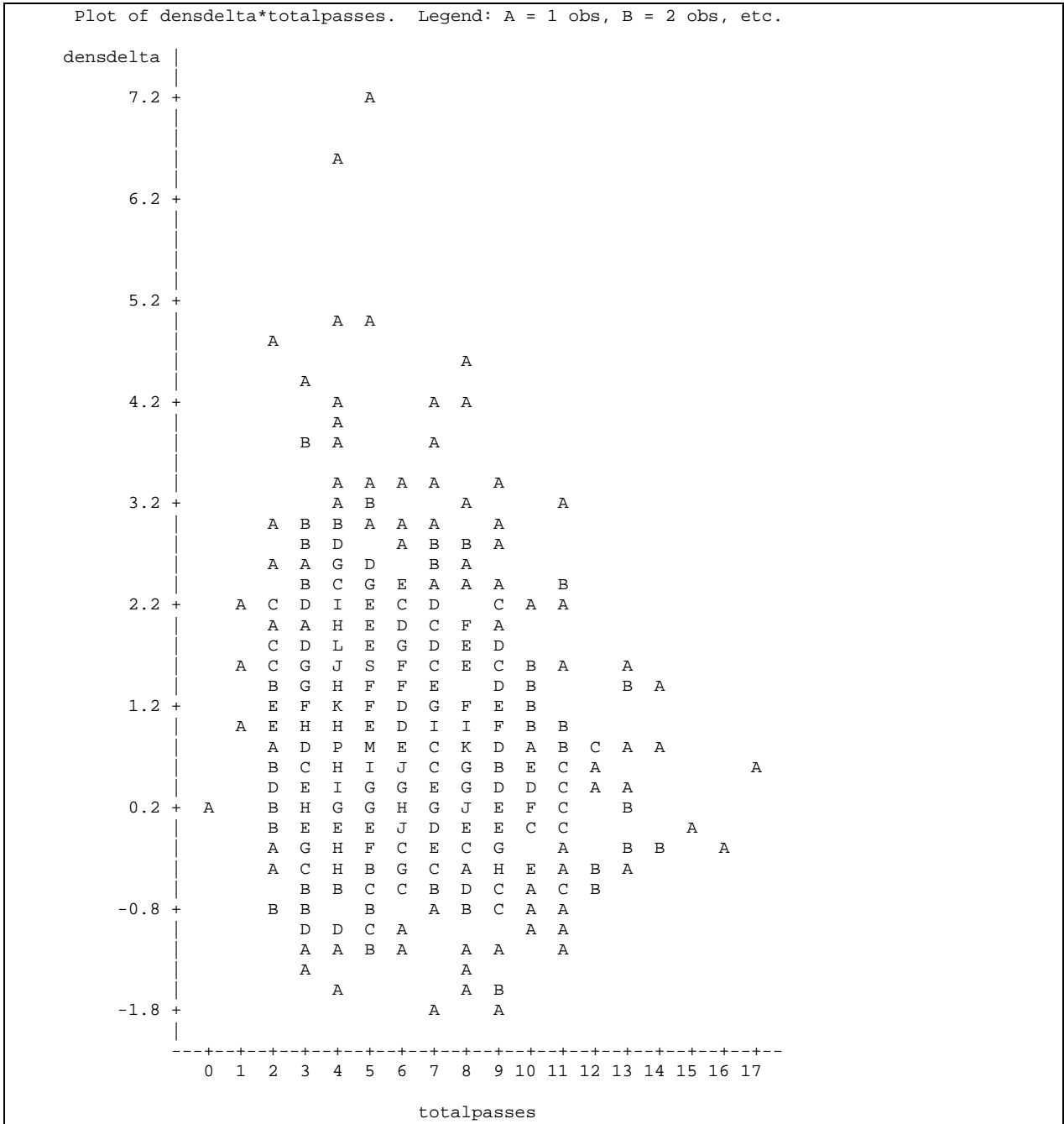


Figure C.5 Finish Roller – Density Gain versus Cumulative Passes

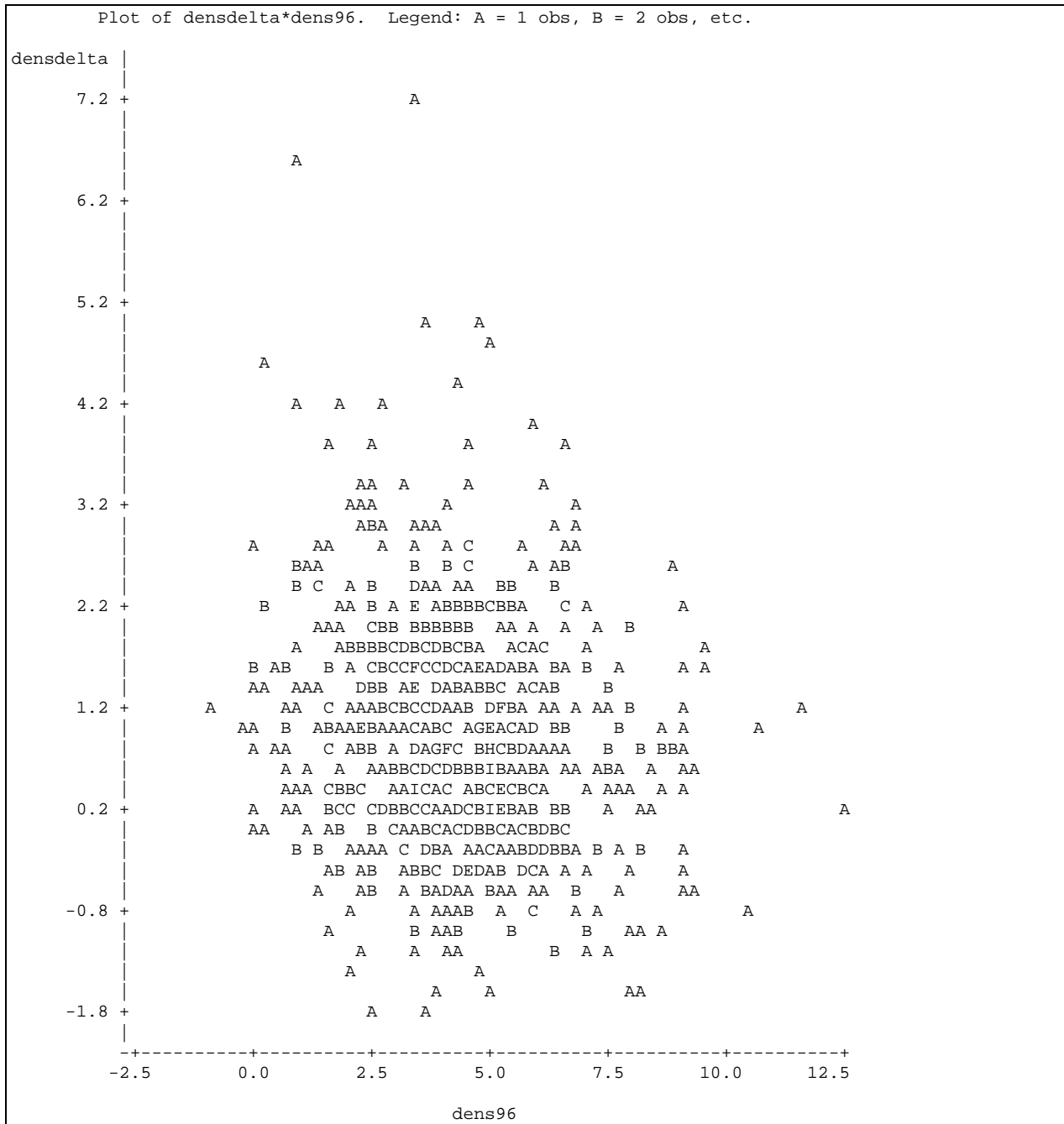


Figure C.6 Finish Roller – Density Gain versus Difference of 96% Gmm

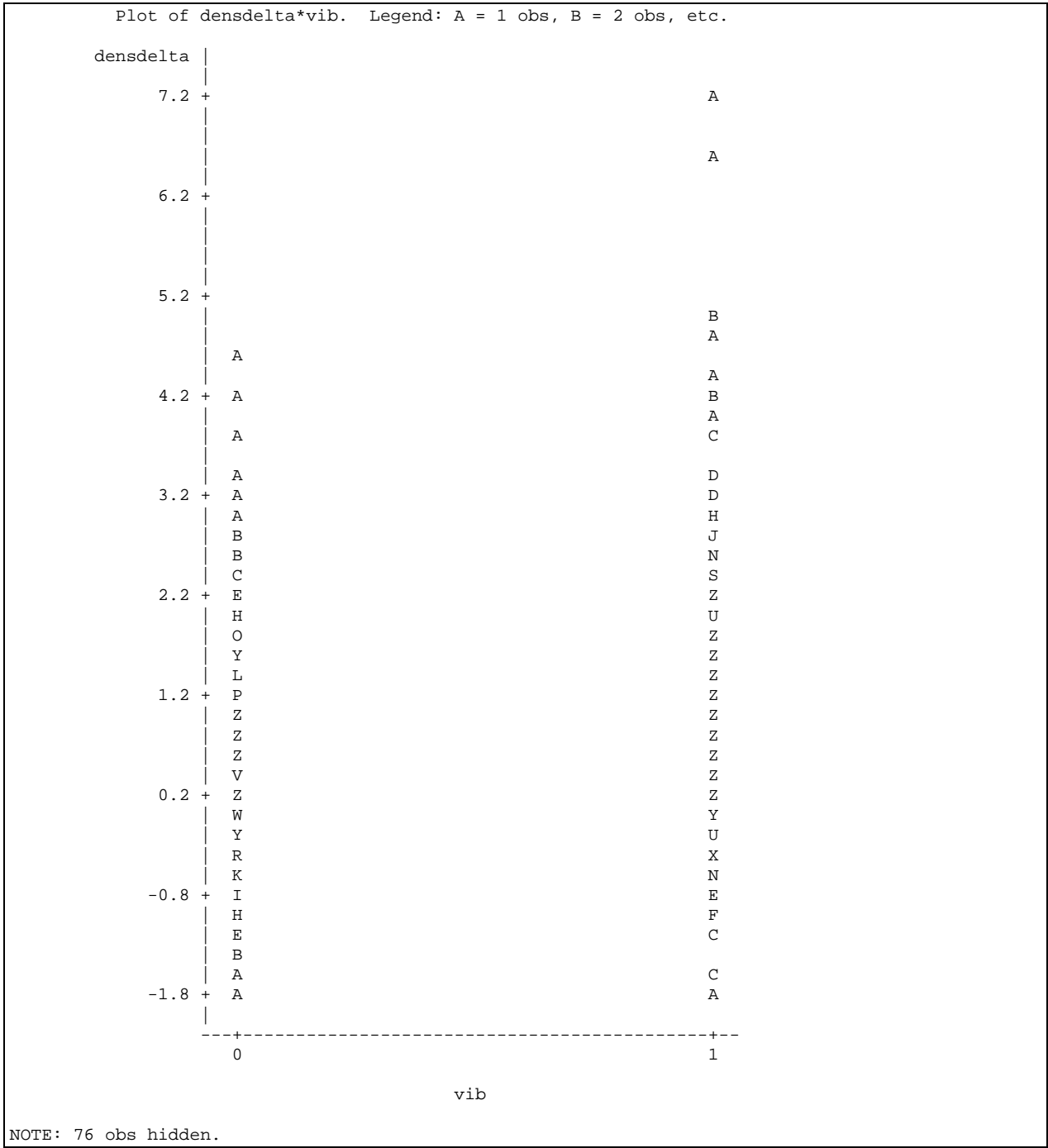


Figure C.7 Finish Roller – Density Gain versus Vibratory Setting

Appendix D Lab Compaction Models

Source	DF	Sum of Squares	Mean Square	F Value	Pr > F
Model	4	215.7580964	53.9395241	40.46	<.0001
Error	109	145.3244554	1.3332519		
Corrected Total	113	361.0825518			

R-Square	Coeff Var	Root MSE	ndes Mean
0.597531	1.226555	1.154665	94.13886

Source	DF	Type III SS	Mean Square	F Value	Pr > F
pg	1	6.1910973	6.1910973	4.64	0.0334
pressure	1	91.1021763	91.1021763	68.33	<.0001
temp	2	118.4648228	59.2324114	44.43	<.0001

Parameter	Estimate	Standard Error	t Value	Pr > t
Intercept	95.58355263 B	0.26855232	355.92	<.0001
pg 58	0.50134615 B	0.23265371	2.15	0.0334
pg 64	0.0000000 B	.	.	.
pressure 300	-1.78789474 B	0.21628862	-8.27	<.0001
pressure 600	0.0000000 B	.	.	.
temp 140	-2.32026316 B	0.26489838	-8.76	<.0001
temp 194	-0.36105263 B	0.26489838	-1.36	0.1757
temp 248	0.0000000 B	.	.	.

Figure D.1 Reduced Model for Lab Compaction Variables

Source	DF	Sum of Squares	Mean Square	F Value	Pr > F
Model	3	209.5669991	69.8556664	50.72	<.0001
Error	110	151.5155526	1.3774141		
Corrected Total	113	361.0825518			

R-Square	Coeff Var	Root MSE	ndes Mean
0.580385	1.246704	1.173633	94.13886

Source	DF	Type I SS	Mean Square	F Value	Pr > F
pressure	1	91.1021763	91.1021763	66.14	<.0001
temp	2	118.4648228	59.2324114	43.00	<.0001

Parameter	Estimate	Standard Error	t Value	Pr > t
Intercept	95.92657895 B	0.21984158	436.34	<.0001
pressure 300	-1.78789474 B	0.21984158	-8.13	<.0001
pressure 600	0.0000000 B	.	.	.
temp 140	-2.32026316 B	0.26924985	-8.62	<.0001
temp 194	-0.36105263 B	0.26924985	-1.34	0.1827
temp 248	0.0000000 B	.	.	.

Figure D.2 Final Reduced Model for Lab Compaction Variables

Source	DF	Sum of Squares	Mean Square	F Value	Pr > F
Model	3	89.9087229	29.9695743	22.69	<.0001
Error	44	58.1233250	1.3209847		
Corrected Total	47	148.0320479			

R-Square	Coeff Var	Root MSE	ndes Mean
0.607360	1.218283	1.149341	94.34104

Source	DF	Type III SS	Mean Square	F Value	Pr > F
pressure	1	37.64791875	37.64791875	28.50	<.0001
temp	2	52.26080417	26.13040208	19.78	<.0001

Parameter	Estimate	Standard Error	t Value	Pr > t
Intercept	96.06937500	0.33178616	289.55	<.0001
pressure 300	-1.77125000	0.33178616	-5.34	<.0001
pressure 600	0.00000000	.	.	.
temp 140	-2.31312500	0.40635340	-5.69	<.0001
temp 194	-0.21500000	0.40635340	-0.53	0.5994
temp 248	0.00000000	.	.	.

Figure D.3 Ndes=60 Final Reduced Model for Lab Compaction Variables

Source	DF	Sum of Squares	Mean Square	F Value	Pr > F
Model	4	114.4046417	28.6011604	36.57	<.0001
Error	43	33.6274062	0.7820327		
Corrected Total	47	148.0320479			

R-Square	Coeff Var	Root MSE	ndes Mean
0.772837	0.937372	0.884326	94.34104

Source	DF	Type III SS	Mean Square	F Value	Pr > F
nmas	1	24.49591875	24.49591875	31.32	<.0001
pressure	1	37.64791875	37.64791875	48.14	<.0001
temp	2	52.26080417	26.13040208	33.41	<.0001

Parameter	Estimate	Standard Error	t Value	Pr > t
Intercept	95.35500000	0.28541503	334.09	<.0001
nmas 12	1.42875000	0.25528296	5.60	<.0001
nmas 19	0.00000000	.	.	.
pressure 300	-1.77125000	0.25528296	-6.94	<.0001
pressure 600	0.00000000	.	.	.
temp 140	-2.31312500	0.31265650	-7.40	<.0001
temp 194	-0.21500000	0.31265650	-0.69	0.4954
temp 248	0.00000000	.	.	.

Figure D.4 Ndes=75 Final Reduced Model for Lab Compaction

Source	DF	Sum of Squares	Mean Square	F Value	Pr > F
Model	3	89.9087229	29.9695743	22.69	<.0001
Error	44	58.1233250	1.3209847		
Corrected Total	47	148.0320479			

R-Square	Coeff Var	Root MSE	ndes Mean
0.607360	1.218283	1.149341	94.34104

Source	DF	Type III SS	Mean Square	F Value	Pr > F
pressure	1	37.64791875	37.64791875	28.50	<.0001
temp	2	52.26080417	26.13040208	19.78	<.0001

Parameter	Estimate	Standard Error	t Value	Pr > t
Intercept	96.06937500 B	0.33178616	289.55	<.0001
pressure 300	-1.77125000 B	0.33178616	-5.34	<.0001
pressure 600	0.00000000 B	.	.	.
temp 140	-2.31312500 B	0.40635340	-5.69	<.0001
temp 194	-0.21500000 B	0.40635340	-0.53	0.5994
temp 248	0.00000000 B	.	.	.

Figure D.5 Ndes=75 Final Reduced Model for Lab Compaction Variables

Source	DF	Sum of Squares	Mean Square	F Value	Pr > F
Model	5	110.5262119	22.1052424	14.19	<.0001
Error	36	56.0892000	1.5580333		
Corrected Total	41	166.6154119			

R-Square	Coeff Var	Root MSE	ndes Mean
0.663361	1.327001	1.248212	94.06262

Source	DF	Type III SS	Mean Square	F Value	Pr > F
nmas	1	21.78000000	21.78000000	13.98	0.0006
source	1	7.16385333	7.16385333	4.60	0.0388
pressure	1	43.02619286	43.02619286	27.62	<.0001
temp	2	43.39989048	21.69994524	13.93	<.0001

Parameter	Estimate	Standard Error	t Value	Pr > t
Intercept	98.24071429 B	0.75213994	130.61	<.0001
nmas 12	-1.65000000 B	0.44130960	-3.74	0.0006
nmas 19	0.00000000 B	.	.	.
source 1	-1.22166667 B	0.56972825	-2.14	0.0388
source 2	0.00000000 B	.	.	.
pressure 300	-2.02428571 B	0.38520660	-5.26	<.0001
pressure 600	0.00000000 B	.	.	.
temp 140	-2.35214286 B	0.47177981	-4.99	<.0001
temp 194	-0.46857143 B	0.47177981	-0.99	0.3272
temp 248	0.00000000 B	.	.	.

Figure D.6 Ndes=100 Reduced Model for Lab Compaction

Source	DF	Sum of Squares	Mean Square	F Value	Pr > F
Model	4	103.3623586	25.8405896	15.12	<.0001
Error	37	63.2530533	1.7095420		
Corrected Total	41	166.6154119			

R-Square	Coeff Var	Root MSE	ndes Mean
0.620365	1.390026	1.307495	94.06262

Source	DF	Type III SS	Mean Square	F Value	Pr > F
nmas	1	16.93627524	16.93627524	9.91	0.0032
pressure	1	43.02619286	43.02619286	25.17	<.0001
temp	2	43.39989048	21.69994524	12.69	<.0001

Parameter	Estimate	Standard Error	t Value	Pr > t
Intercept	97.01904762 B	0.51436560	188.62	<.0001
nmas 12	-1.40566667 B	0.44659441	-3.15	0.0032
nmas 19	0.00000000 B	.	.	.
pressure 300	-2.02428571 B	0.40350158	-5.02	<.0001
pressure 600	0.00000000 B	.	.	.
temp 140	-2.35214286 B	0.49418649	-4.76	<.0001
temp 194	-0.46857143 B	0.49418649	-0.95	0.3492
temp 248	0.00000000 B	.	.	.

Figure D.7 Ndes=100 Final Reduced Model for Lab Compaction

Appendix E Aggregate Source Analysis

In Chapter 5, aggregate source was identified as having a marginal effect on lab compactive effort (p-value ≈ 0.02), where gravels yielded a lower density of 1.2% when compared with limestone. This factor was further investigated by evaluating the JMF for specific aggregate properties, such as quarry/pit location, crushed face counts, percent thin and elongated pieces (by weight), and fine aggregate angularity (FAA). Gradation analysis was not possible since the actual measured gradation data were not readily available. There was potential for incorrectly classifying the geologic source of the aggregate by location, so a quantitative approach was taken using the percentage of crushed faces (2 faces), percentage of thin and elongated particles, and FAA percentage.

Figures E.1 and E.2 plot the CDI against the percentage of 2 crushed face for E-3 and E-10 mixes, respectively. For the E-3 mixes, lower values of 2 crushed faces generally yielded lower compactive effort. There was a slight upward trend for 600 kPa, but a more pronounced effect for 300 kPa pressure. No relationship was observed for the E-10 mixes at 600 kPa, and a negative correlation was observed for the 300 kPa mixes, counter to what would be expected.

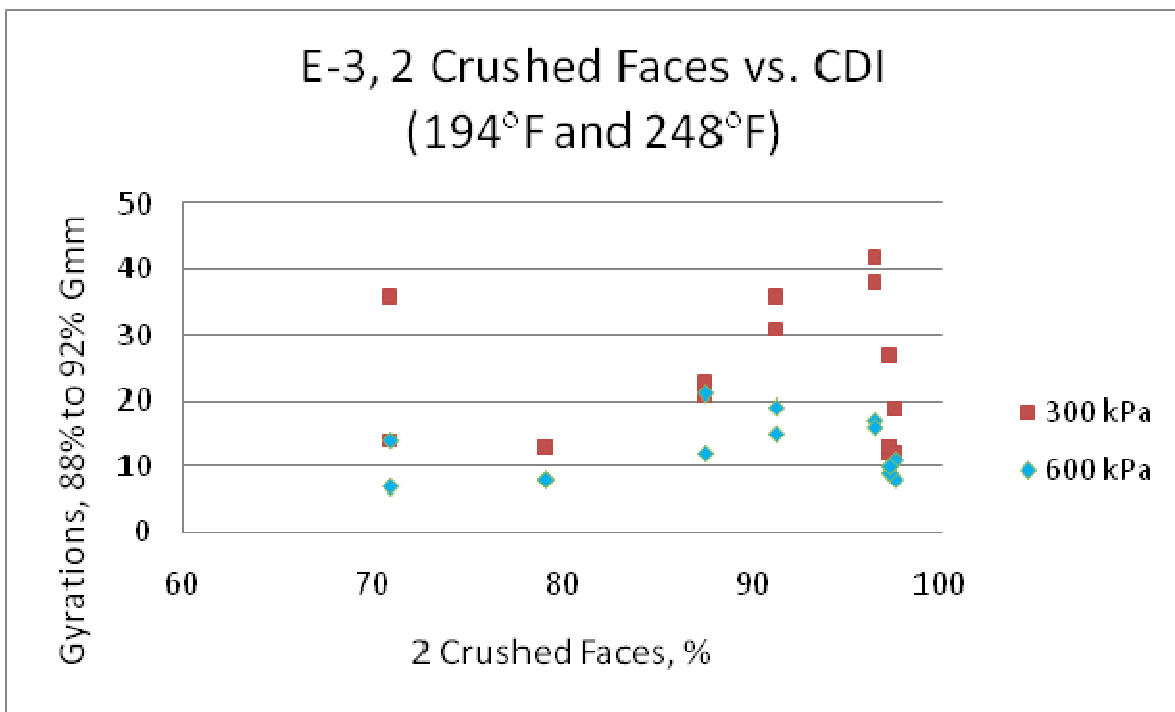


Figure E.1 E-3 Crushed Faces relationship with Compactive Effort

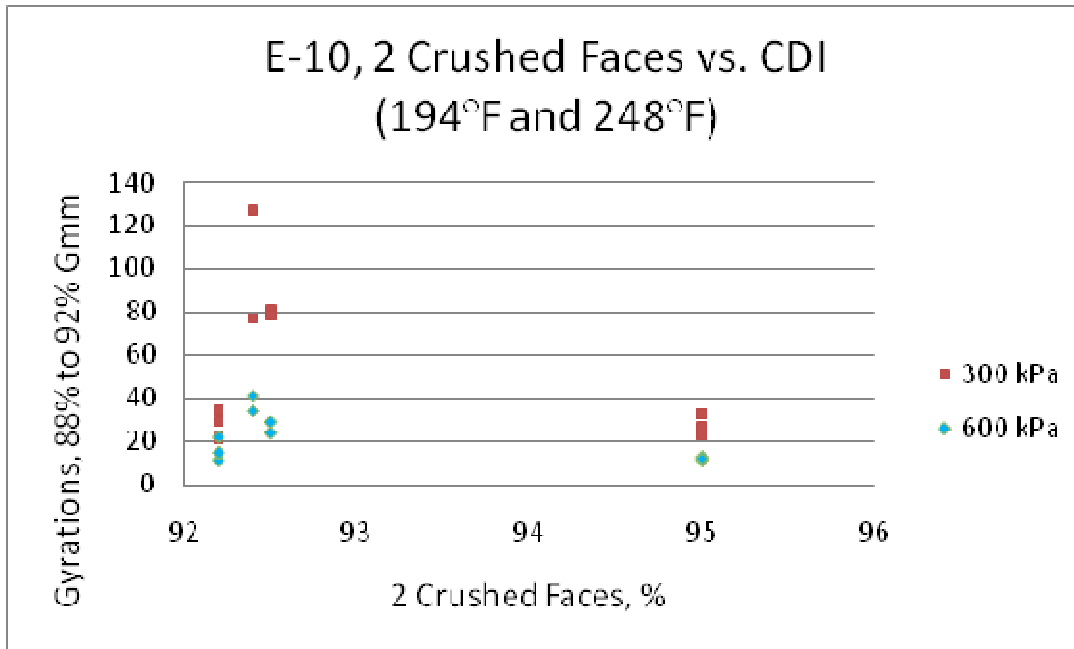


Figure E.2 E-10 Crushed Faces relationship with Compactive Effort

Plots were prepared for FAA versus compactive effort (CDI) in Figures E.3 and E.4. Compaction at lower 140°F temperatures required more compactive effort, so those data points were eliminated from the plots. E-3 mixture FAA values ranged from 42.5% to 45.2%, and indicated an increase in compaction level with an increase with FAA.

No trend was observed for the E-10 mixes; however, it must be noted that the FAA range was very narrow, from 45.2% to 46.6%. This finding may be contrary to the expected result, where it becomes increasing difficult to compact the mixture with greater void levels in the fine aggregate. Based on the data, there are no strong trends, and only moderate evidence, between aggregate properties and compaction effort. Additionally, it must be noted that the IH 39 Marquette County project had material properties out of specification limits, resulting in low field density of about 90%. These findings are limited to initial exploratory analysis, and it is recommended that additional comprehensive research be conducted with aggregate analysis, since the principal objective of the study was understanding the effect of temperature and pressure to achieve density. A complete data set of as-built aggregate properties and measures is needed.

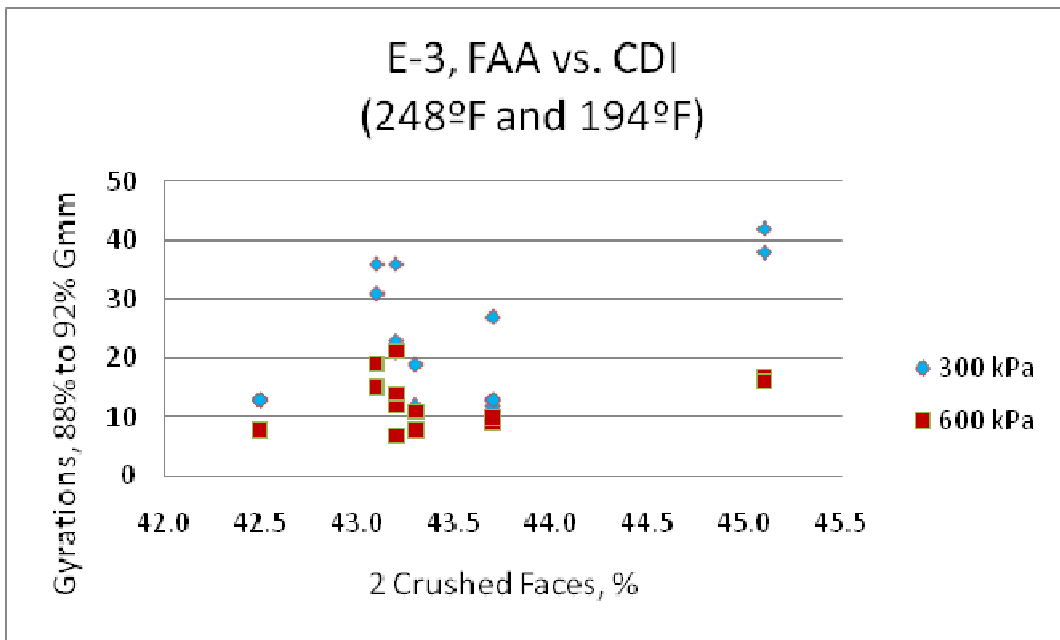


Figure E.3 FAA relationship with Compactive Effort for E-3 Mixes

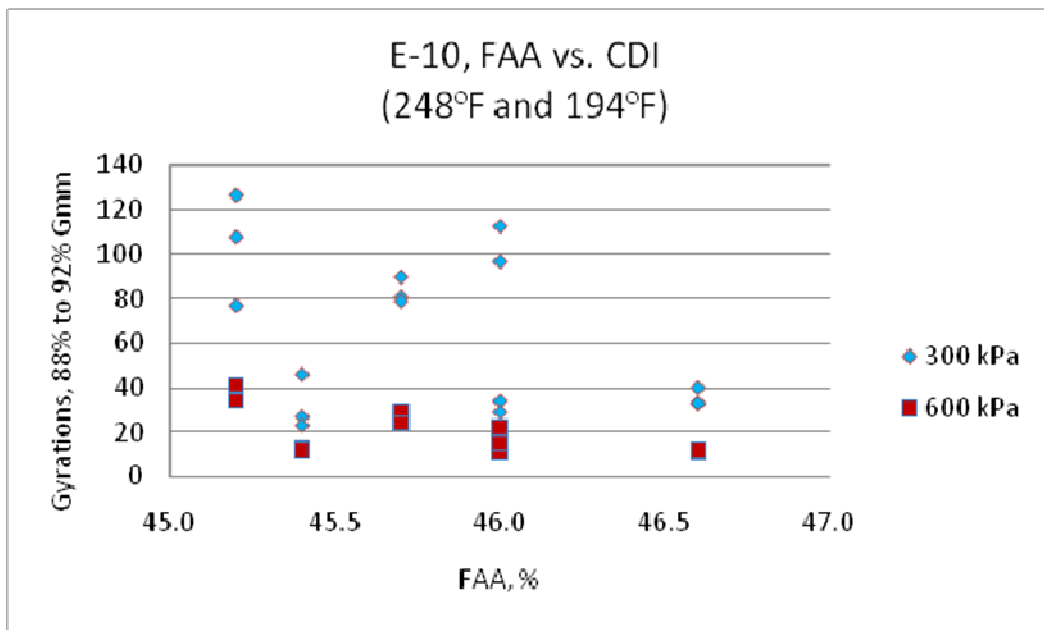


Figure E.4 FAA relationship with Compactive Effort for E-10 Mixes